THE K-CYCLE ENGINE

by

Brian J. Lanoway

A Thesis Submitted to

THE FACULTY OF GRADUATE STUDIES

UNIVERSITY OF MANITOBA

in Partial Fulfillment of the Requirements

for the Degree of

MASTER OF SCIENCE IN MECHANICAL ENGINEERING

Winnipeg, Manitoba

August, 1979

THE K-CYCLE ENGINE

BY

BRIAN JOHN LANOWAY

A dissertation submitted to the Faculty of Graduate Studies of the University of Manitoba in partial fulfillment of the requirements of the degree of

MASTER OF SCIENCE

© 1979

Permission has been granted to the LIBRARY OF THE UNIVERSITY OF MANITOBA to lend or sell copies of this dissertation, to the NATIONAL LIBRARY OF CANADA to microfilm this dissertation and to lend or sell copies of the film, and UNIVERSITY MICROFILMS to publish an abstract of this dissertation.

The author reserves other publication rights, and neither the dissertation nor extensive extracts from it may be printed or otherwise reproduced without the author's written permission.

ABSTRACT

The K-Cycle Engine is an axial cylinder, opposed piston, rotating cylinder block, stationary cam internal combustion engine. The extended expansion stroke of such a mechanism offers the theoretical potential of a 50% increase in thermal efficiency as compared to a conventional Otto Cycle engine.

To realize some portion of such an increase in thermal efficiency K-Cycle Engines Ltd. constructed two prototype engines and entered into a research and development program. Although the first two engines performed satisfactorily for early prototypes, several sub-systems would have to demonstrate improved performance in order to obtain respectable engine output.

To circumvent some of the identified problem areas and reduce development time by taking advantage of existing conventional technology, the design of a third K-Cycle prototype engine was initiated.

With the benefit of a re-examination of the design intent of the original prototypes, this thesis evolves a method of optimizing the configuration of the third engine concept in terms of basic engine design variables. At the same time

means of minimizing mechanical losses are examined and methods of improving indicated power output through combustion chamber shape are investigated.

For the sake of brevity, it is assumed that the reader is conversant with conventional internal combustion engines and is acquainted with the K-Cycle Mechanism.

ACKNOWLEDGEMENTS

The author wishes to express his sincere gratitude to K-Cycle Engines Ltd. for its assistance during the course of this thesis. Special thanks are forwarded to Hoken Kristiansen, President of K-Cycle Engines Ltd., who provided stimulative thought and moral support in many 'after hours' discussions.

At the same time, he would like to thank his thesis advisor, Prof. W. D. Alexander, without whose teaching, criticism and patience this thesis would not have been possible and whose many years of influence have culminated in this thesis.

In addition, the author would like to thank the staff members of K-Cycle Engines Ltd. and the Department of Mechanical Engineering who so willingly offered their help during the course of this study.

TABLE OF CONTENTS

LIST OF TABLES, FIGURES AND GRAPHS

CHAPTER 1

INTRODUCTION

Since January 1975, K-Cycle Engines has been heavily involved in the development of an internal combustion engine mechanism that can convert the "K-Cycle theory", of improved thermodynamic efficiency via an extended expansion stroke, into reality.

To demonstrate the feasibility of the K-Cycle thermodynamic principle two prototype engines were constructed and a research program was initiated to realize the full potential, indicated by theory, on the test bench and in an automotive environment. Although both engines demonstrated adequate performance for early prototypes, their output fell short of demonstrating the predicted increased efficiency.

Bench testing of both engines revealed that the original concept had a number of inherent deficiencies where certain sub-systems were designed to perform outside the bounds of conventional technology. These sub-systems would require a concentrated development program to bring their individual performance up to the required level in order to demonstrate the full viability and potential of the total engine mechanism.

As the primary goal of K-Cycle Engines is to demonstrate in the most expedient manner the potential gain in fuel economy that its internal combustion engine concept offers, and not to involve itself in a tedious development program of the

concept's sub-systems, it was decided to design a third prototype engine--designated the Dash-3 Engine--that would circumvent the problem areas of its predecessors. In addition, the new engine concept would be optimized and revalued in light of the limited but significant test data that had been obtained during the testing of the first two prototypes.

The author, an employee of K-Cycle Engines, was assigned the task of evolving the Dash-3 Engine concept (within the Company design parameters outlined in Chapter Three) and has taken the opportunity to record within this thesis the engineering rationale incorporated in the new engine.

For the sake of brevity, it has been assumed that the reader of this document is fully conversant with the conventional internal combustion engine and the K-Cycle principle of the extended expansion stroke and is acquainted with the mechanisms of the first two K-Cycle prototype engines.

CHAPTER 2

A HISTORICAL REVIEW OF THE FIRST TWO PROTOTYPE ENGINES

2.1 INTRODUCTION

An optimization process of the Dash-3 Engine configuration would not achieve the required focus unless it was evolved with the benefit of a re-examination of the original intent, goals and philosophy of the first two K-Cycle Engines.

The design of the first engine was based on a distinct design philosophy. This philosophy was arrived at with feasibility analysis and extrapolation from similar applications being substituted for the lack of past test experience.

To get the first prototype engine to run under its own power, a number of basic changes were made which often did not coincide with the intent of the original design. One particular example of such a change is the substitution of spark ignition and carburetion for the continuous combustion ignition and continuous fuel injection. Although the majority of these changes were warranted, some were based on superficial test data, and the subsequent repair might not be capable of the performance that its predecessor might have been if more development time had been available.

The original design philosophy, modified by these compromises and changes, was carried over into the Mark II Engine and, via the design goals stated in Chapter Three, to the third generation Dash-3 Engine.

2.1 Introduction (Con't)

The following background information is therefore presented to provide the historical perspective required to properly evaluate the rationale behind the optimization of the Dash-3 Engine configuration presented in the remaining chapters.

2.2 THE DESIGN PHILOSOPHY AND GOALS OF THE FIRST PROTOTYPE ENGINE

During the feasibility studies conducted prior to the detailed design of the first engine, a number of basic design goals and philosophies emerged, all of which were based on an axial-cylinder drum-cam engine.

This section will outline the original design intent, unmodified by the subsequent test and development programs, of the first prototype engine.

2.2-1 Rotating Cylinders and Stationary Cams

At an early stage, it was decided that the prototype engine would have a rotating cylinder block or rotor and stationary opposed cams. The other possibility, stationary rotor and rotating cams, was rejected for a number of reasons. By having the rotating cylinder ports interfacing with stationary inlet and exhaust ports in a stationary casing or "combustor ring", the need for conventional inlet and exhaust valves, and their associated mechamism, is eliminated. An obvious advantage is the potential of attaining high volumetric efficiencies. Along with improved breathing, the overall mechanical efficiency of the engine is increased with the elimination of a valve train mechanism.

2.2-1 Rotating Cylinders and Stationary Cams (Con't)

Another improvement is that if a single inlet port is used to supply the fuel/air mixture to all the cylinders, the need for complex manifolding found in conventional engines no longer exists. In a carbureted version of the K-Cycle, this would mean better control of the range of mixtures being supplied to all the cylinders and the subsequent possibility of running at leaner than conventional air/fuel ratios.

Because the exhaust gases of the K-Cycle Engine will be released at a pressure just above atmosphere, the single stationary exhaust port and pipe is more desirable as it would allow a freer flow of the exhaust gases with less back pressure than would an exhaust poppet valve and collection manifold. The elimination of the exhaust valve also removes a potentially troublesome hot spot that would otherwise be present in each cylinder.

It was also felt that it would be easier to lubricate the running surface of a stationary cam rather than fight centrifugal force in trying to keep an adequate amount of oil on a spinning cam.

It was recognized that the rotating rotor stationary cam configuration had several inherent design difficulties. Although a revolving rotor is a natural for an air-cooled engine, it had been previously decided that the first engine would be water cooled. This was dictated by the requirement of suiting an automotive environment. The moving rotor

2.2-1 Rotating Cylinders and Stationary Cams (con't)

presented the design problem of getting water into a rotating cylinder block, around each cylinder and out again to a stationary outlet in the required manner with a minimum of sealing losses.

Another recognized difficulty was that the cylinder ports of the moving cylinders had to be sealed with respect to the stationary inlet and exhaust ports of the combustor ring. Although it was felt that such a sealing system would require careful design, the recent advances in sealing technology resulting from the development of the Wankel Engine provided great encouragement. It was felt that the operating parameters of the Wankel seal were much more severe than those of the constant velocity K-Cycle seal. This then reduced the design problem to one of gleaning useful information from the Wankel seal design and incorporating it successfully into the first K-Cycle prototype.

2.2-2 Combustion

Three different methods of combustion initiation were possible in the first prototype engine. Two of these methods have been used by other cycles in the past: spark ignition (Otto Cycle) and auto ignition (Diesel), while the third method, continuous combustion, is unique to the K-Cycle Engine.

A spark ignition K-Cycle Engine would have all the characteristics at the high pressure end of the P-V curve as that of an Otto Cycle Engine. With spark ignition the K-Cycle Engine

2.2-2 Combustion (Con't)

would require variable ignition advance, fuels insensitive to detonation, etc.

The high compression "diesel" version of the K-Cycle Engine would have all the thermodynamic advantages of the conventional auto-ignition diesel in addition to those of the longer expansion ratio. The proposed K-Cycle mechanism allows an interesting variation in the method of fuel delivery in that the injection of the fuel could be continuous rather than intermittent.

The third proposed method of ignition--continuous combustion--is unique to the K-Cycle mechanism. Continuous combustion is obtained when the hot gases of a cylinder that has just fired are used to ignite the unburned charge of the following cylinder. Some of the proposed advantages of continuous combustion over spark ignition are reduced ignition lag and, therefore, the reduction of ignition advance required. The continuous combustion ignition gases are a reliable source of ignition in comparison to the conventional electronic spark ignition mechanism, and do not require continual purging of the ignition electrode gap with a fresh air/fuel charge.

Advantages of continuous combustion over Diesel auto-ignition are that the hot gas ignition has all the advantages of auto ignition without the associated work of compression. If continuous fuel injection, rather than intermittent injection, is used with the hot gas ignition of continuous combustion, the possibility exists of obtaining detonation-free combustion.

2.2-2 Combustion (Con't)

Detonation is avoided if the fuel is burned as it is injected preventing the collection of unburned fuel which is susceptible to end gas auto-ignition[3]. This would allow the engine to maintain a reasonable compression ratio and use low grade fuels. Without detonation, a lower rate of pressure rise also results and the engine mechanism can be made lighter than that required by a conventional Diesel. The continuous injection of fuel also does not require the complex fuel injection timing equipment associated with intermittent injection.

Even prior to any detailed analysis, it had been decided to incorporate continuous combustion of one form or another into the first engine. The first engine was to be a showcase for all the possible K-Cycle advantages and, therefore, spark ignition was considered only as an interesting possibility for future specific applications. Diesel auto-ignition was included in future test plans for the first engine. It was decided to design the continuous combustion ignition system into the engine because of its more forgiving compression ratios and its unique advantages inherent only to the K-Cycle operating principle. Continuous fuel injection was specified because of its potential detonation-free combustion and its simplicity relative to conventional intermittent fuel injection systems. Initial ignition was to be provided with a glow plug.

2.2-3 A Peripheral Port Rotor

There were several options available as to the manner in which the cylinder ports could be positioned. The initial engine

2.2-3 A Peripheral Port Rotor (Con't)

concepts examined had the stationary member or combustor ring, incorporating the inlet and exhaust ports, located in the center of the engine with the sealing system operating on a surface perpendicular to the axis of rotation of the rotor. This stationary member would also act as a common cylinder head for the opposed banks of pistons.

Such a configuration had a number of design problems, such as coolant flow from one bank of cylinders to the other, and was soon replaced by the peripheral cylinder port system. There are numerous advantages of the former porting method over the latter. With the elimination of the cylinder head, a one-piece cylinder sleeve could be used by each pair of opposed pistons. Consequently, the rotor halves could be combined into a single unit requiring only two main support bearings located at each end. The removal of the common cylinder head also resulted in a significant reduction of total engine length. With each pair of pistons sharing a common combustion chamber, the gas pressure acting on each piston would be equal resulting in a perfectly balanced, vibration free engine.

The peripheral port rotor also resulted in an improved combustion chamber shape, as it was more suited to the continuous fuel injected version of continuous combustion which had already been designated as the system the first engine would use. The elimination of the cylinder head reduced the surface to volume ratio of the combustion chamber.

2.2-4 The Circumferential Sealing System

The choice of a rotating rotor with peripheral ports and a stationary combustor ring with a single inlet and exhaust port necessitated the use of a gas seal between the relative moving surfaces of the two components.

A seal concept was decided upon that used two circumferential ring seals around the circumference of the rotor, on either side of the ports, to seal the cylinder ports from the inside of the engine casing. To obtain cylinder port to cylinder port sealing, the two circumferential seals were intersected by inter-cylinder port cross-seals. These cross-seals were to be sufficiently narrow so that any interruption of the continuous fuel injection spray would be insignificant.

The circumferential seals were to have oil grooves in their running surfaces. Pressurized oil was to be supplied from stationary ports in the combustor ring to these grooves to enable the seals to ride on a hydrodynamic oil film and avoid metal to metal contact. The running surfaces of the cross-seals were to be lubricated as they passed through the continuous spray of the diesel fuel.

The seals were positioned by light sub-seal springs but were to be pressure activated and pressure balanced under operating conditions.

2.2-5 The Drum Cam

The actual physical size of any stationary cam that would be used is dictated by the cylinder PCD, engine displacement, and desired expansion ratio.

2.2-5 The Drum Cam (Con't)

Several types of cam motion were examined: simple harmonic, cycloidal and parabolic motion. Although cycloidal motion exhibits theoretical peak accelerations of greater magnitude than the other motions considered, it was the only one to have finite jerk.[4] In theory, simple harmonic motion results in peak accelerations less in magnitude than cycloidal motion, but in reality the opposite is true when a dwell is involved. In fact, the actual acceleration megnitudes of parabolic and harmonic motions are twice that indicated by theory if the motion is preceded or followed by a dwell, while those of cycloidal motion approach the theoretical values in the same situation.[5]

To meet some of the constraints imposed by the continuous combustion process, a flat spot or dwell was inserted at the end of the compression stroke. The TDC dwell made it possible to provide ignition at what was thought to be the optimum point because it reduced the amount of ignition advance required. It should be noted that this ability to control the piston motion at TDC was considered to be one of the major advantages of the new concept. The requirement of a TDC dwell made the cycloidal motion with its finite jerk the obvious choice for the piston motion.

Unlike the conventional four stroke crankshaft engine, a cam generated four cycle is not restricted to stroke lengths of equal angular duration. If desired, each stroke could have an angular duration that is different from the other three.

2.2-5 The Drum Cam (Con't)

It was decided that for simplicity, the intake and compression strokes would initially be of equal duration, with the same being the case for the expansion and exhaust strokes. The angular split between the intake/compression and expansion/exhaust was determined by setting equal the peak accelerations for all four strokes. This was done in an attempt to optimize the engine's balance.

Several cam cross-sectional shapes were examined with the following requirements in mind: the piston loads should be transmitted in a symmetrical axial fashion and the piston should not have to be disassembled to remove it from the cam. Although a 'T'-shaped cam cross-section is more attractive from a loading point of view, the assembly/disassembly requirements resulted in a 'L'-shaped cross-section being chosen.

2.2-6 The Pistons

The final form that a piston concept would arrive at was primarily governed by these variables: bore diameter, stroke lengths, operating speed and combustion gas loading.

It was initially concluded that the piston concept would have to survive a peak combustion pressure of 1,000 psi (arbitrarily set) and a maximum engine speed of 4,000 RPM. Maximum piston assembly weight was targeted at 1 pound. The top piston roller would have to survive the previous loads with a reasonable bearing life and for obvious reasons off-the-shelf bearings were specified. To survive the contact stresses of

2.2-6 The Pistons (Con't)

the roller to cam line contact, the roller would have certain contact width and diameter requirements. The contact stresses generated required either a small diameter roller to be compensated by a large roller width or a small line contact by a large roller diameter.

The narrow roller concept was favoured as this would reduce the frictional losses that resulted from the sliding action of the roller on the cam. This sliding action would result from the tendency of the outer edge of the roller to have a higher surface velocity than that of the inner edge.

Due to the cycloidal motion and high gas pressure loading, it was felt that the negative roller would be loaded for a small portion of the entire four stroke cycle. Because of its spin up inertia and the differential rotation sliding, it was concluded that a negative roller would slide under load and not roll. For this reason, and total piston weight considerations, a negative slider or lug was substituted for the roller. To rationalize the choice of a negative load slider comparisons were made to the conventional automotive camshaft with its tappet follower.

The piston body was seen as having several distinct functions. It has to transmit the gas force to the top roller, support the top roller assembly and the negative slider, transmit the cam pressure angle induced positive thrust force and resist the negative cam induced thrust force and the centrifugal force from the piston weight. It was felt that a semi-circular

2.2-6 The Pistons (Con't)

cross-section would be able to serve all these functions, as long as it had a suitable length to diameter ratio to prevent the piston from tilting and binding in its bore.

One function that the semi-circular piston body could not perform was to resist the twisting torque that resulted when the negative slider contacted the cam. To resist this, and keep the piston in proper angular alignment with respect to the axis of the rotor (as it travelled up and down its bore), a key was added to the piston body concept. This key would slide in a properly positioned keyway in the cylinder bore. The importance of the piston key was increased when a TDC dwell was added to the cam profile. Because the dwell is flat, the natural aligning tendency is absent and the possibility exists that the top roller would have less than optimum line contact when it starts the expansion stroke.

2.2-7 The Cooling System

As previously mentioned in Section 2.2-1, it was decided that the first prototype engine would be watercooled because of its automotive nature. Although the rotating rotor is a natural for air cooling as a Francis Fan (axial inlet, radial outlet), it was felt that the confined conditions in an indoor test cell favoured water cooling.

It was initially thought that the engine could be oil cooled with the oil also serving a parallel lubrication function. The more complex water cooling was chosen after a feasibility

2.2-7 The Cooling System (Con't)

analysis showed that an unreasonable flow rate of the cooling oil was required.

There are two ways that an engine cooling system can be designed: one method uses a large amount of water moving at a slow rate as in a conventional engine, or one can use a small amount of water moving at high velocities. In order to keep the rotating rotor weight at a minimum the latter concept was chosen.

To obtain a uniform rotor temperature a parallel coolant path to each cylinder was specified, rather than a series path with the cooling of one cylinder after another.

Because of its different cooling requirements the combustor ring, which contained the exhaust port, was to have a separate cooling system.

2.2-8 The Lubrication System

Because of the absence of a crankshaft in the K-Cycle prototype a dry sump lubrication system was thought to be more suitable than a wet sump. The lubrication system was to supply pressurized oil to each piston travel area. The oil would then migrate around the piston lubricating the bearings and then collect on outward portion of the cylinder bore. Aided by centrifugal force, the oil would then pass through drainage holes in the outside of the rotor, spray against the inside of the engine casing and fall to the bottom where it would be scavanged by the dry sump system.

2.2-8 The Lubrication System (Con't)

The cams, rollers and negative sliders would be lubricated by the oil mist generated inside the engine casing. The combustor ring would have a separate pressurized supply and drain for the seals.

2.2-9 Engine Size and Displacement

With future publicity requirements in mind, an engine size suitable to current automotive requirements was specified. At that time, the average mid-size domestic car was equipped with approximately a 150 HP engine and this became the target of the first engine. Comparisons were made to the then new G.M. Buick V6 powerplant.

2.2-10 Prototype Engine Purpose

It was intended that the first prototype engine be designed as a "pre-production prototype". In other words, it was to be designed so that small production runs could be fabricated on a limited basis by a manufacturer with Winnipeg-level shop technology. It was envisioned that after the initial tests of the first prototype were completed, interested licensees would require "field trial" engines based on the design of the first prototype.

Some component interchangeability (piston heads, cams, combustor rings) was to be designed into the engine so that its torque and breathing characteristics could be modified to suit the demands of specific "field trial" engines.

Engine adjustments were to be limited to those variables required in the fine tuning of the finished engine.

2.3 THE EVOLUTION OF THE FIRST PROTOTYPE INTO A RUNNING ENGINE

2.3-1 The Engine on the Test Bench

After the first engine was assembled, it was installed in a test bench and a series of motoring trials was initiated to break-in the mechanism, check out the auxiliary systems, measure compression pressures, and evaluate the roller/cam/slider mechanism.

The motoring tests revealed two problems with the new mechanism: low compression pressures and a galling action between the negative slider of the piston and the bottom running surface of the cam. The poor compression pressures were attributed to the circumferential seals and cross-seals sticking in their grooves. The cam galling was felt to be caused by insufficient running clearances and inadequate surface lubrication. Despite attempts to rectify these problems, they persisted until the completion of the motoring trials.

It was felt that the seal leakage and cam galling problems would diminish in a running engine where increased engine speed would attenuate the effect of seal leakage and combustion pressure would reduce the excessive negative slider loading (caused by the sub-atmospheric over-exapsnion at the end of the expansion stroke in a non-fired engine).

The initial attempts to run the engine were unsuccessful and the lack of combustion obtained was blamed on the inability of the glow plug to initiate the burning of the

2.3-1 The Engine on the Test Bench (Con't)

injected diesel fuel. Alternate ignition systems were installed and all that was obtained at the best of times was sporadic and ineffectual combustion.

The inability to obtain meaningful combustion was thought to be caused by inadequate ignition and improper fuel distribution and atomization. The marginally acceptable compression pressures, due to seal leakage, did not permit a conversion to compression ignition as a possible solution.

In order to reduce the number of variables associated with the fuel injection and continuous combustion, it was decided to "conventionalize" the engine and convert to spark-ignition and carburetion. This move was intended as a temporary one, with the return to fuel injection and continuous combustion to occur after the engine was running.

After the conversion, firing trials were resumed and the same type of sporadic ineffectual firing was again obtained.

Because of the marginal compression pressures, suspicion was re-directed at the peripheral seals. Examination of the motoring cylinder pressure traces revealed that although compression pressures at the start of the TDC dwell were marginally acceptable, the seal leakage reduced the compression pressures to just above atmosphere at the end of the dwell. This explained the ineffective combustion.

Consideration was given to various means of raising the

2.3-1 The Engine on the Test Bench (Con't)

engine starting speed to a level where the effect of seal leakage could possibly be overcome, but sufficient motoring power was not available.

Close examination of the circumferential ring--cross-seal sealing grid revealed several leakage paths in the seal underside and a program was initiated to design a new seal that could be easily incorporated into the existing rotor.

The resulting seal configuration, the 'L' element seal, differed significantly from the original one in that each cylinder port now had its own autonomous sealing grid that could function independent of the events occurring in adjacent cylinders.

The new seal was installed in the engine and firing trials were resumed. Once again, the same type of sporadic firing was obtained as was the case with the original seal design. This time, the performance of the new seals was suspected immediately.

Testing of the 'L' element seal in a static test rig revealed that the metallic elements that were to seal between the primary seal and the rotor seal bed were unable to pressure-activate properly. A commercial silicone "O-ring" packing was substituted for the faulty elements and reduced seal leakage was obtained.

The modified seal design improved the seal performance to

2.3-1 The Engine on the Test Bench (Con't)

the extent that effective combustion was obtained and the engine could now run under its own power.

2.4 THE SECOND PROTOTYPE ENGINE, THE MARK II

During the testing of the first engine, it quickly became apparent that the existence of only one prototype engine severely hindered the progress of the development program.

The de-bugging of the first engine required significant changes to be made to the mechanism, each of which involved periods of "down-time" where the engine was dismantled and components were modified. The promotion of the concept by the Company also required that the engine be made available for private and public demonstrations. Because of these demands, test time was at a premium and the need for a second prototype was quite obvious if the engine development program was to continue at a meaningful rate. The need was also apparent o have a working K-Cycle Engine installed in an automobile as soon as possible, and this reinforced the requirement for a second engine.

2.4-1 Purpose of the Second Prototype

At the time of the design initiation of the second engine it was felt that the Mark I configuration was the optimum one for the K-Cycle Engine mechanism: that the initially weak performance of the Mark I could be improved upon by performance tuning and small detail design refinements.

2.4-1 Purpose of the Second Prototype (Con't)

In other words, the original concept was assumed to be fundamentally correct and the second engine would essentially be a copy of its predecessor with a few minor changes and improvements.

The second engine was not intended as a multi-variable research engine but as a fixed design "production type" engine. After a short period of development in the test stand, where it would share test and demonstration duties with the Mark I, the Mark II was to be installed in an automobile for on-the-road evaluation and demonstration purposes.

2.4-2 Performance Orientated Design Changes

Unlike the Mark I Engine, the Mark II was intended to be a carbureted spark-ignition engine from the start, with the capability of converting to continuous combustion and fuel injection at some point in the future.

To accommodate the spark ignition, the combustion chamber shape was modified to have less of a volume between the pistons as well as to promote purging of the spark plug by a fresh air/fuel charge. No attempt was made to examine and subsequently alter the basic characteristics of the combustion chamber shape.

The sealing system specified for the second engine was to be substantially different from that of the first. A "button and rail" peripheral seal was designed which would

2.4-2 Performance Orientated Design Changes

improve intake sealing as well as maintain mini-chamber combustion pressure for future continuous combustion ignition (refer to Figure 4-17 for a description).

In addition the new seal was to overcome inherent performance defects encountered in the Mark I Engine, such as: high seal friction and wear and poor intake manifold vacuum at part throttle.

A third area where the initial Mark I design was deviated from was the cam generated piston motion. Early testing of the first engine showed that the TDC dwell severely magnified the effect of the seal leakage. The inability to maintain constant pressure over the dwell greatly reduced the indicated power potential of the combustion process. At the same time, the poor combustion of the Mark I Engine raised concern over the possibility of over-expansion at the end of the expansion stroke if the initial 2.5:1 expansion ratio was maintained.

To overcome these problems, the Mark II cam motion was changed to dwell-free simple harmonic with a 2.0:1 expansion ratio.

To enable the piston to follow this motion without encountering severe cam wear, a negative cam follower roller was specified similar to that of the repaired Mark I piston.

2.4-3 Manufacturing and Assembly Orientated Design Changes

As was indicated at the beginning of this section, one of the reasons for the fabrication of a second engine was to reduce "down-time" due to demonstration and engine modifications.

2.4-3 Manufacturing and Assembly Orientated Design Changes (Con't)

The disassembly down-time of the second engine was to be shortened by the reduction of the number of components as well as the adoption of design standards that would allow fully interchangeable components.

The interchangeable components would allow the easy fabrication of spare parts and sub-systems. This was quite difficult to achieve with the first engine since many of its components were custom fitted to obtain the desired fits and clearances.

To reduce manufacturing time and cost, numerous detail changes were made. The piston design retained the off-the-shelf piston head and wrist-pin of the repaired Mark I piston. The piston cam follower bearings were changed to heavier single unit commercial track runner bearings located on a dead axle. To simplify the piston further, the bottom roller clearance adjustment mechanism was removed, and the oil retention grooves on the surface of the piston body were eliminated. Modifications were also made to the outer casing to reduce the number of casing bolts, and the cam timing adjustment and separate oil drainage sumps were eliminated.

CHAPTER 3

INTENT AND DESIGN GOALS OF THE DASH-3 ENGINE

3.1 INTRODUCTION

The K-Cycle Research and Development Program revealed that the first two prototype engines, as initially designed, were capable of limited net output and performance. The development program aimed at improving this output was handicapped by the inflexible nature of both the engines which hindered research and made it difficult to incorporate progressive design changes and improvements.

In addition it was also discovered that certain sub-systems of the Mark I and II Engines were designed to operate outside the bounds of existing available technology. To overcome this and obtain respectable engine output these subsystems required a development program of their own.

To circumvent the problems associated with the initial engines, it was decided to design a third "multi-variable research" engine--the Dash-3--with design parameters similar to those found in conventional engines.

To guide the evolution of the Dash-3 Engine, a design manual was issued which specified its intent and design goals.

3.2 EVENTS LEADING UP TO A THIRD ENGINE

3.2-1 Why Another Engine?

As the test and development programs of the Mark I and Mark II Engines unfolded, it became apparent that the eight cylinder-

3.2-1 Why Another Engine? (Con't)

peripheral seal engine configuration was not conducive to the generation of optimum power output and speed.

Evaluation of the preliminary test results showed that the low net power output was not due to one or two isolated deficiencies, but rather that the peripheral seal concept and its associated combustion chamber shape resulted in high seal frictional losses, resulting from the large seal diameter with its associated velocities and centrifugal losses, and poor combustion efficiency (with spark ignition). Both of these areas will be dealt with in detail in subsequent chapters.

In an effort to isolate and characterize these problem areas, a "piston/cam test rig" and a "peripheral seal test rig" were constructed. The rigs were designed to duplicate some of the operating conditions of these systems as well as measure the performance variables that were almost impossible to measure in the actual engines. Although the rigs were able to isolate these performance variables, difficulty was encountered in calibrating the test results obtained in the test rigs with those obtained in the actual engine. A possible explanation was that the combustion process is a key aspect in the performance of the seals and the cam-piston combination, and since this could not be simulated in the test rigs (without actually building another engine) the test rig data could never be wholly applicable.

3.2-1 Why Another Engine? (Con't)

The difficulty in isolating the poor performance characteristics of the prototype engines was further compounded by their inflexible design: component modifications were expensive and time consuming with some key areas impossible to alter. For example, seal design modifications were quite limited because a major seal design change would require a new seal bed and in the case of the first two engines, the prohibitive requirement of a new rotor. Design changes to other important areas such as the combustion chamber shape were quite impossible.

Rather than depend on the two test rigs with their contentious test data to define the direction required for a development program, it was decided to build a third prototype engine that would be designed around the problem areas already pinpointed. This engine would be of such a flexible design that its characteristics could easily be changed to provide meaningful test data and it could keep pace with research developments with the assistance of component and sub-system interchangeability.

3.3 INTENT AND GOALS OF THE THIRD ENGINE

3.3-1 The Design Manual

To ensure that the third engine would satisfy the requirements of the projected engine development program, a design manual was issued. In this design manual, the goals and

3.3-1 The Design Manual (Con't)

intent of the third engine, now designated as the Dash-3 Engine, were detailed along with the process that the evolution of the third engine concept would take. To expedite the completion of the Dash-3 design the concept goals were frozen when the design manual was issued: this would ensure that they would not be deviated from during the design process.

3.3-2 The Design Manual Goals

One of the first goals specified within the design manual was that the design parameters of the third engine stay within the bounds of conventional technology.

Conventional technology was defined as that commonly used in conventional engine design, or performance parameters that were known to be a success in the first two K-Cycle Engines. One particular example of this is that the troublesome peripheral seals were designed to operate at pressures and velocities not commonly found in similar conventional applications. It was hoped that this philosophy would enable the third engine to circumvent areas that would require their own development program before they could be successful.

The second goal stated was that the Dash-3 Engine take advantage of, and not exceed, conventional seal technology. As will be discussed in Section 4.1-3, the peripheral seals of the first two engines were designed to operate at higher

3.3-2 The Design Manual Goals (Con't)

than conventional surface velocities which imposed severe limits on engine performance until the appropriate technology is developed. To avoid this the seals of the third engine were to operate at velocities no greater than those encountered by the most successful of engine gas seals: piston rings.

The third major design goal was that the Dash-3 Engine attempt to attain peak combustion pressures and indicated horsepower magnitudes comparable to those of a conventional spark ignition engine. To do this, it was specified that its combustion chamber shape approach that of a successful conventional spark ignition engine and that the Dash-3 Engine start out with a 8:1 compression ratio. With future engine development in mind it was also specified that the third engine must be designed to easily convert from spark ignition to continuous combustion, through component interchange.

The fourth goal was that the Dash-3 Engine attempt to approach the mechanical efficiency of a conventional crankshaft engine. It was intended that the primary means of reducing frictional losses be via massive piston weight reduction with secondary gains obtained through refinement of the slider mechanism. To reinforce this goal a maximum piston weight of 1.0 to 1.2 pounds was specified. This arbitrarily set maximum was a reaffirmation of the original design goal for the Mark I piston (Section 2.2-6) and was designed to prevent overweight pistons as currently found in the first two prototype engines.

3.3-2 The Design Manual Goals (Con't)

The fifth goal outlined in the design manual was that the engine have easily interchanged components to attain variable engine characteristics. In other words, rather than being designed as a "pre-production prototype" as its predecessors were, the Dash-3 Engine was to be designed as a "multi-variable" research engine. The true worth of the Dash-3 would not be in what it could do once it was built, but in how easily it could continue to accommodate the changes required and specified by the K-Cycle research program.

Several areas were pinpointed to have the design flexibility via component interchangeability:

* The rotating combustion chamber shape
* The seals and their associated seal bed and running surface.
* The portion of the cylinder bore not used by the piston rings so as to allow the use of different piston bodies and cam followers.
* The cams
* The stationary combustion chamber shape

The sixth goal was that although the Dash-3 was to be primarily designed as a research engine, it should be able to take the place of the Mark II Engine in the auto installation if required.

In addition to the previous goals, the design manual required

3.3-2 The Design Manual Goals

that component function and weight would have priority over manufacturing short cuts and that the engines ancillary systems and accessories be conventional in all respects.

CHAPTER 4

THE OPTIMIZATION OF THE DASH-3 ENGINE CONFIGURATION

4.1 RE-EVALUATION OF THE GAS SEALING REQUIREMENTS

The initiation of a redesign of the basic K-Cycle Engine was prompted by the realization that several aspects of the initial concept would have to be optimized and improved, so as to obtain a more respectable engine output.

One of the deficient areas that was highlighted by the testing of the first two prototype engines was seals. The peripheral sealing system was found to have a number of inherent characteristics that were outside the bounds of conventional technology.

4.1-1 Comparing the Peripheral Seals to Conventional Seals

The large diameter at which the peripheral seals were required to operate results in unusually high seal surface velocities. Table 4-1 compares the seal velocities of the first K-Cycle prototypes to the surface velocities in engine sealing situations. The average maximum piston ring surface velocity of approximately 65 ft/sec. for the conventional engines listed while the apex seal in the Wankel rotary engine peaks with a maximum velocity of approximately 100 ft/sec. When comparing the K-Cycle peripheral seal velocities to those of the highly reliable piston ring, it is obvious that above 1500 RPM, the K-Cycle seal surface

TABLE 4-1

Engine Type	RPM	Maximum Seal Velocity Ft/sec	Reference
Honda C-92	5000	66.8	6
Chrysler 318 V8	5000	63.5	6
Mercedes Benz 220	5000	62.3	6
Austin Maxi 1.75 l	5500	90.5	7
Audi 80 GT 1.6 l	6000	82.5	7
Fiat 131 1.3 l	5400	66.3	7
Volvo 264 2.6 l	6000	75.2	7
Alfasud 1.2 l	6000	60.8	7
Curtis-Wright Rotary RC2-60 Apex Seals	5000	42.5-108	6
NSU Wankel KK M 250	5000	29.2- 67.0	8
K-Cycle KC75 MKI	1000	51.5	
	2000	102.9	
	3000	154.4	

4.1-1 Comparing the Peripheral Seals to Conventional Seals (Con't)

velocities start to exceed those found in most piston engines; and above 2000 RPM velocities greater than those of the newly developed apex seal in the Wankel rotary engine are encountered.

As is the case with the Wankel engine apex seal, the K-Cycle peripheral seals are subject to centrifugal force. Unlike the Wankel sealing system, where the side seals escape the influence of centrifugal force, the entire K-Cycle peripheral sealing grip must cope with this effect. Even with low friction coefficients and a light weight peripheral seal,the friction losses due to centrifugal force, even with a non-pressure activated, non spring loaded seals are unacceptably high.

The presence of the centrifugal component will also make it difficult to design the peripheral seal for minimum pressure activation throughout the entire engine RPM range: the spring force remaining constant throughout the speed range while the centrifugal force varies as the square of the engine RPM.

The large seal diameter also results in a large seal friction torque and hence a significant seal friction horsepower loss throughout the entire RPM range.

4.1-2 Peripheral Seal Disadvantages

In addition to minimizing friction losses, a successful seal must seal its cylinder's gases with a minimum of leakage.

4.1-2 Peripheral Seal Disadvantages (Con't)

The leakage of any seal design is a function of two basic characteristics: the number of designed gaps per seal, and the total sealing surface grid length per volume sealed. The number of leakage holes or gaps is governed by the type of seal design used and is independent of variables such as seal diameter. The grid length design variable is directly proportional to seal diameter. As no metallic contact provides a perfect seal it is highly desirable to keep the grid length per volume sealed to a minimum.

It is assumed that any seal will operate at a higher temperature than that of its seal bed, and its design will therefore have to allow for the differential thermal expansion between the seal and its bed. With a peripheral seal, the required thermal expansion clearance will increase with seal diameter and this increased clearance means a gap whose difficulty in sealing increases with size. This differential thermal expansion problem is aggravated even further by the use of dissimilar metals for the seals and rotor and inadequate seal cooling.

Regardless of the number of cylinders that any K-Cycle Engine has, an increased seal diameter (with respect to the cylinder diameter) also results in an increase in cylinder head space. To maintain reasonable compression ratios, this head space can be limited by reducing the width of the cylinder port: such an action has the associated

4.1-2 Peripheral Seal Disadvantages (Con't)

disadvantage of hindering volumetric efficiency because of small port cross-sectional flow areas. Reducing the port width also results in an increased surface to volume ratio for the combustion chamber; another disadvantage.

It can be shown that combustion chamber performance deteriorates with increased flame front travel distance for a spark ignition engine[9]. The peripheral seal design results in relatively long flame travel distances.

In summary, the disadvantages of large diameter peripheral seals are: high seal velocities and resultant friction losses, difficulty in optimizing seal pressure activation for all conditions, increased seal leakage, differential thermal expansion clearances that are difficult to seal, reduced volumetric efficiency, and a less than optimum combustion chamber shape with a poor surface to volume ratio. It should also be noted that the high surface velocity of the peripheral seal can make the maintenance of an oil film on the running surface quite difficult.

4.1-3 A Low Velocity Face Seal Design

As indicated in Section 2.4-2, the peripheral type of sealing system was specified for the first prototype engine primarily to suit the continuous combustion ignition with continuous fuel injection. In light of the sealing problems experienced with the peripheral seal design, and the conversion to carbureted spark ignition, the advantages of such a system

4.1-3 A Low Velocity Face Seal Design (Con't)

are outweighed by its design problems.

One of the goals of the third engine was to design the sealing system within the bounds of conventional technology--specifically piston ring technology. With piston ring velocities such as those illustrated in Table 4-1, the design goal for the third engine was that it have a maximum seal surface velocity of 60 ft/sec. at maximum engine speed (3000 RPM).

At first glance, it becomes very obvious that only a face seal engine could meet this goal, and that such an engine would have to be different from the eight cylinder 8 inch PCD version which was the basis of the first prototype engine. Graph 4-2 illustrates the various engine configurations that are able to meet the seal design goal and the first prototype engine is not among them.

4.2 AVAILABLE CAM MOTIONS

One of the significant advantages that the K-Cycle Engine configuration has over the conventional crankshaft engine is that unlike the latter, where the piston motion is confined to that provided by the cranking motion, the barrel cam controlling the K-Cycle piston can generate a great number of different motions.

ENGINE CONFIGURATIONS THAT CAN INCORPORATE A FACE DEAL WITH A SURFACE VELOCITY OF 60 FT/SEC. AT 3000 RPM

Minimum Cylinder Port Opening = 45°

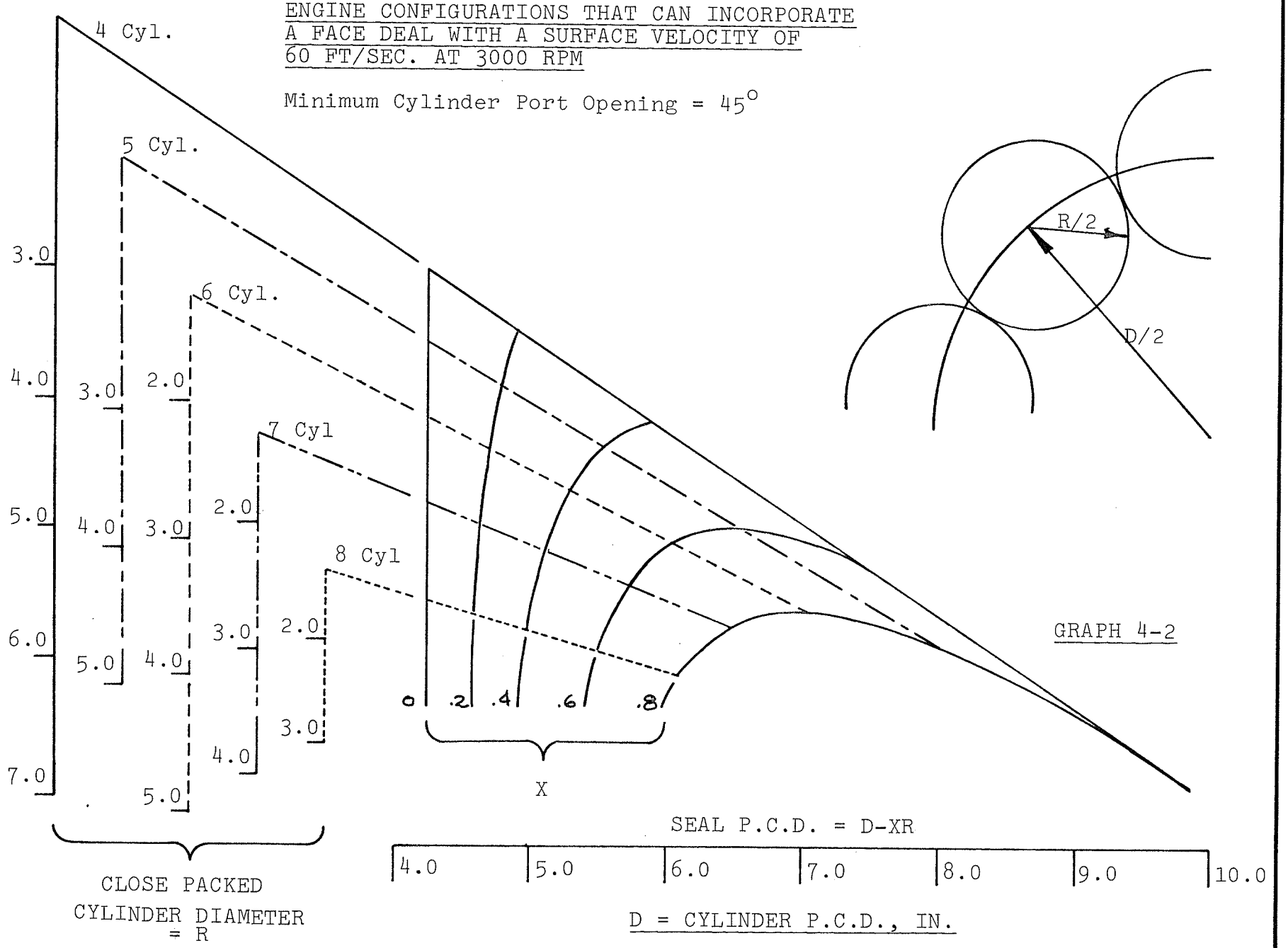

GRAPH 4-2

4.2-1 Comparison of Cam Motions

Graph 4-3 illustrates some of the more conventional cam profiles available. The first four motions: the parabolic, cubic no. 1, cubic no. 2, and the 2 - 3 polynomial are not considered as serious candidates because of their infinite jerk and included for informational purposes only.

At first glance, the "combination modified trapezoidal acceleration" motion seems to be the most likely of the remaining motions because of its low acceleration magnitudes and finite jerk. Although the "simple harmonic" motion has an equally impressive acceleration magnitude, it suffers from infinite jerk at the beginning and end of each stroke when preceded and followed by a dwell since maximum acceleration occurs at the start of the curve. Because the K-Cycle cam will encounter unusually high follower velocities finite jerk is most advisable.

The acceleration magnitudes in Graph 4-3 should be viewed with caution for accelerations encountered in practice can differ significantly from those predicted by theory with a dwell at the beginning or end of the curve. In a comparison[10] of parabolic (P), simple harmonic (H), and cycloidal (C) motions, the ratio of the theoretical maximum accelerations P:H:C is 1.0:1.23:1.57. Reference found that in an undamped system the ratio of actual measured accelerations was P:H:C = 1.0:.834:.584.

FIGURE 4-3: COMPARISON OF CAM MOTIONS

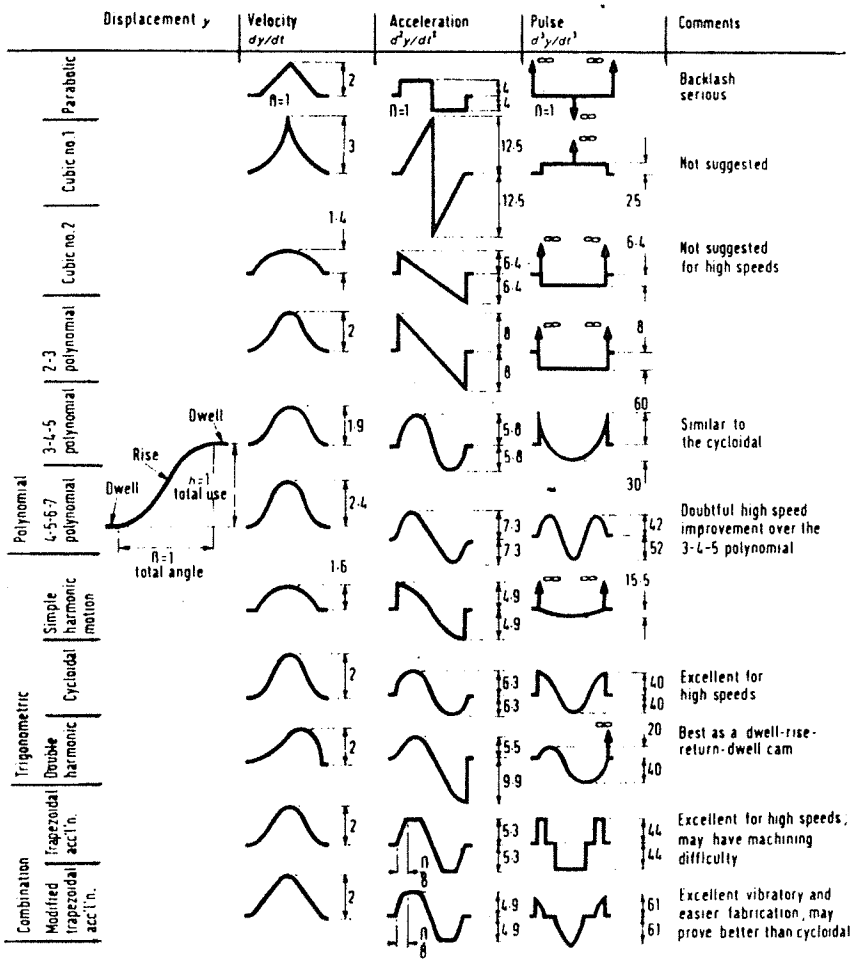

4.2-1 Comparison of Cam Motions (Con't)

With damping this discrepancy is not as great, but its existence is a caution that a cam motion should not be picked solely because of its low acceleration magnitudes. The comparison of actual and theoretical accelerations indicates the importance of damping or conversely that of finite jerk when a dwell is involved.

Unlike the conventional radial cam, such as that used in automotive cam shafts, the K-Cycle drum cam does not have to have its motion preceded and followed by a dwell.

Without a starting dwell, the acceleration peak at the beginning of the simple harmonic motion can be set equal to the acceleration peak of the preceeding curve eliminating the infinite jerk. Each stroke on the K-Cycle drum cam is always preceeded by another stroke and not necessarily by a dwell. Therefore, on a drum cam with all strokes generating simple harmonic motion and without any inter-stroke dwells the simple harmonic motion's infinite jerk is eliminated. The resulting motion has both the lowest acceleration and jerk peak magnitudes of those presented in Graph 4-3.

The inclusion of a dwell anywhere in the K-Cycle cam motion would require either the trapezoidal acceleration or cycloidal motion which exhibit a combination of low acceleration and jerk magnitudes in both theory and real life.

4.2-1 Comparison of Cam Motions (Con't)

Experience with the MK I cycloidal/dwell motion has shown that with the significant leakage of the present K-Cycle seals, a TDC dwell greatly magnifies the effect of seal leakage.

At the same time, since the positive and negative effects of a TDC dwell on combustion efficiency have yet to be documented, a TDC dwell was not seriously considered for the Dash-3 engine; at least for the initial design iteration.

With only textbook comparisons available, and without the benefit of experimental data on the influence of various types of cam motions on the K-Cycle piston cam follower, we shall continue to define the engine optimization based on simple harmonic cam motion.

4.3 CONFIGURATION OPTIMIZATION

Arriving at an optimum configuration for the K-Cycle barrel/cam engine is a great deal different than the optimization process required for a conventional engine. Once the required displacement is determined for the conventional crankshaft engine, the number and layout of the cylinders is usually derived from the minimum number of cylinders that can achieve dynamic balance and make optimum use of the space available. Configuration optimization of conventional multi-cylinder crankshaft engines is confined to in-line, vee or horizontal opposed arrangements.

4.3 CONFIGURATION OPTIMIZATION (Con't)

The K-Cycle Engine on the other hand is totally confined to the axially opposed piston drum cam configuration. This configuration, which has complete dynamic balance, is controlled in size by the following primary variables: intake displacement, expansion ratio, bore/stroke ratio, cylinder or cam pitch circle diameter and the number of cylinders. By varying these variables, an almost overwhelming combination of engine types are possible for a given intake displacement. Configuration optimization is obtained via secondary variables, such as type of cam motion, stroke angular duration, piston weight and friction, as well as gas seal requirements and combustion restraints. After these have been taken into account only a few optimum configurations will be possible for a given intake displacement.

In the following sections these variables will be examined and the general method for finding the optimum geometric engine configuration will be developed. At the conclusion the optimum Dash-3 engine, defined by the general parameters of Chapter 3, will be specified.

4.3-1 Optimum Total Cylinder Area

A preliminary attempt at optimizing the displacement/engine volume would involve the examination of the amount of available cylinder area per cross-section of engine. Figure 4-4 illustrates the cross sections that are available in going from a two cylinder engine to eight cylinder configuration. Note that only close-packed arrangements are

THE UNIVERSITY OF MANITOBA LIBRARIES

2 Cyl.

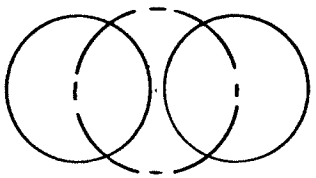

3 Cyl.

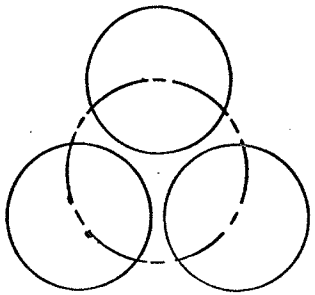

4 Cyl.

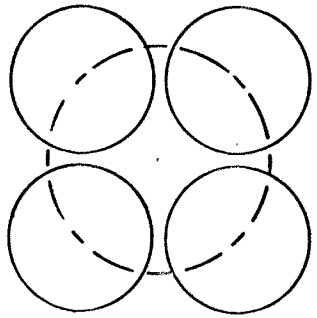

5 Cyl.

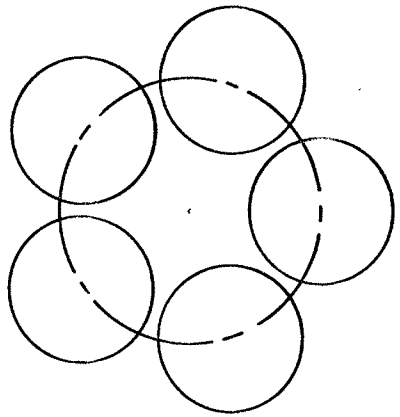

6 Cyl.

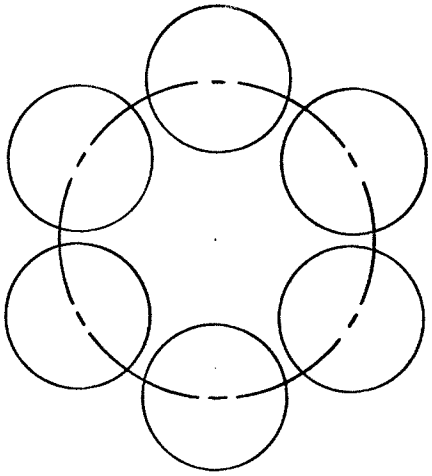

7 Cyl.

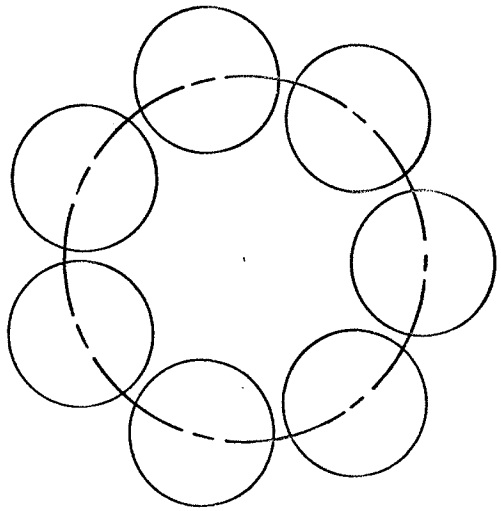

8 Cyl.

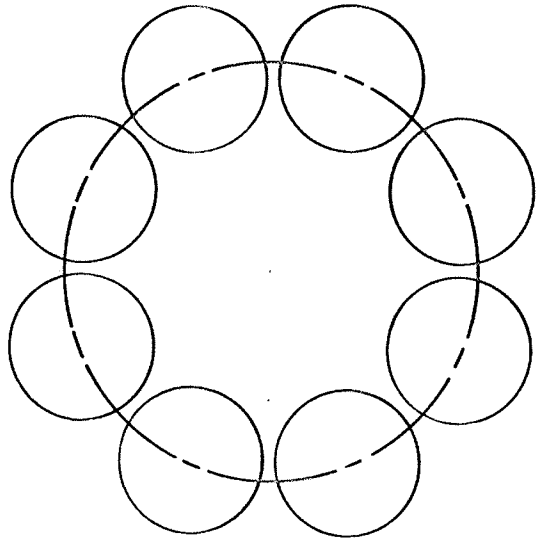

Figure 4-4

POSSIBLE ARRANGEMENTS OF CLOSE-PACKED CYLINDERS

GRAPH 4-5

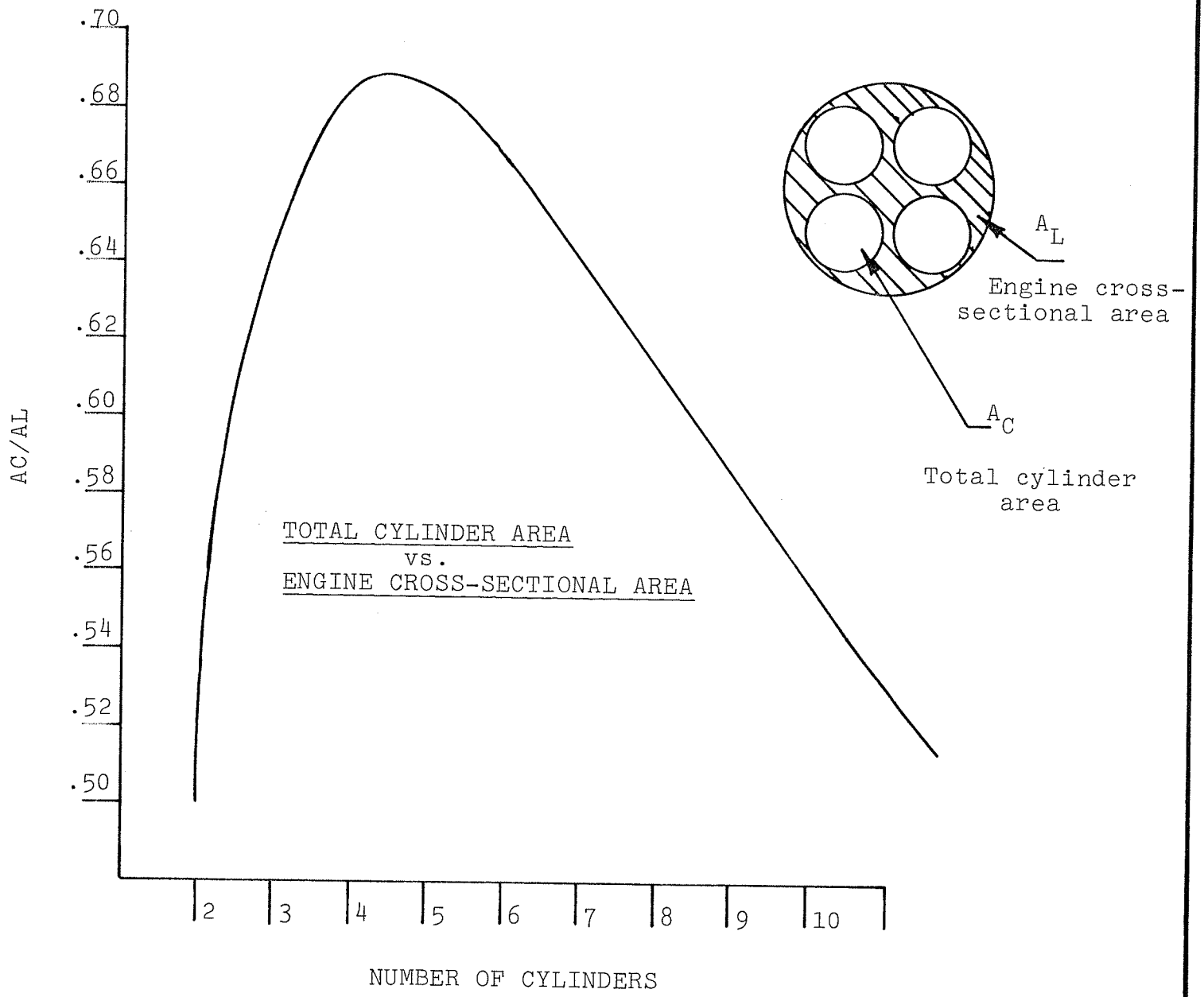

N	AC/AL
2	.500
3	.646
4	.686
5	.685
6	.667
7	.641
8	.613
9	.585
10	.557
11	.531

4.3-1 Optimum Total Cylinder Area (Con't)

considered as this is the most efficient way to use any number of cylinders.

It quickly becomes obvious that the 8-cylinder engine, such as that used for the MK I and MK II engines make inefficient use of the available engine cross sectional area because of the large amount of wasted space at the centre of the engine. Graph 4-5 compares the ratio of cylinder area to engine cross-sectional area for various numbers of cylinders and concludes that a four or five cylinder engine makes optimum use of the available area. In spite of this, the configuration cannot solely be examined as a two-dimensional entity: stroke length, cylinder PCD, etc. also have to be considered.

4.3-2 The Optimum Cam Motion

It was concluded in the comparison of available types of cam motions (Section 4.2-1), that a dwell-free simple harmonic cam will generate a piston motion with the lowest possible piston/cam follower/cam inertia loading.

The actual cam profile that is used is a function not only of the type of motion but of the angular duration of the stroke lengths as well as the expansion ratio required.

To equalize the peak accelerations of an adjacent short stroke and long stroke, the following relation must be followed:

4.3-2 The Optimum Cam Motion (Con't)

$$E_R = \frac{\beta^2}{\alpha^2} \quad \text{(Equation 4-1)}$$

WHERE,

E_R = The expansion ratio or the ratio of the long stroke to the short stroke.

β = Angular duration of the long stroke, rad.

α = Angular duration of the short stroke, rad.

Because the K-Cycle motion requires the 4 strokes of each cycle to be completed in one revolution, we have:

$$\pi - \alpha - B = 0 \quad \text{(Equation 4-2)}$$

Or combining Equation 4-1 and 4-2,

$$E_R = \frac{\beta^2}{(\pi - \beta)^2} \quad \text{(Equation 4-3)}$$

The relationship is illustrated graphically in Graph 4-6.

The third variable, the expansion ratio, is governed primarily by the extent that one wishes to apply the K-Cycle expansion principle. Ideally it would be desirable to expand the combustion gases to just above atmosphere but not to the point that the gases reach a sub-atmospheric pressure prior to being exhausted.

Graph 4-7 illustrates the relationship between exhaust pressure and expansion ratio. This was derived from a combustion chart analysis of an 8:1 compression ratio spark-

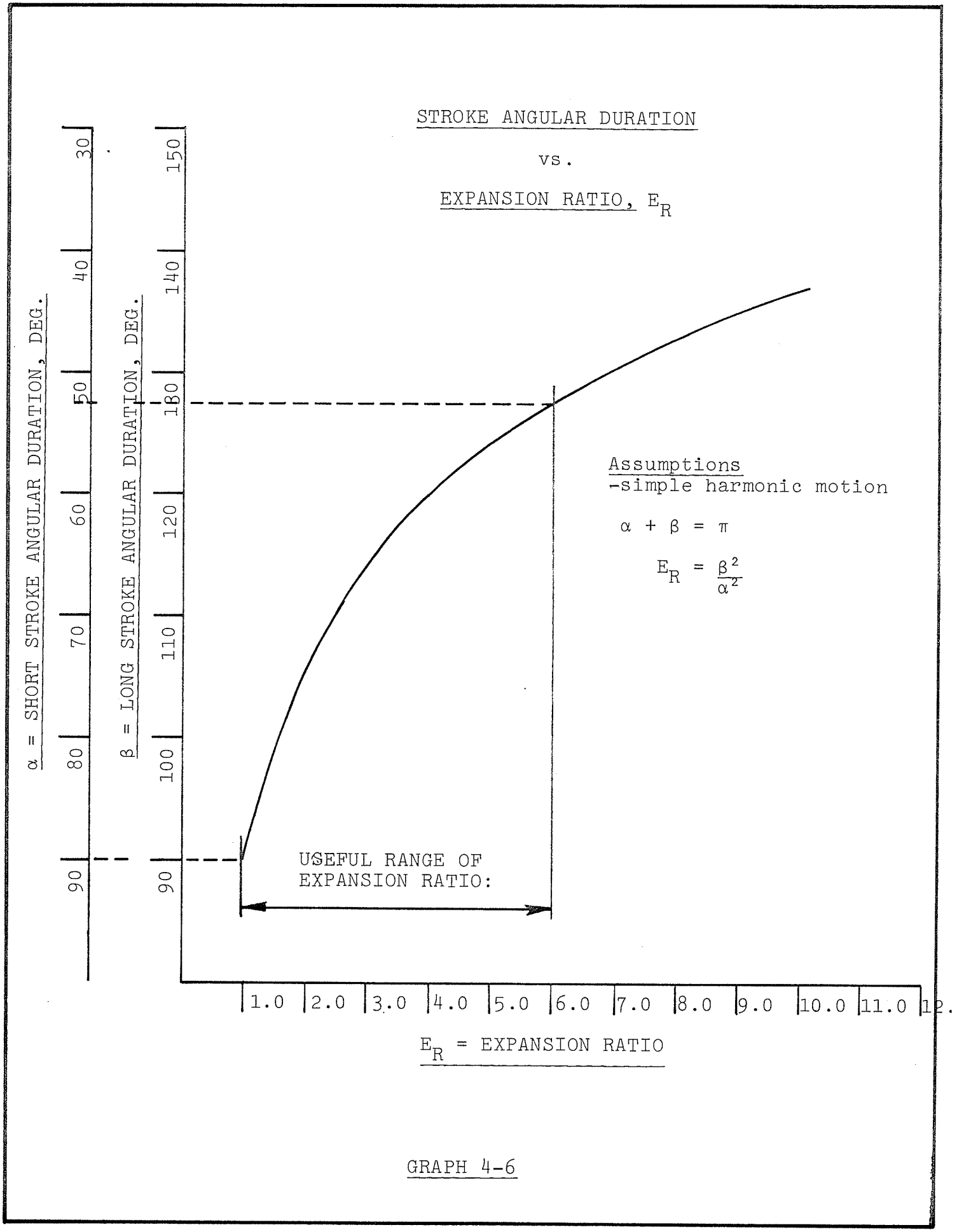
STROKE ANGULAR DURATION
vs.
EXPANSION RATIO, E_R
α = SHORT STROKE ANGULAR DURATION, DEG.
β = LONG STROKE ANGULAR DURATION, DEG.
30
40
50
60
70
80
90
150
140
180
120
110
100
90
Assumptions
-simple harmonic motion
$\alpha + \beta = \pi$
$E_R = \frac{\beta^2}{\alpha^2}$
USEFUL RANGE OF EXPANSION RATIO:
1.0
2.0
3.0
4.0
5.0
6.0
7.0
8.0
9.0
10.0
11.0
12.
E_R = EXPANSION RATIO

GRAPH 4-6

PRESSURE AT THE END OF THE EXPANSION STROKE

vs. E_R = EXPANSION RATIO

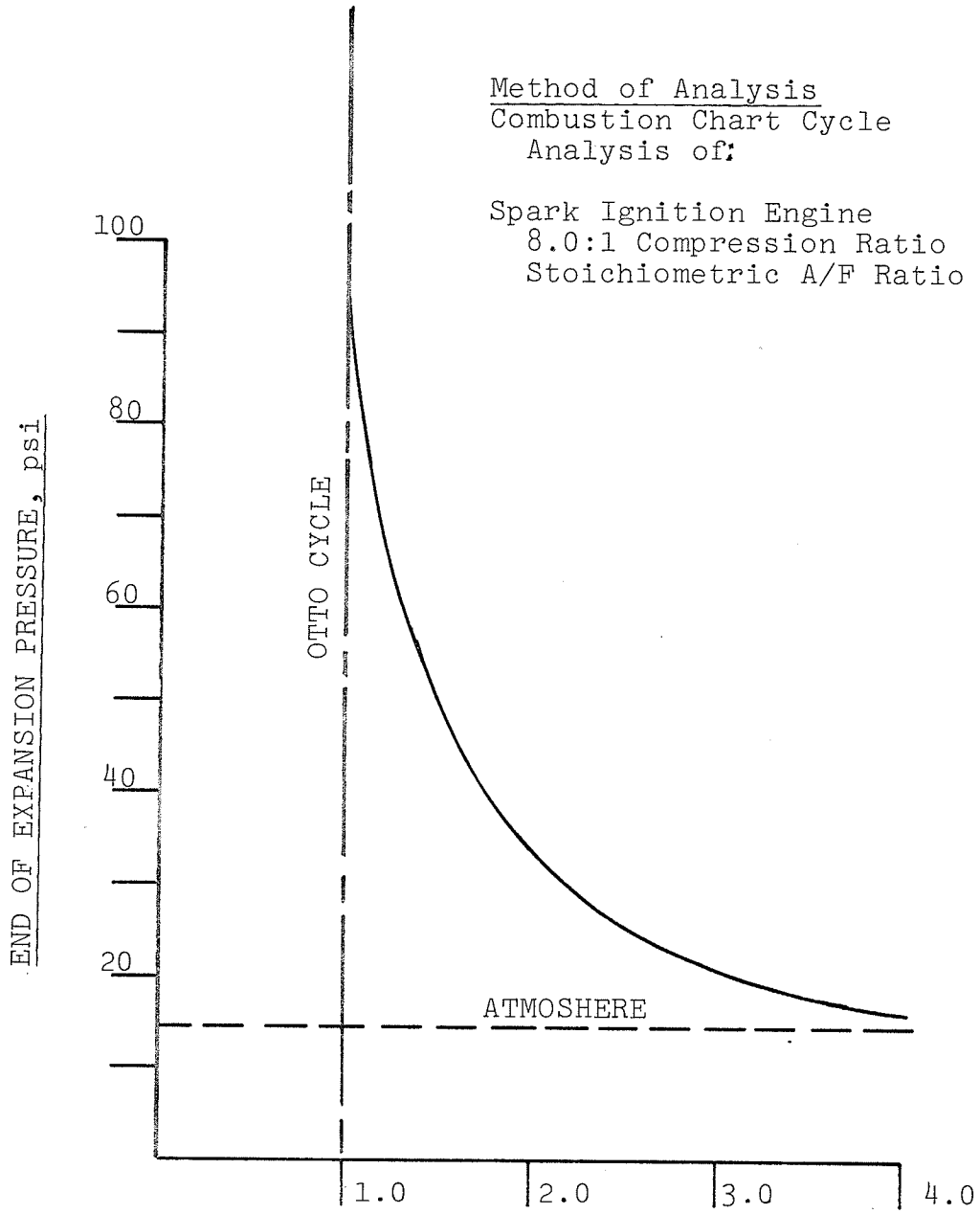

GRAPH 4-7

4.3-2 The Optimum Cam Motion (Con't)

ignition engine burning a stoichiometric mixture at wide open throttle. This analysis shows that such an engine can have expansion ratios as great at 4:1 and still have an exhaust pressure several psi above atmosphere. This is not the case in an actual engine where heat losses, volumetric efficiencies and throttling all contribute to a reduction in exhaust pressure. In an attempt to determine the expansion ratios at which the combustion gas pressure would go subatmospheric in an actual engine, the K-Cycle combustion model computer simulation was used to generate the series pressure-volume curves shown in Graph 4-8. This simulation was calibrated to the actual performance characteristics observed in the MK I K-Cycle Engine.

The curves in Graph 4-8 which have a 2:1 expansion ratio, are identical except for their reaction rates. A reduction in reaction rate has the effect of reducing cylinder pressures similar to that of throttling. To analyze the effect of longer expansion ratio each of these simulations was extrapolated and allowed to expand down to atmosphere. The resulting point of overexpansion is documented as a function of reaction rate and peak cylinder pressure in Graph 4-9.

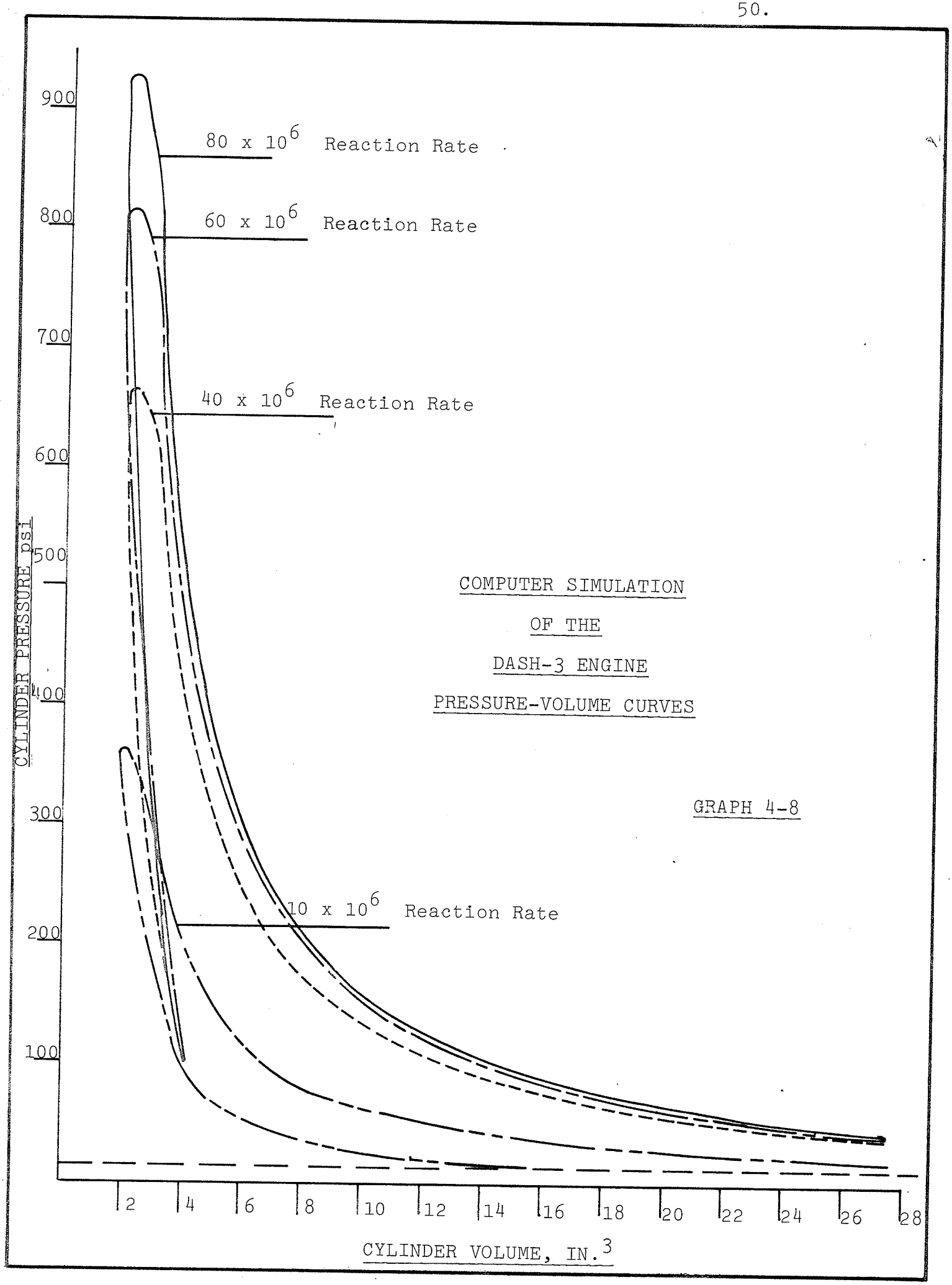

COMPUTER SIMULATION

OF THE

DASH-3 ENGINE

PRESSURE-VOLUME CURVES

GRAPH 4-8

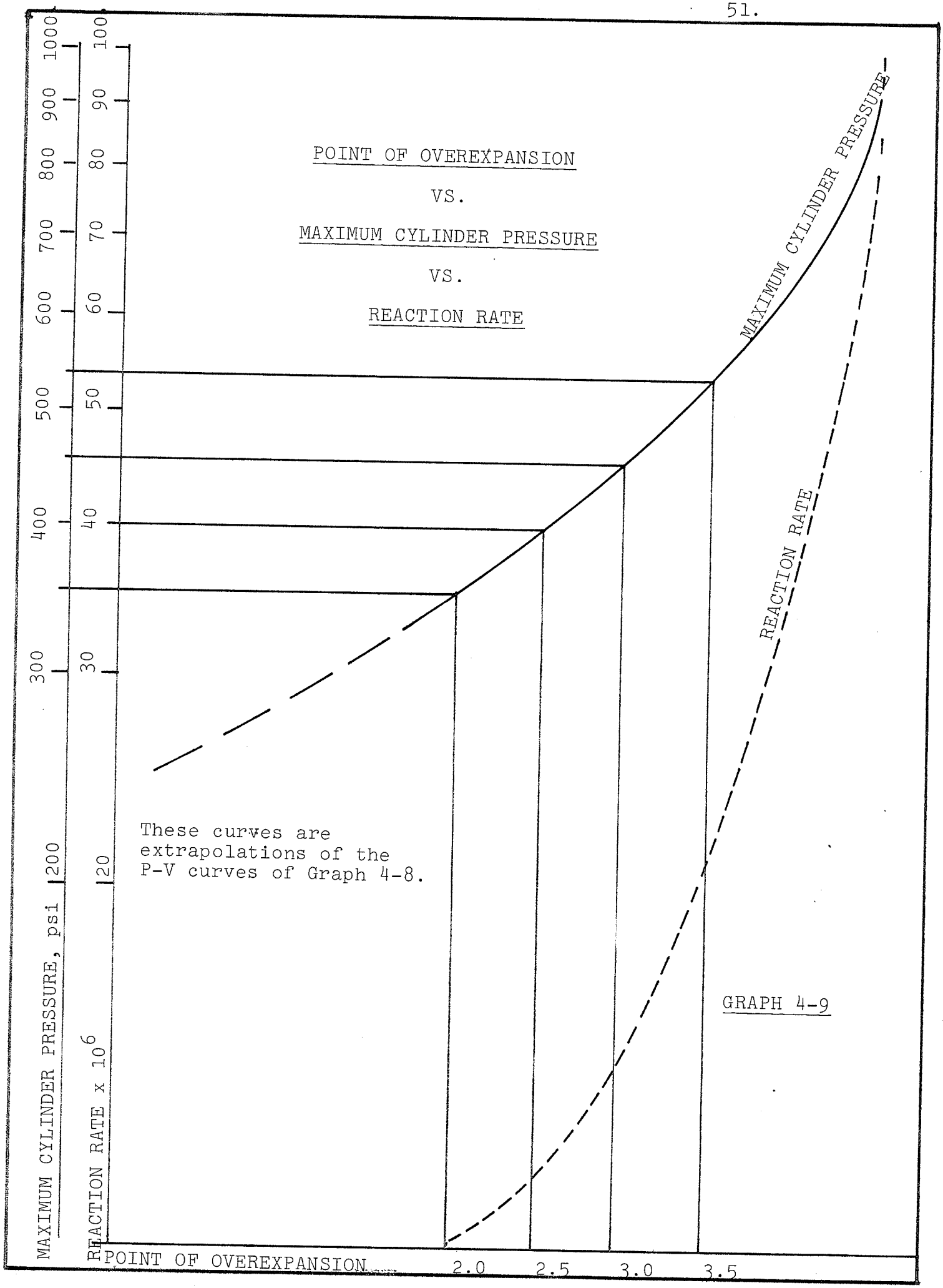
POINT OF OVEREXPANSION
VS.
MAXIMUM CYLINDER PRESSURE
VS.
REACTION RATE
MAXIMUM CYLINDER PRESSURE
REACTION RATE
These curves are extrapolations of the P-V curves of Graph 4-8.
MAXIMUM CYLINDER PRESSURE, psi
REACTION RATE x 10^6
POINT OF OVEREXPANSION
100
90
80
70
60
50
40
30
20
1000
900
800
700
600
500
400
300
200
2.0
2.5
3.0
3.5

GRAPH 4-9

4.3-2 The Optimum Cam Motion (Con't)

Experience acquired during the testing of the Mark I and Mark II Engines has shown that the peak cylinder pressures obtained during the early stages of development were in the 350 - 400 psi range. Comparative testing of the Ford Fairmont 4 cylinder engine[13] indicated a maximum cylinder pressure for that engine under full load conditions of 600 psi.

It seems quite likely that the Dash-3 Engine's combustion and sealing efficiency will not exceed that of the Ford Fairmont Engine. Therefore cylinder pressures in excess of 650 psi[14] seem unlikely at full load and wide open throttle.

Therefore, in light of the expected initial performance capabilities as well as part throttle performance, expansion ratios in the 2.0:1 to 2.5:1 range seem to be the most suitable with the 2.0:1 ratio being the more conservative choice. If overexpansion is encountered at the end of the expansion stroke one possible method of avoiding the pumping losses associated with this is to add a one way valve to add atmospheric air.

As a result, a 2.0:1 expansion ratio was specified for the third engine, this ratio offering the best balance between avoiding overexpansion and adequately demonstrating the increased cycle efficiency of the K-Cycle thermodynamic principle.

4.3-2 The Optimum Cam Motion (Con't)

Now that the cam motion has had the following parameters defined:

* Simple harmonic motion with no dwells and equal maximum accelerations.
* An expansion ratio of approximately 2.0:1

A third variable--the maximum pressure angle--must be considered: With this variable defined, the physical dimensions of the cam, such as stroke length and cam pitch circle diameter can be defined.

For any number of cylinders and cylinder PCD, a larger pressure angle will allow a longer stroke length, a greater engine displacement and an increased stroke to bore ratio for a given expansion ratio. On the other hand, a smaller pressure angle will reduce the side loading of the piston against the side of the cylinder wall and is, therefore, more desirable from a piston friction point of view. Unfortunately, at this point in time, no test experience has been aquired on the effect of various cam pressure angles on piston side loading and subsequent friction.

References[15] indicate that maximum pressure angles of 30^{o} to 35^{o} are the largest that one can normally use with conventional cams without encountering difficulties and until more experience is obtained a maximum pressure angle of 30^{o} was specified for the Dash-3 engine as a conservative limit. Future research will provide a more analytical method of defining cam pressure angle constraints.

4.3-2 The Optimum Cam Motion(Con't)

The relationship between maximum pressure angle, expansion ratio, cam pitch circle diameter, and stroke length is illustrated in Graph 4-10. A 2.0:1 expansion ratio and a maximum pressure angle of 30^{o} results in a cam pitch circle diameter to long stroke length ratio which we shall designate as "R", of approximately 2.9:1.

Now that the parameters of the cam motion have been optimized a relationship between the number of cylinders and cam pitch circle diameter can be evolved. The mathematical expression for this geometrical relationship is:

$$\text{DISPLACEMENT} = \frac{\pi\, d^3\, Q}{2\, \kappa\, \text{SIN}\left(\frac{360}{2Q}\right) R\, E_R} \qquad \text{(Equation 4-4)}$$

WHERE:

DISPLACEMENT = Engine Intake Displacement, in^3

Q = No. of cylinders

k = Ratio of bore diameter to minimum diameter allowed by the close packing of the cylinders. k is less than 1.0 and allows for cylinder sleeve and water jackets.

D = Cam pitch circle diameter, in.

R = Ratio of D to the long stroke length obtained from Graph 4-6.

E_R = Expansion ratio

d = Cylinder bore diameter, in.

Equation 4-4 is graphically illustrated in Graph 4-11. It is interesting to note the effect of optimizing the packaging of the cylinder cross-sectional area as shown in Graph 4-5.

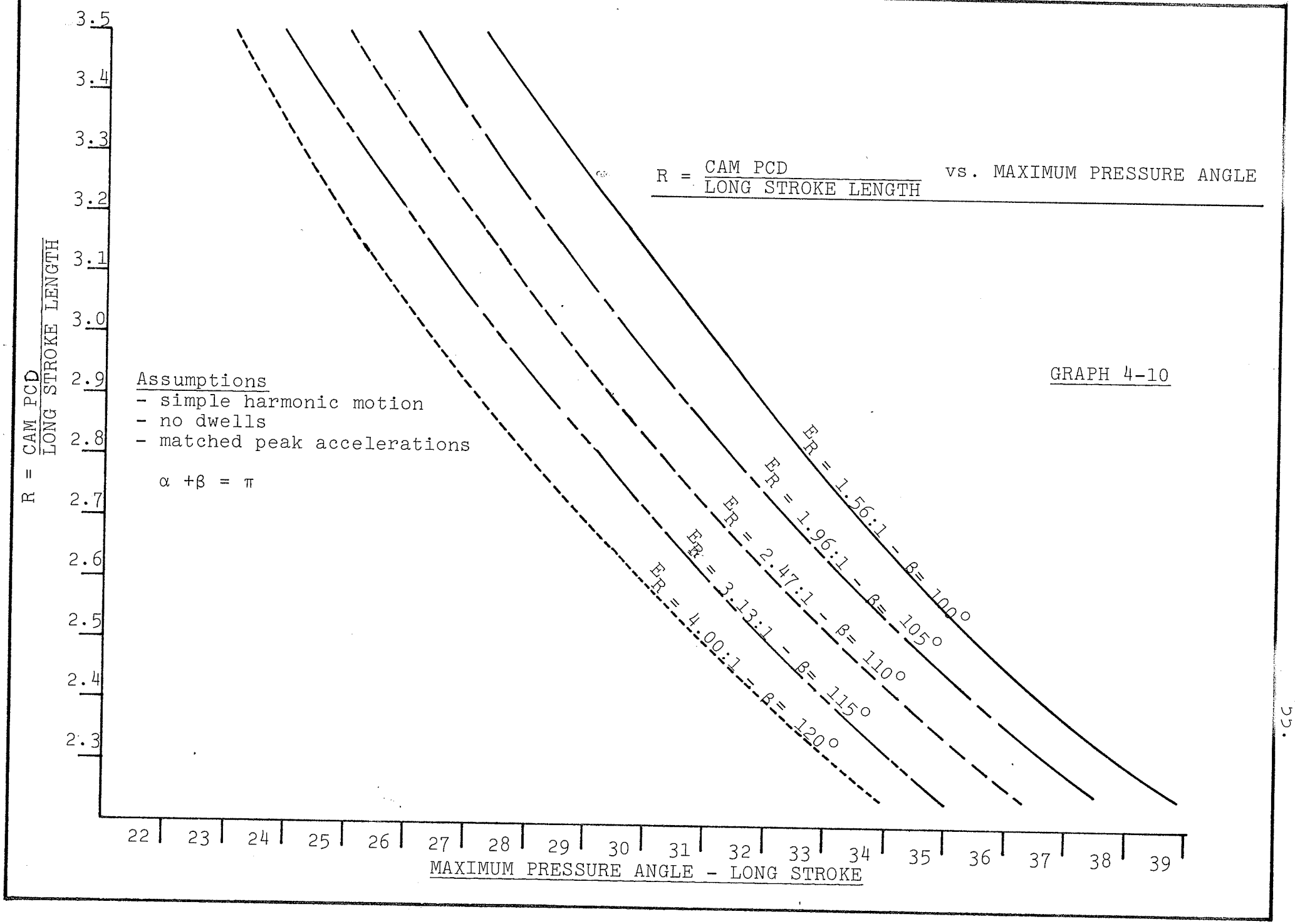
R = CAM PCD / LONG STROKE LENGTH vs. MAXIMUM PRESSURE ANGLE
GRAPH 4-10
Assumptions
- simple harmonic motion
- no dwells
- matched peak accelerations
α +β = π
ER = 1.56:1 - β= 100°
ER = 1.96:1 - β= 105°
ER = 2.47:1 - β= 110°
ER = 3.13:1 - β= 115°
ER = 4.00:1 - β= 120°
R = CAM PCD / LONG STROKE LENGTH
3.5
3.4
3.3
3.2
3.1
3.0
2.9
2.8
2.7
2.6
2.5
2.4
2.3
22 23 24 25 26 27 28 29 30 31 32 33 34 35 36 37 38 39
MAXIMUM PRESSURE ANGLE - LONG STROKE

ENGINE INTAKE DISPLACEMENT vs. CAM P.C.D.

Assumptions
- simple harmonic motion-no dwell
- matched peak accelerations
- $\alpha + \beta = \pi$
  $K = 0.85$
  $E_R = 2.0:1$
- maximum pressure angle = 30°

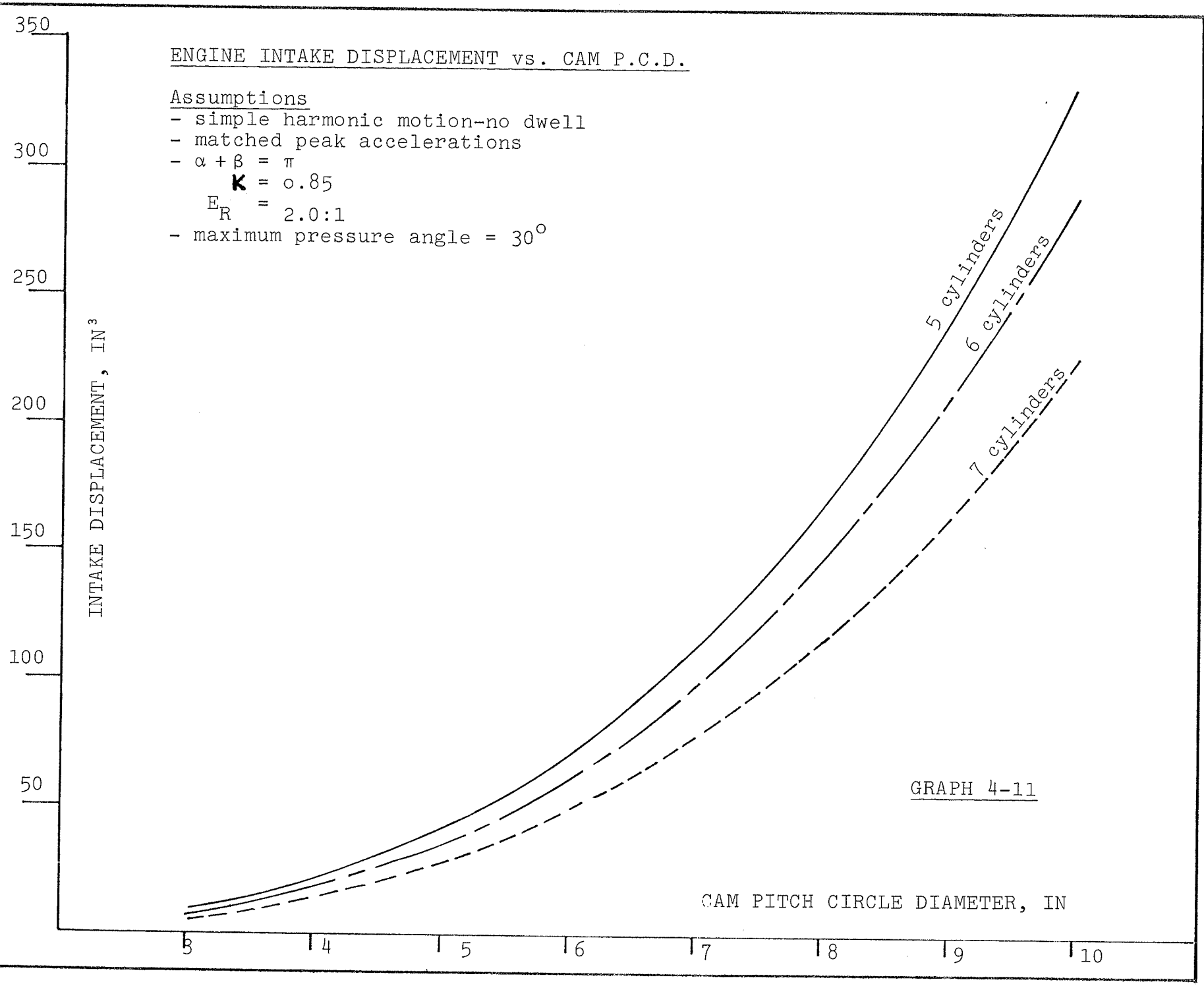

GRAPH 4-11

4.3-2 The Optimum Cam Motion (Con't)

It can be clearly seen that for any given cam pitch circle diameter, and the engine design constraints evolved to this point, that a 5 cylinder engine allows for a 47% greater intake displacement and a 6 cylinder a 28% greater intake displacement than an 8 cylinder engine with the same cylinder pitch circle diameter.

4.3-3 Piston Friction and Piston Size

The previous section showed that within the design constraints considered there exists an optimum number of cylinders for a given size of engine in so far as intake displacement is concerned. It is not enough to optimize the engine package with respect to its energy input capacity; the associated losses inherent in such a configuration must also be considered.

Our optimization has, to this point, considered the packaging of the engine as a function of the number of cylinders, the piston diameter, and, therefore, piston area and resulting intake displacement within the confines of allowed piston motion.

The primary losses that are a function of the same variables should be considered in the engine configuration optimization. These are the losses arising from the piston itself. These friction losses can be categorized as: losses resulting from the centrifugal loading of each piston against its cylinder wall, side thrust reactions between the piston and

4.3-3 Piston Friction and Piston Size (Con't)

its cylinder wall dependent on the cam pressure angle, and losses due to the sliding action of the cam follower against the cam running surface.

If these frictional losses are analyzed in the classical sense where the friction force is a function of the normal force and the friction coefficient, and not as a function of the loaded surface area, they are all then directly proportional to the weight of the piston.

For example, the total power loss resulting from the centrifugal action can be expressed as:

HP_{CF} = Centrifugal Loading Power Loss, HP

$$HP_{CF} = (C_F)\ \mu\ (DIST)\ \frac{N}{33000}\ T \quad \text{(Equation 4-6)}$$

WHERE,

C_F = Centrifugal force per piston, lbf.

μ = Coefficient of friction

DIST = Distance of each piston slides each revolution, ft.

N = Engine rev/min.

T = Number of pistons

$$C_F = \frac{M}{32.2}\ \frac{D}{(2)(12)}\ N^2\ \frac{4\pi^2}{(60)^2} \quad \text{per piston}$$

WHERE,

M = Weight of each piston, lbf.

D = Cam, PCD, in.

4.3-3 Piston Friction and Piston Size (Con't)

$$DIST = (2)(\text{Intake Stroke}) + (2)(\text{Expansion Stroke})$$

$$= \frac{2}{12}\left\{\frac{D}{R(E_R)}\right\} + \frac{2}{12}\left\{\frac{D}{R}\right\}$$

$$= \frac{2D}{12R}\left\{\frac{1}{E_R} + 1\right\}$$

WHERE,

R = Cam pressure angle ratio (Section 4.3-2)

E_R = Expansion ratio

$$T = \text{Number of Pistons} = 2Q$$

WHERE,

Q = Number of cylinders

$$D = \frac{d}{\kappa \, SIN\left(\frac{360}{2Q}\right)}$$

WHERE,

d = Cylinder bore diameter, in

κ = Cylinder close packing constant

$$\kappa = \frac{\text{Cylinder bore diameter}}{\text{Maximum cylinder diameter allowed by close packing}}$$

$\kappa < 1$ to allow for water jackets and cylinder sleeves around the cylinder bore

Combining the above relationships we have:

$$HP_{CF} = \{1.44 \times 10^{-10}\} \frac{\mu \, MQd^2N^3}{R \, \kappa^2 \, SIN^2\left(\frac{360}{2Q}\right)} \left\{\frac{1}{E_R} + 1\right\}$$

(Equation 4-7)

If the piston weight could be expressed as a function of piston diameter then the centrifugal losses could be expressed solely as a function of piston diameter or cam PCD and the number of pistons which are the key variables of this optimization. It could then be established whether

4.3-3 Piston Friction and Piston Size (Con't)

or not for a given engine displacement a four cylinder or an eight cylinder engine would have greater total centrifugal losses.

The total piston weight for the style of cam follower being considered for the Dash-3 engine is the summation of the weights of four areas of any such piston: the piston head (aluminum), the bearing carrier (aluminum), the connection between the two latter areas (aluminum) and the cam follower bearings and rollers (steel).

Assuming that required bearing capacity is directly proportional to piston area (in other words combustion gas loading) a series of "off-the-shelf" commercially available "track runner" bearings and rollers were examined to establish the relationship between bearing dynamic capacity and bearing weight. Graph 4-12 illustrates this relationship for SKF nast series[16] bearings: it can be seen that bearing weight increases at a greater than linear rate with respect to bearing capacity or with respect to piston area or piston diameter squared.

The remaining aluminum components of our hypothetical piston are sized so as to keep with in allowable stress limits of the material.

A relationship between total piston weight and piston diameter results:

SKF TRACK RUNNER BEARINGS
NAST SERIES

BEARING AND ROLLER RADIAL DYNAMIC
LOAD CAPACITY

vs.

TOTAL BEARING WEIGHT

Reference:

SKF general catalogue
3000 E/GB 666
November 1975

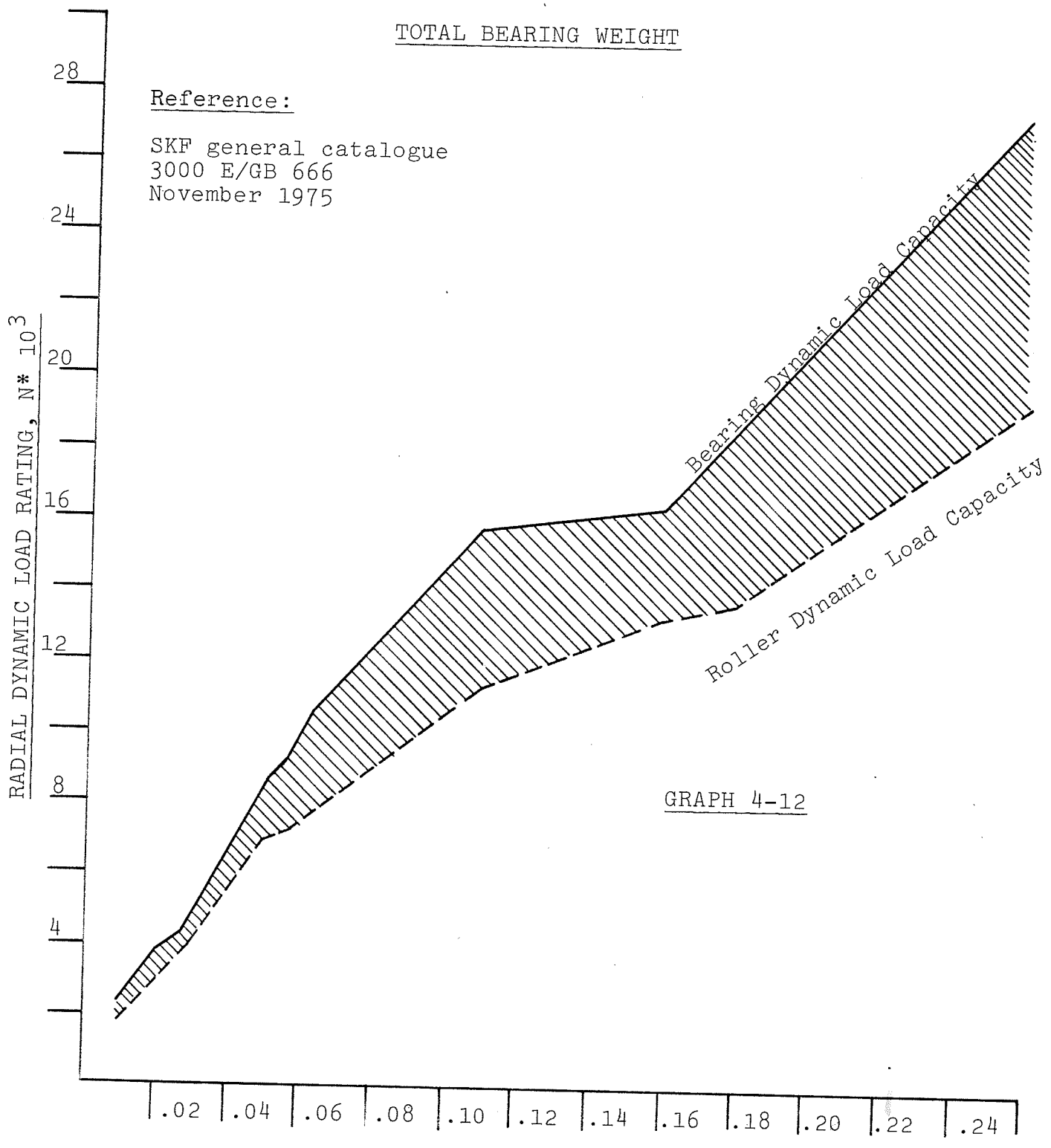

GRAPH 4-12

4.3-3 Piston Friction and Piston Size (Con't)

$$\text{Piston Weight} = K_1 (d)^{\eta} \qquad \text{(Equation 4-8)}$$

WHERE,

K_1 = constant, or for our example, with the nast bearings

η = 2.21

K_1 = 0.123

This particular exponent and constant were derived from a hypothetical piston with its weight evenly split between the aluminum body and the bearings and then extrapolated to larger sizes with the aluminum body weight increasing as the square of the piston diameter, and the bearing weight increasing with respect to piston diameter at the rate shown in Graph 4-12.

The friction losses resulting from the sliding of the cam follower on the cam running surface and the side thrust reaction between the piston and the cylinder wall are a function of the combined gas and inertia loads applied to the piston along its axis. For engines of equal displacements and operating conditions, the gas loading should be constant.

The inertia loading is a function of the piston weight and the acceleration forces imposed on it by the cam motion.

The acceleration resulting from simple harmonic motion is:

$$\ddot{y} = \frac{d}{2} \left(\frac{\pi\omega}{A}\right)^2 \cos\left(\frac{\pi\theta}{A}\right) \qquad \text{(Equation 4-9)}$$

4.3-3 Piston Friction and Piston Size (Con't)

WHERE,

$\underline{d}$ = The total stroke length, ft.

$\underline{\omega}$ = Angular velocity, rad./sec.

$\underline{A}$ = Total angular duration of the stroke length, radians

$\underline{\theta}$ = Angular position during the stroke for which $\ddot{y}$ is desired, radians

An expression for the average inertia loading on each piston during each four stroke cycle can be obtained by the summation of the cubic mean acceleration for each of the stroke lengths. The cubic mean is used rather than the arithmetic mean so as to compensate for the sudden pressure loading during combustion and the cyclic nature of the inertia loading.

The cubic mean pressure loading will be assumed to be constant for all engine configurations.

The cubic mean average or the cyclic acceleration can be obtained via:

$$\ddot{y} = \frac{1}{2}\left\{\frac{\int_0^{\alpha/2} \ddot{y}_s^3 d\theta}{\alpha/2}\right\}^{1/3} + \frac{1}{2}\left\{\frac{\int_0^{\beta/2} \ddot{y}_l^3 d\theta}{\beta/2}\right\}^{1/3}$$

(Equation 4-10)

4.3-3 Piston Friction and Piston Size (Con't)

WHERE,

α = Angular duration of the short strokes, radians

β = Angular duration of the long strokes, radians

y_s = Acceleration during the stroke at any θ, ft./sec.

y_l = Acceleration during the long stroke at any θ, ft./sec.^{2}

Setting the total short stroke length to "l" and that of the long stroke to "s" and substituting (Equation 4-9) into (Equation 4-10) and solving for the cubic mean acceleration we have

$$y\Big|_{\text{cubic mean}} = \frac{3\pi}{4}\,\omega^2\,\left(\frac{l}{\alpha^2} + \frac{s}{\beta^2}\right) \qquad \text{(Equation 4-11)}$$

and since $E_R = \frac{s}{l} = \frac{\beta^2}{\alpha^2}$

$$y\Big|_{\text{cubic mean}} = \frac{3\pi}{2}\,\omega^2\,\frac{s}{\beta^2}$$

from Graph 4-6

$$R = \frac{D}{S}$$

Therefore

$$y\Big|_{\text{cubic mean}} = \frac{3\pi}{2}\,\omega^2\,\frac{D}{R\beta^2} \qquad \text{(Equation 4-12)}$$

The total force acting axially on the piston can be expressed as:

$$F_T = \frac{P\pi d^2}{4} + \frac{M}{32.2}\,\frac{3\pi}{2}\,\omega^2\,\frac{D}{R\beta^2} \qquad \text{(Equation 4-13)}$$

WHERE,

P = The cubic mean gas pressure in the cylinder for each revolution., lbf./in.^{2}

4.3-3 Piston Friction and Piston Size (Con't)

The power loss due to the sliding of the cam follower on the cam can be expressed as:

$$HP_{RS} = (COS\phi)\ F_T\ \mu Z\ \frac{N}{33000}\ (2Q)$$

(Equation 4-14)

WHERE,

ϕ = R.M.S. average of the cam pressure angle throughout the four strokes. This is constant if R is constant.

Z = The distance that the roller slides on the cam each revolution.

The distance that the roller slides is a function of the roller contact width, b; for any cam/roller combination the roller contact width is a function of the allowable contact stress of the material. This in turn is a function of F_T. Therefore, $b = K' F_T$ (Equation 4-15)

WHERE,

K' = constant for rollers of the same width to diameter ratio

The sliding motion of the roller on the cam results from the outside edge of the roller attempting to travel at a greater surface velocity than that of the inside edge. The distance that the roller slips each revolution is:

$$Z = \frac{(D + b)\pi - (D - b)\pi}{2} \quad \text{(Equation 4-16)}$$

$$Z = \pi b$$

Or $$Z = \pi K' F_T$$

Substituting (Equation 4-16) and (Equation 4-13) into (Equation 4-14) and setting as constant

4.3-3 Piston Friction and Piston Size (Con't)

if K_a = constant, $\frac{HP}{lbf^2}$, K_b = constant, $\frac{lbf.}{in.^2}$, K_c = constant, $\frac{1}{FT.}$ we have

$$HP_{RS} = K_a Q \left\{ K_b^2 d^4 + \frac{K_b K_c 2Md^3}{SIN(\frac{360}{2Q})} + \frac{K_c^2 M^2 d^2}{\sin^2(\frac{360}{2Q})} \right\} \quad \text{(Equation 4 - 17)}$$

If we use our hypothetical Dash-3 piston where its weight is

$$M = 0.123d^{2.21}$$

$$HP_{RS} = K_a Q \left\{ K_b^2 d^4 + \frac{0.246 K_b K_c d^{5.21}}{SIN(\frac{360}{2Q})} + \frac{0.123 K_c^2 d^{4.21}}{SIN^2(\frac{360}{2Q})} \right\}$$

The power loss due to the sliding motion and cam induced side force as the piston travels up and down its bore can be expressed as:

$$HP_{SF} = (TAN\phi)\ F_T\ \mu\ \frac{N}{33000}\ 2Q\ F$$

(Equation 4-18)

WHERE:

F = Distance that the piston travels axially in its bore each revolution

WHERE:

$$F = 2s + 2s = 2s\{\frac{1}{E_R} + 1\} \quad \text{(Equation 4-19)}$$

AND

$$F = 2\frac{D}{R}\{\frac{1}{E_R} + 1\}$$

Substituting (Equation 4-19) and (Equation 4-13) into (Equation 4-18) we have with

4.3-3 Piston Friction and Piston Size (Con't)

if K_d = constant, $\frac{HP}{Ft.\ lbf}$, K_e = constant, $\frac{lbf.}{in.^2}$, K_f = constant, $\frac{1}{Ft.}$

$$HP_{SF} = \frac{K_d Q}{SIN(360/2Q)} \left\{ K_e d^3 + \frac{K_f d^2}{SIN(\frac{360}{2Q})} \right\} \quad \text{(Equation 4-20)}$$

Substituting $M = 0.123 d^{2.21}$

$$HP_{SF} = \frac{K_d Q}{SIN\ \frac{360}{2Q}} \left\{ K_e d^3 + \frac{K_f M d^{4.21}}{SIN(\frac{360}{2Q})} \right\}$$

(Equation 4-21)

The total power loss due to the centrifugal loading of the piston as it slides in its bore (Equation 4-7) is illustrated in Graph 4-13. For an engine of a given intake displacement, increasing the number of cylinders results in an increase in the centrifugal power loss. It should be noted that these losses increase at a greater than linear rate with respect to intake displacement. Because these losses also are proportional to the cube of the engine speed, engines with an intake displacement considerably larger than that being considered for the Dash-3 will be of the low speed variety.

Graph 4-14 shows that the frictional power loss due to the sliding motion of the roller contact width against the cam running surface (Equation 4-19) decreases for an increasing number of cylinders for an engine of a given intake displacement. Graph 4-15 illustrates that the total power loss arising from the cam pressure angle induced side force

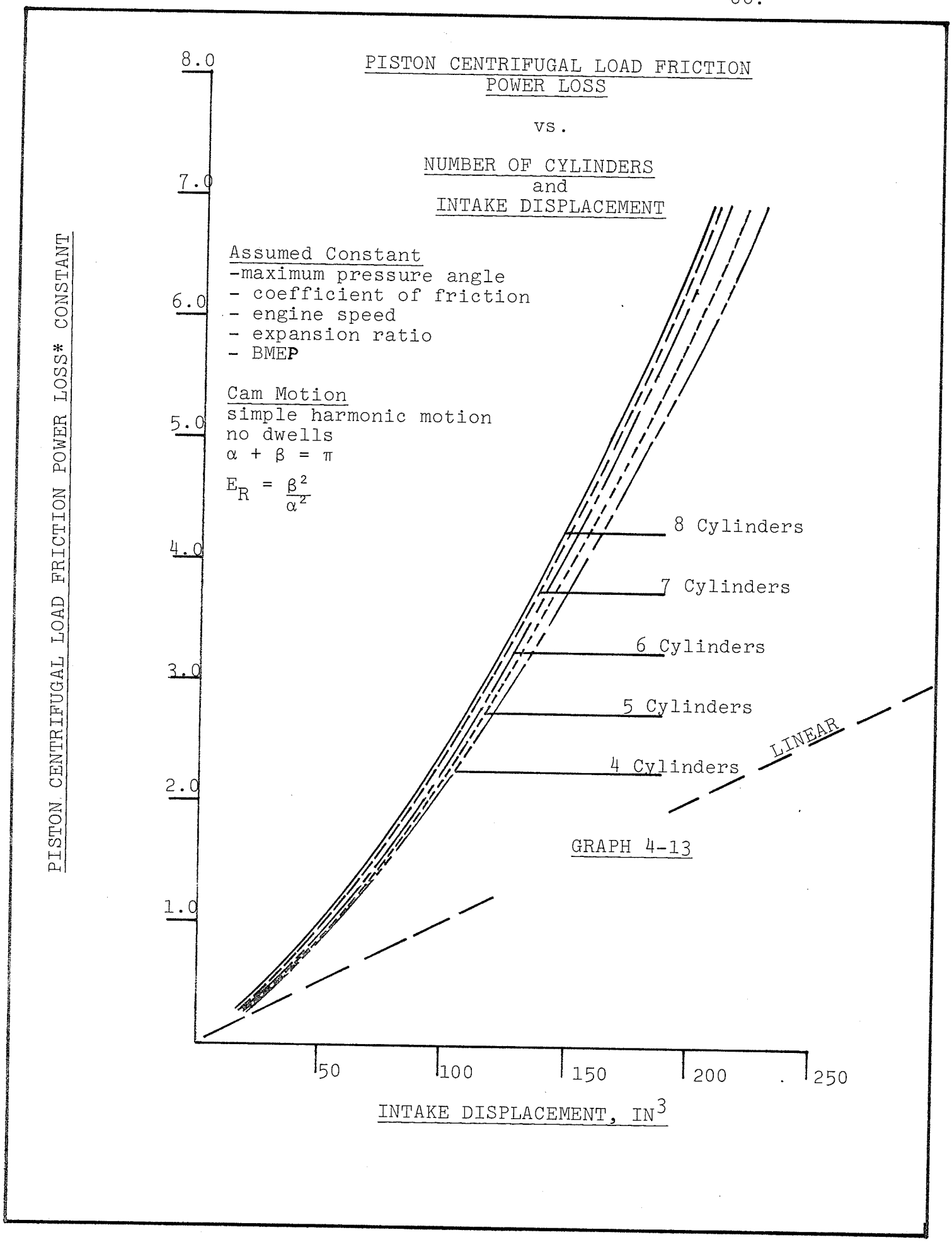
PISTON CENTRIFUGAL LOAD FRICTION POWER LOSS
vs.
NUMBER OF CYLINDERS
and
INTAKE DISPLACEMENT
Assumed Constant
-maximum pressure angle
- coefficient of friction
- engine speed
- expansion ratio
- BMEP
Cam Motion
simple harmonic motion
no dwells
α + β = π
$E_R = \frac{\beta^2}{\alpha^2}$
PISTON CENTRIFUGAL LOAD FRICTION POWER LOSS* CONSTANT
8.0
7.0
6.0
5.0
4.0
3.0
2.0
1.0
8 Cylinders
7 Cylinders
6 Cylinders
5 Cylinders
4 Cylinders
LINEAR
50
100
150
200
250
INTAKE DISPLACEMENT, IN^3

GRAPH 4-13

PISTON ROLLER/CAM SLIDING FRICTION POWER LOSS
vs.
NUMBER OF CYLINDERS and INTAKE DISPLACEMENT

GRAPH 4-14

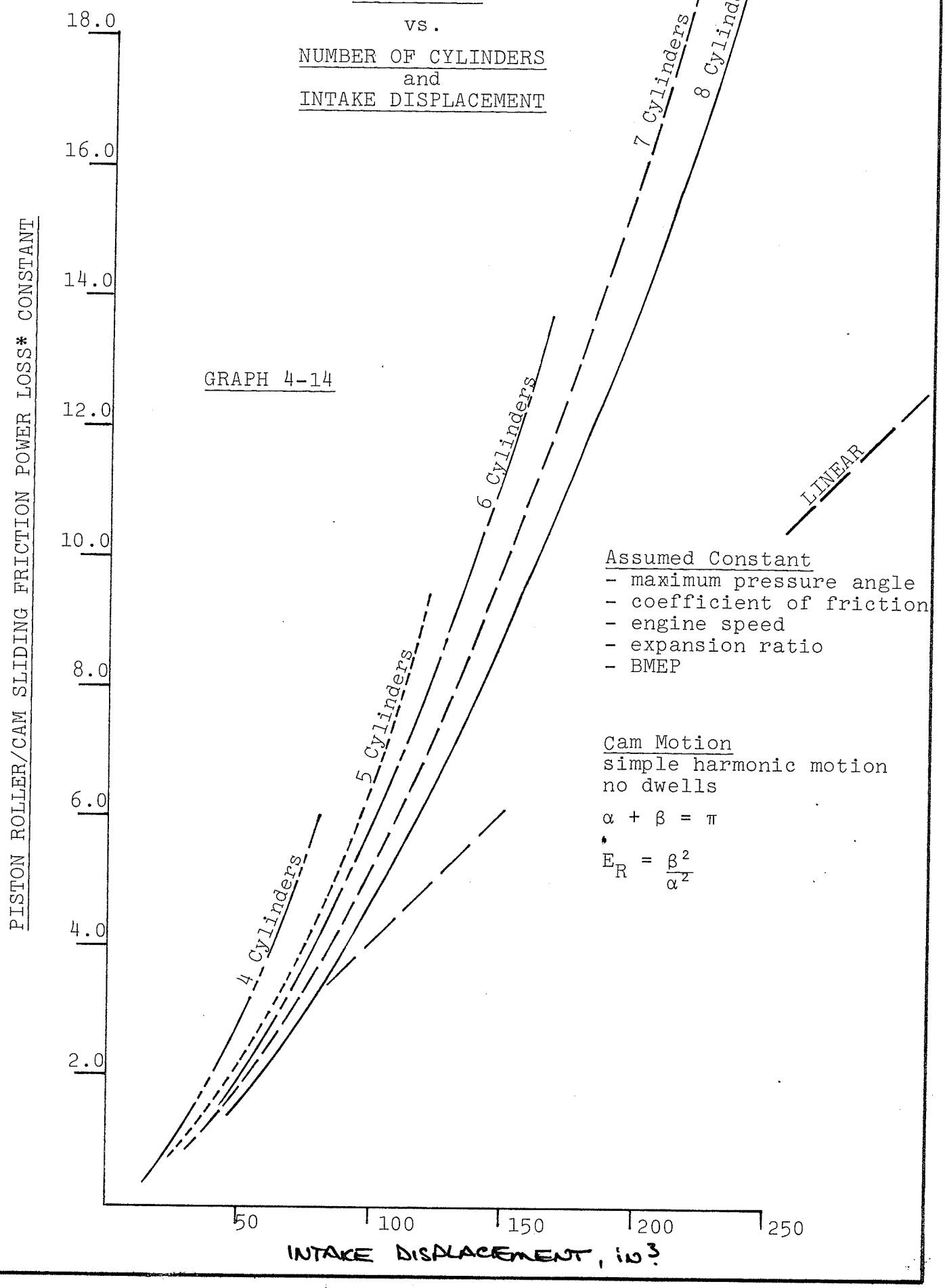

Assumed Constant
- maximum pressure angle
- coefficient of friction
- engine speed
- expansion ratio
- BMEP

Cam Motion
simple harmonic motion
no dwells

$\alpha + \beta = \pi$

$E_R = \frac{\beta^2}{\alpha^2}$

PISTON SIDE FORCE FRICTION POWER LOSS

vs.

INTAKE DISPLACEMENT

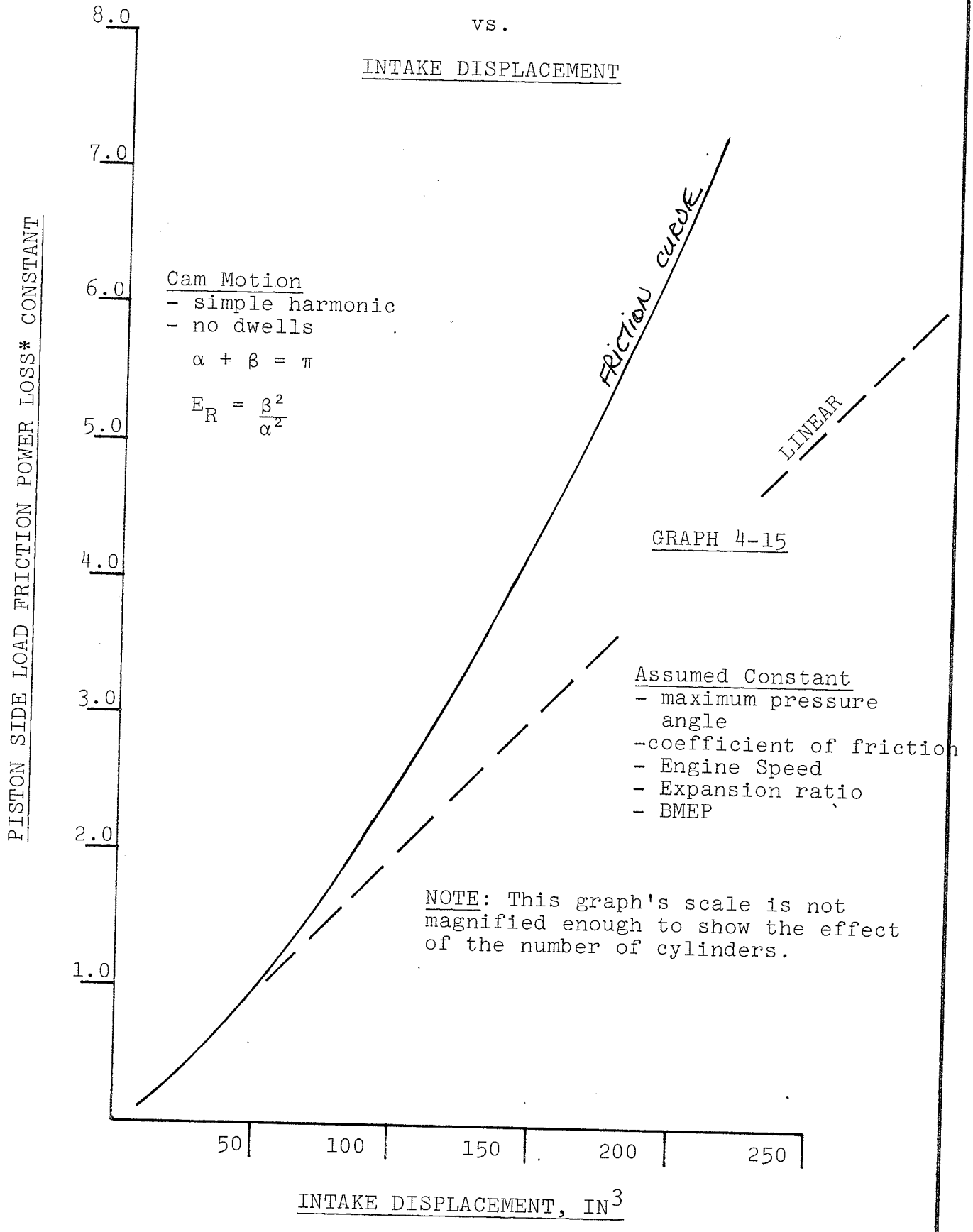

GRAPH 4-15

4.3-3 Piston Friction and Piston Size (Con't)

on the pistons will be virtually the same for engines of the same size regardless of the number of cylinders. As was the case with the centrifugal power losses, the latter two losses also increase at a greater than linear rate with intake displacement and as the cube of the engine speed; strengthening the caution that large scale K-Cycle engines must be limited rotational speed.

As both the centrifugal and roller to cam power losses are equally significant (refer to test data of the existing prototype engines in Section 5.1-3) and as they cannot be simultaneously reduced by adjusting the geometric design variables, the configuration optimization of the Dash-3 engine will not be able to provide a significant reduction in these losses as compared to the Dash-3's predecessors.

4.3-4 Continuous Combustion

The design goals stated in Chapter three point out that the Dash-3 engine be able to convert to continuous combustion hot gas ignition after an initial research period using spark ignition.

There are two methods proposed by continuous combustion theory to attain the ignition of the air fuel mixture, as it approaches TDC, by a jet of hot combustion gases from a preceeding cylinder.[17] The first method uses a "bleedback" or a "by-pass" tube

4.3-4 Continuous Combustion (Con't)

to transfer the ignition gases from the burning cylinder to the one following. This method is illustrated in Figure 4-16. Although the "by-pass" tube ignition system has the advantage of being able to provide the optimum timing for the pick-up and discharge of the ignition gases regardless of engine configuration used, the flow of high velocity gas through the required orifice presents some design problems from a heat transfer point of view. Another undesirable characteristic is that the percentage of the total gas volume required increases as engine speed is reduced.

The second method of obtaining continuous combustion is by the use of a small stationary "mini-chamber" to vent the hot ignition gases at the appropriate time (illustrated in Figure 4-17). The mini-chamber gases are at the same pressure as the burning gases of the cylinder that coincides with the mini-chamber. This pressure is retained in the mini-chamber in between cylinder ports as they rotate by and are released into the preceeding cylinder when leading edge of its port uncovers the mini-chamber orifice. The more uniform ignition characteristics such as discharge volume and temperature are much easier to control with the mini-chamber design,but such a design has the disadvantage of having its ignition timing set by the engine configuration used.

SCHEMATIC OF CONTINUOUS COMBUSTION IGNITION USING A BLEEDBACK TUBE

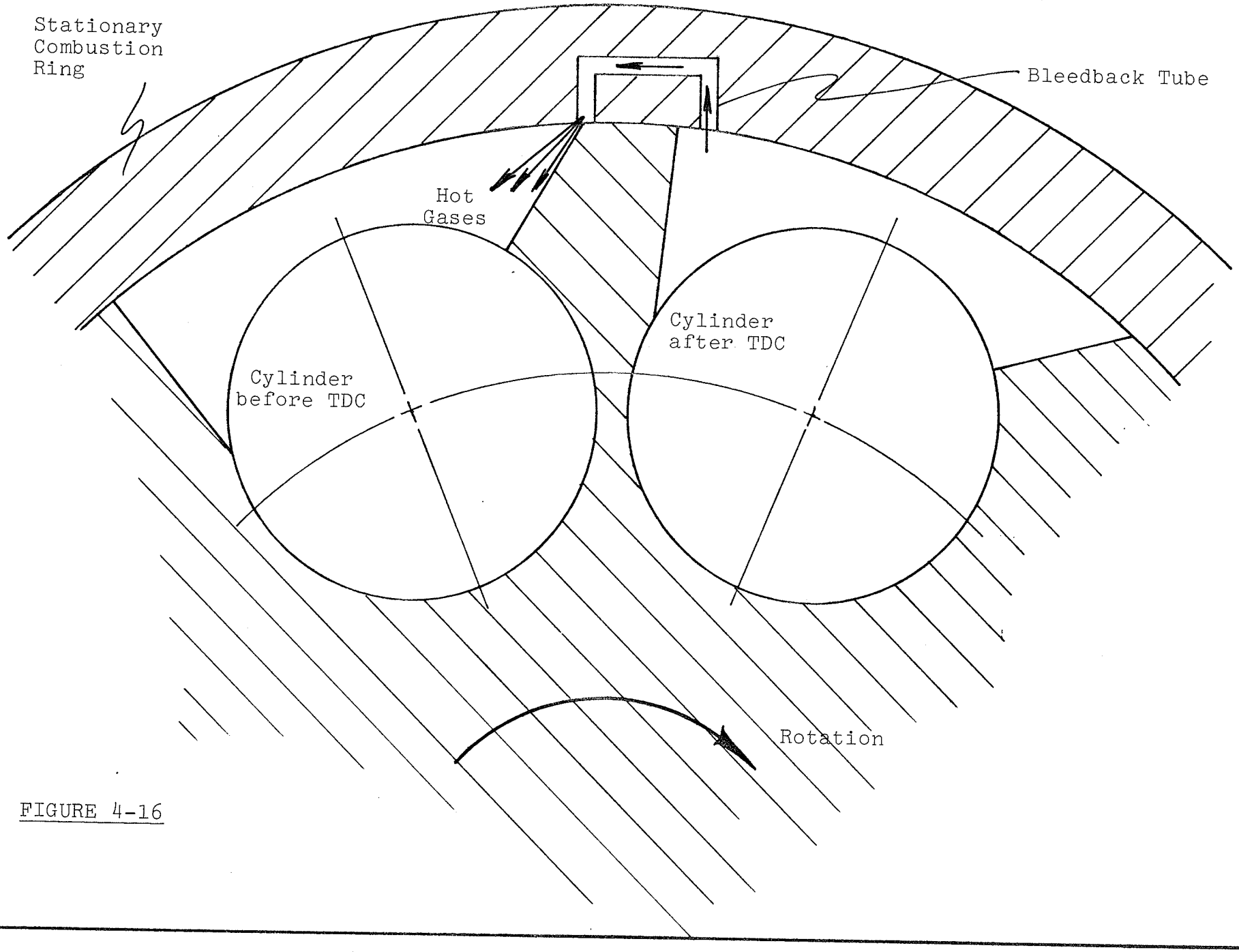

FIGURE 4-16

SCHEMATIC OF CONTINUOUS COMBUSTION IGNITION USING A STATIONARY MINI-CHAMBER

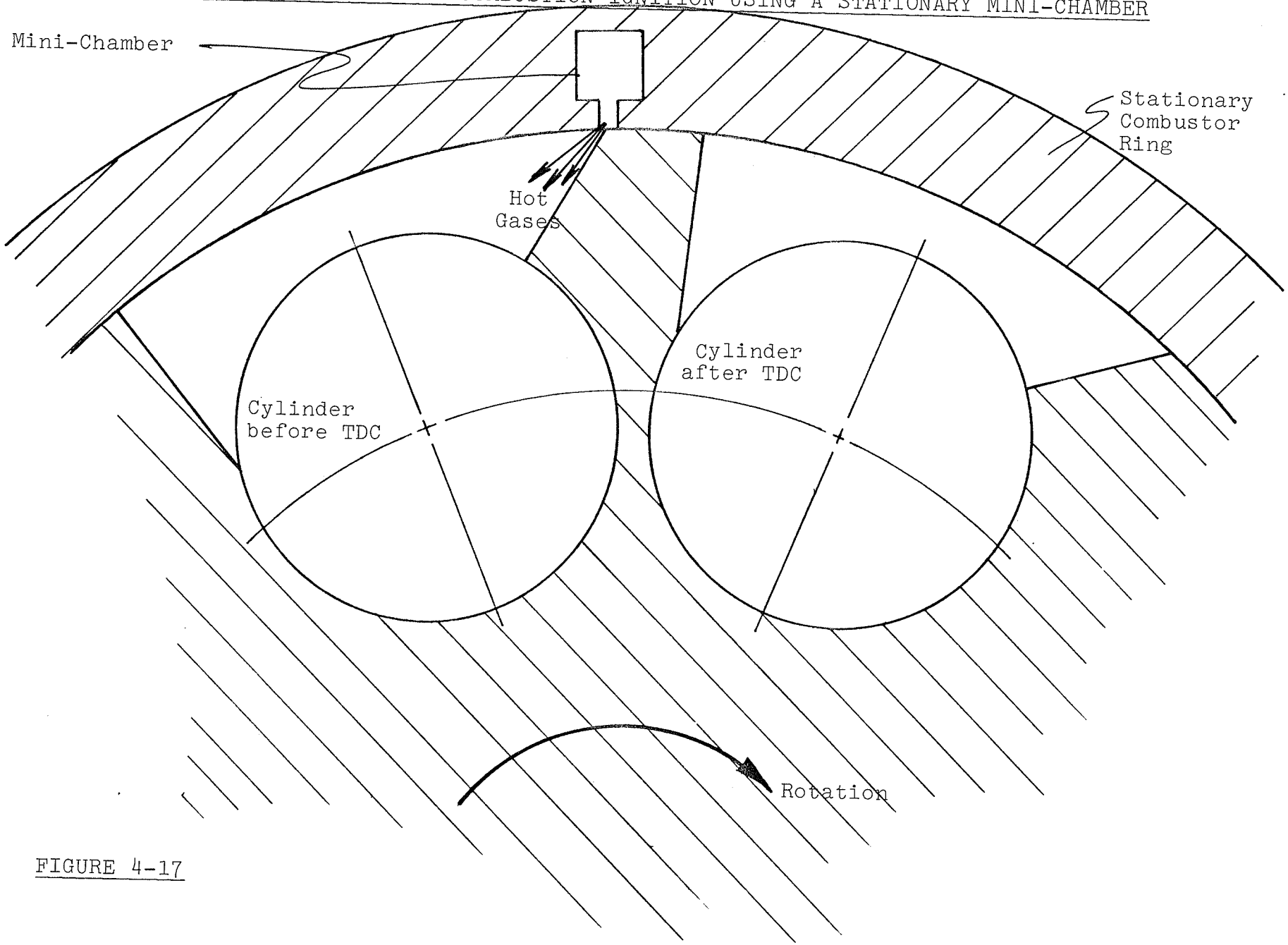

FIGURE 4-17

4.3-4 Continuous Combustion (Con't)

The combustion gases stored in the mini-chamber must be released into the to-be-ignited cylinder at pressure greater than that already present. The ideal pressure ratio would 2.0:1. Pressure ratios greater than 2.0:1 are allowable (even though they will result in sonic flow) but ratios significantly less than 2.0:1 may not be able to provide the required pressure differential at part throttle settings.

Graph 4-18 shows several cylinder pressure-engine rotation curves for a hypothetical Dash-3 engine. These curves were evolved by the K-Cycle computer combustion simulation.

This graph shows the size of cylinder port opening required to obtain a 2.0:1 pressure ratio and also have the ignition initiation occur at the desired time. It is thought that this form of combustion initiation will result in very little ignition lag[17] making a significant degree of ignition advance unnecessary. Graph 4-18 shows that in order to meet these pressure ratios and ignition timing constraints the maximum allowable cylinder port opening is 45 to 50 degrees.

The effect of this port opening requirement on the allowable engine configuration is shown in Graph 4-19. This graph is based on the seal and port design parameters evolved in Graph 5-1 for a seal surface velocity of 60 ft/sec. Note that this is not the maximum available cylinder port opening--that restricted by the cylinder bore--but is 10% less to allow room for a seal bed at the ends of the port opening.

CYLINDER PRESSURE vs. ANGULAR LOCATION

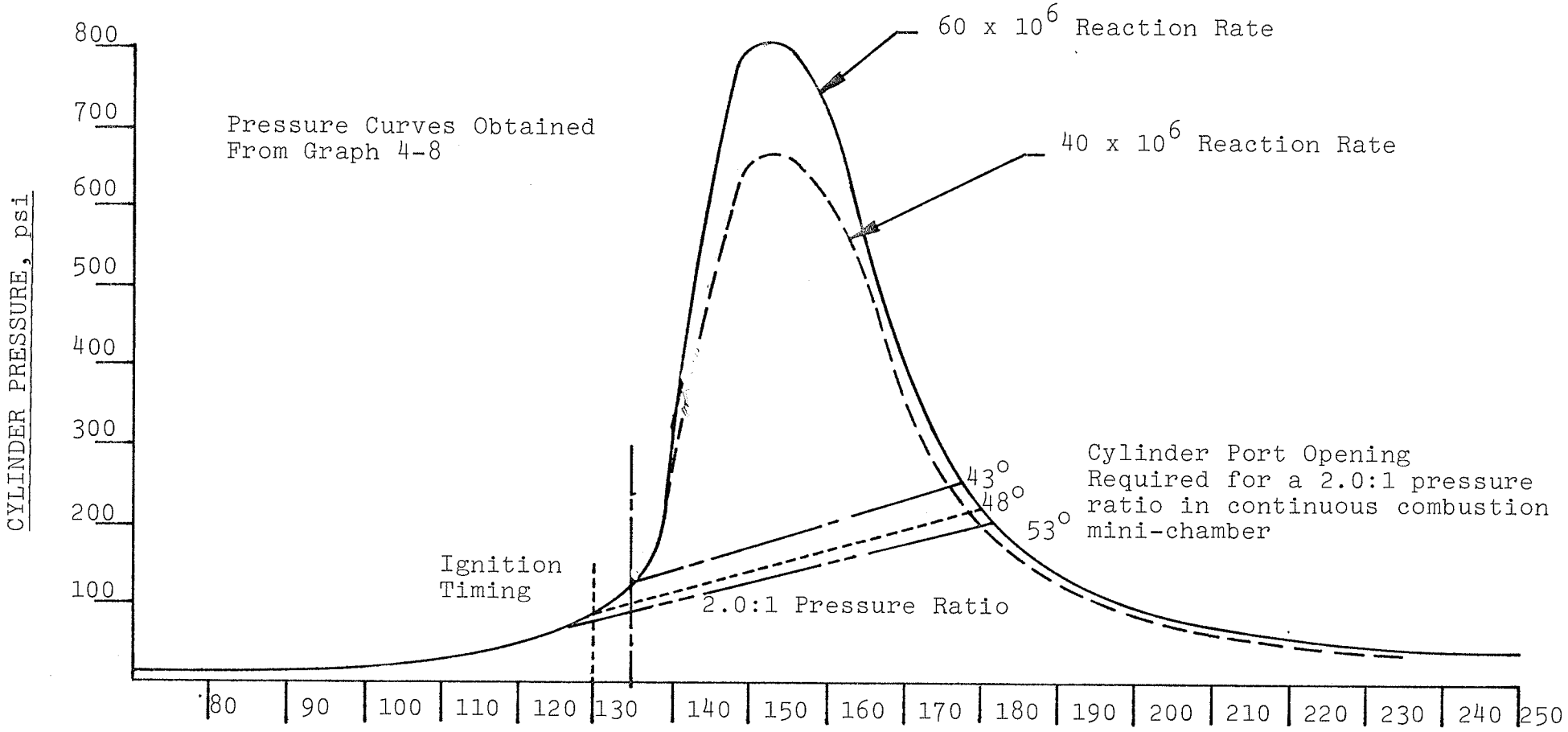

GRAPH 4-18

ENGINE CONFIGURATION ENVELOPE
for engines with the following parameters:
- simple harmonic motion - no dwell
- maximum pressure angle = 30^{o}
- expansion ratio = 2.0:1
- maximum seal surface velocity is 60 ft/sec/ @ 3000 RPM

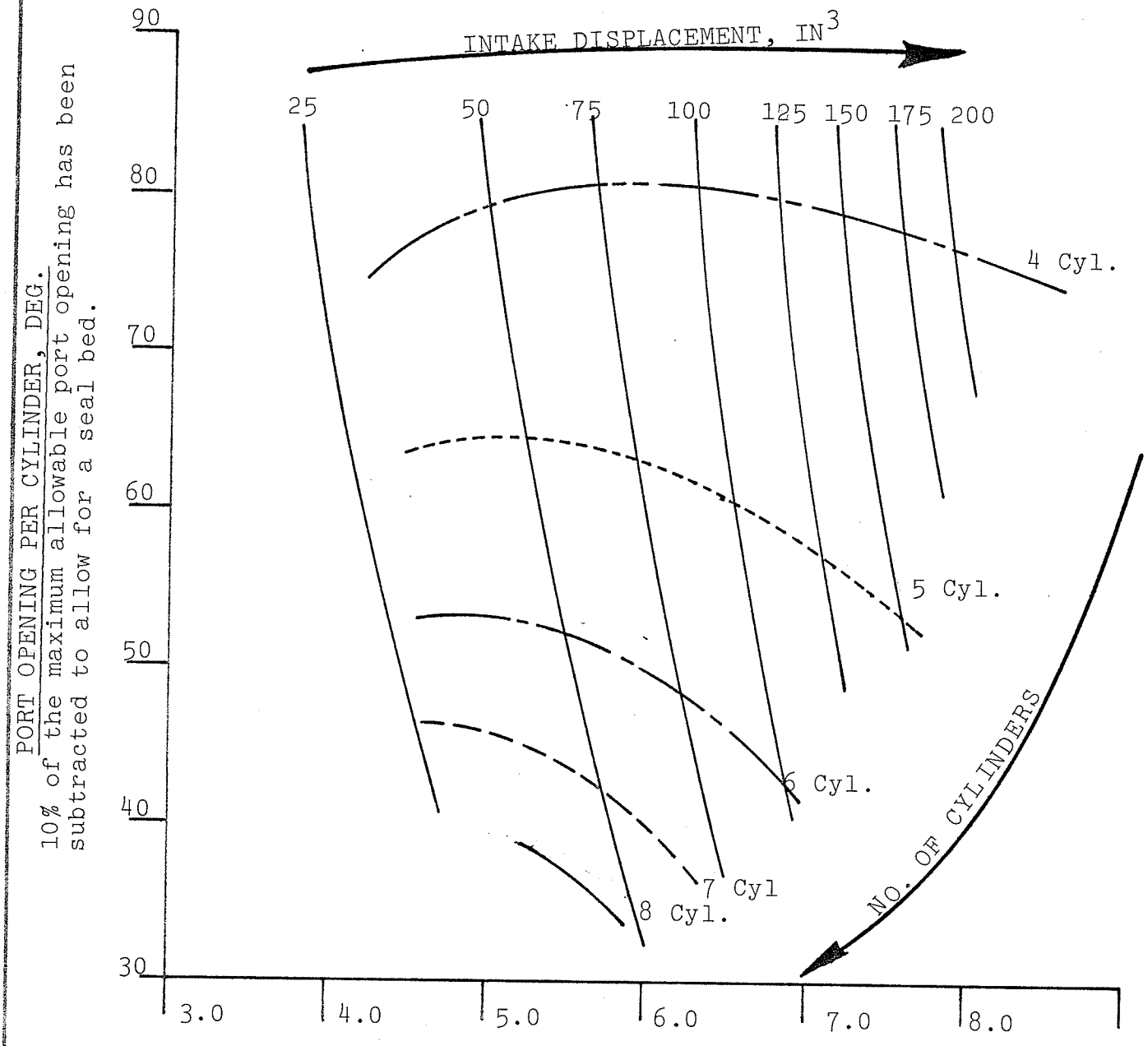

GRAPH 4-19

4.3-4 Continuous Combustion (Con't)

The cylinder port opening does not have to utilize the maximum opening that the engine configuration allows; it can be reduced as required. For example, the maximum port opening of a 5 cylinder engine at a 5 inch cam can be reduced from the 60° maximum to say, 40° to meet the continuous combustion requirements. A reduction of this kind will reduce the breathing capacity and such a penalty should be avoided in trying to reach the optimum engine configuration and will not be considered here.

4.3-5 Selection of an Engine Configuration

Prior to selecting a particular engine configuration for the Dash-3 engine, the parameters that our optimization process has evolved should be reviewed.

Section 4.3-1 shows that to make optimum use of the cross-sectional area of the K-Cycle envelope, one should choose either a four cylinder or five cylinder engine with the cylinders packaged in a "close packed" manner.

The engine intake displacement is a function of the number and size of the cylinders as well as the stroke length with the latter being controlled by the cam motion and expansion ratio.

Section 4.2-1 and 4.3-2 showed that a dwell-free cam which generates simple harmonic motion will result in a peak acceleration of the least magnitude and therefore minimum inertia loads for the cam motions considered.

4.3-5 Selection of an Engine Configuration (Con't)

Section 4.3-2 also concluded that in order to avoid over-expansion in the Dash-3 Engine a 2.0:1 expansion ratio would be the most suitable. At the same time a maximum cam pressure angle of 30^{o} was selected as a conservative approach to a design variable with which we have had little practical experience.

Section 4.3-3 concluded there is a high probability that piston weight will at least be proportional to piston diameter squared for the type of piston that is being considered for the Dash-3 Engine. It was also illustrated that for the same intake displacement fewer and larger pistons will result in fractionally greater total piston friction. It is felt that the significant increase in engine packaging efficiency on the basis of intake displacement per engine volume easily balanced the slight increase in total piston friction.

The range of cylinder pitch circle diameters available to the Dash-3 Engine are restricted by two design constraints: that a face seal configuration with a maximum seal surface velocity of 60 ft/sec. be used, and that the engine be able touse the continuous combustion method of ignition if required. The former is illustrated in Graph 4-2 and the latter in Graph 4-19.

The combination of the seal design constraints with the previously optimized variables results in the range of possible engine configurations shown in Grpah 4-19.

4.3-5 Selection of an Engine Configuration (Con't)

It can quickly be seen that the engine with the largest possible displacement that meets all of our design criteria is a 75 to 100 cubic inch 6 cylinder engine.

The final engine configuration decided upon was influenced by the availability of suitable off-the-shelf piston rings and the desire to have major engine dimensions in a manageable form for the design and manufacturing processes.

The configuration can be summarized as:

Number of cylinders = 6

Cylinder bore= 2.75"

Maximum allowable close-packed cylinder diameter = 3.25

($k = 0.85$)

Cam PCD = 6.5"

Seal PCD = 4.58"

Cam Motion = Simple harmonic with no dwells

Long stroke length = 2.25"

Long stroke angular duration = 105^{o}

Short stroke length = 1.147"

Short stroke angular duration = 75^{o}

Expansion ratio = 1.96:1

Engine intake displacement = 81.75 in^3

CHAPTER 5

THE PISTON/CAM FOLLOWER MECHANISM

5.1 INTRODUCTION

One of the main attractions of the K-Cycle rotating cylinder - stationary cam concept is its inherent simplicity with fewer moving parts when compared to the conventional crankshaft engine. The K-Cycle piston/cam follower mechanism is the most important of these dynamic components in that it must translate the work potential of the engine into useful output with a minimum of losses.

The piston/cam follower has a more complex function than that of its conventional counter-parts, and this complexity can be a source of significant performance constraints if it is improperly dealt with. Examination of the performance characteristics of the first two prototype engine's piston/cam followers indicates that significant improvements are possible and these must be incorporated into those of the Dash-3 Engine so as to obtain a respectable engine output.

This chapter will re-define the requirements of a successful piston/cam follower mechanism (refered to as "piston" hereafter) and will then re-examine the design of its predecessors in an attempt to determine what the optimum concept should be.

5.2 CURRENT PISTON TECHNOLOGY

5.2-1 Piston Performance Requirements

The piston required by the K-Cycle Engine is much more complex than that of the conventional crankshaft engine. In the latter, the piston essentially forms the lower part of the combustion chamber and, with its piston rings, acts as a moveable sealing plug that slides up and down the cylinder bore.[18] The connecting rod and crankshaft transforms the cylinder pressure into useful work and defines the motion that the piston is to follow.

The K-Cycle piston serves as a combination piston and connecting rod, while acting as an autonomous engine component whose only link with the rest of the engine arises through sliding contact and not via a fixed linkage.

There are three basic differences between the K-Cycle and conventional piston and they can be summarized as follows:

* The K-Cycle piston will have a much greater weight than that of a comparable conventional piston, because in addition to the piston head and rings of the latter, the K-Cycle piston also includes two sets of bearings and cam follower rollers.

* In addition to major and minor side thrust loads (comparable to those of the conventional piston), the rotating motion of the K-Cycle cylinder block or rotor results in a third

5.2-1 Piston Performance Requirements (Con't)

centrifugal component which is imposed on the K-Cycle piston, and in turn results in a friction power loss that is proportional to the cube of engine speed.

* In the conventional engine, the gas and inertia loads are transferred to the output shaft via bearings with a capacity that is a function of their projected load carrying area. In the K-Cycle Engine these loads are transmitted via roller cam followers that rely on line contact for load transmission.

In addition to being able to cope with these differences, a K-Cycle piston must have the following properties, some of which will be part of the refinement process, to perform properly:

A. The piston must be able to withstand the extremely high pressures and temperatures generated by the combustion process.

B. It must be able to withstand the bending forces imposed by combustion pressures.

C. It must have an adequate heat path to prevent excessive piston head temperatures.

D. It must prevent the transfer of excessive heat to the cam follower bearings which would reduce bearing life.

5.2-1 Piston Performance Requirements (Con't)

E. The piston must exhibit minimum dimensional changes due to thermal distortion and expansion.

F. The piston head to cylinder bore clearance must be maintained at a minimum to keep blow-by low.

G. It must have minimum weight so as to keep side forces and centrifugal sliding friction losses down.

H. To minimize frictional losses and wear, hydrodynamic friction coefficients must be approached during the sliding motion.

I. The piston must have high scuff and wear resistance for a long life.

J. To maximize bearing life, adequate contaminate-free lubricant must be supplied and sufficient lubricant drainage must be allowed for.

K. Piston motion must be sufficiently controlled so as to maintain maximum roller to cam line contact. The piston structure must also be stiff enough to maintain parallelity of the roller axis with the cam surface to maintain line contact.

L. The cam follower roller must be designed to minimize the frictional losses arising from the sliding of the roller on the cam.

M. The roller/cam/roller clearance must be kept to a minimum so as to reduce impact loading and noise.

5.2-1 Piston Performance Requirements (Con't)

Because of the complexity and sheer number of the variables involved, experts in the field have claimed that the design of a successful piston for the conventional crankshaft engine is more of an art than a science.[19] The complexity of the K-Cycle piston is even more overwhelming and many of its additional sub-systems, such as its high speed roller/cam followers are without significant engineering and real world precedents. In addition, its location in a rotating cylinder as well as its autonomous nature make laboratory duplication and instrumentation difficult if not impossible. Despite the lack of background knowledge required by the refinement process, a few basic rules can be established so as to optimize the initial piston concept.

5.2-2 The Mark I and Mark II Prototype Engine Pistons

The piston presently installed in the Mark I Engine, has been modified to such an extent that it is barely recognizable when compared to its original design described in Section 2.4-4.

The original piston design is illustrated in Figure 5-1 and its final form in Figure 5-2. These modifications increased the total piston weight to the extent that friction losses increased dramatically resulting in poor engine output and performance. One of the first changes made to the original piston was the substitution of a cam follower roller for the slider so as to take up the negative axial loads. The

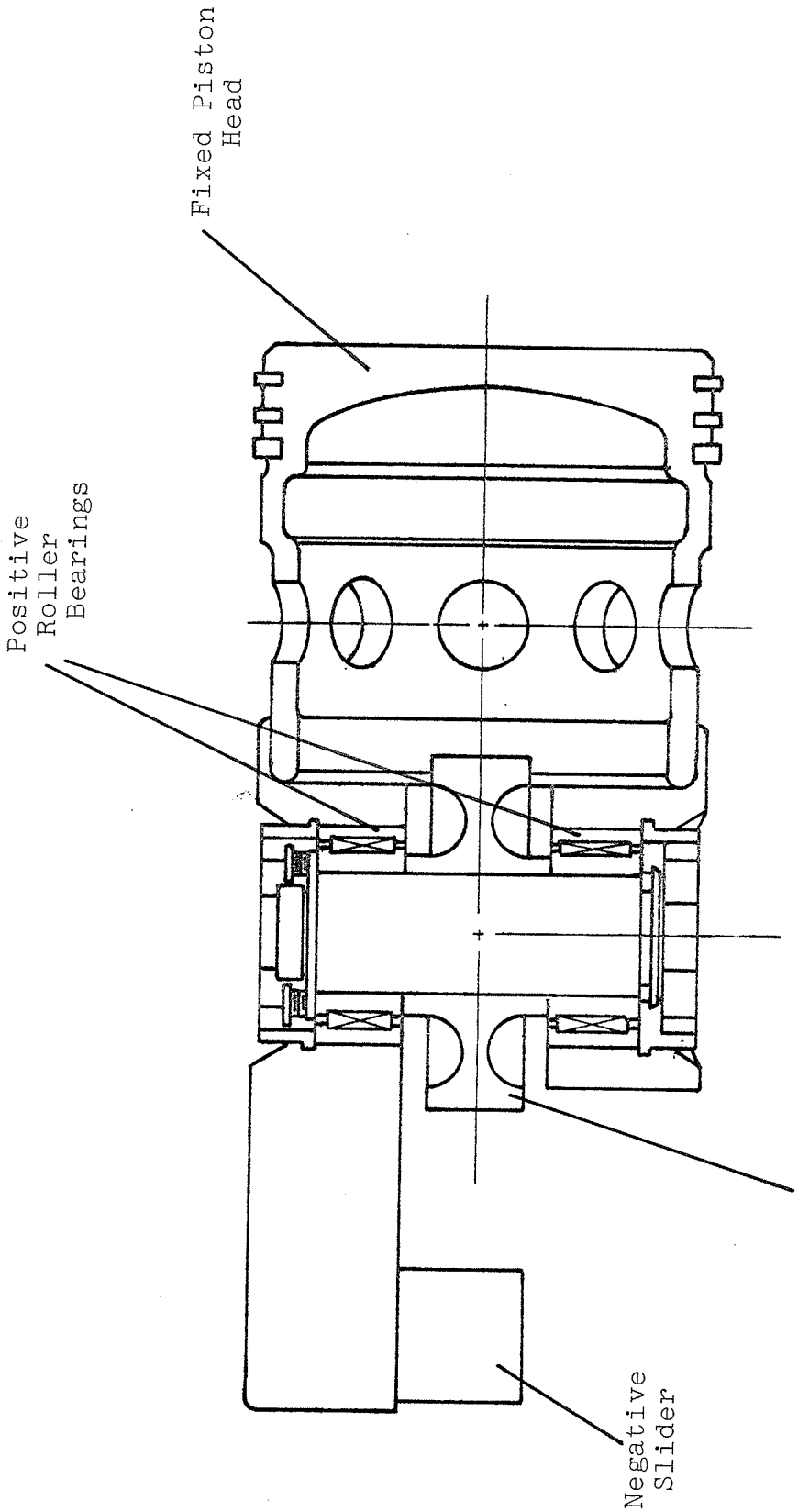

FIGURE 5-1

THE ORIGINAL MARK I PISTON ASSEMBLY

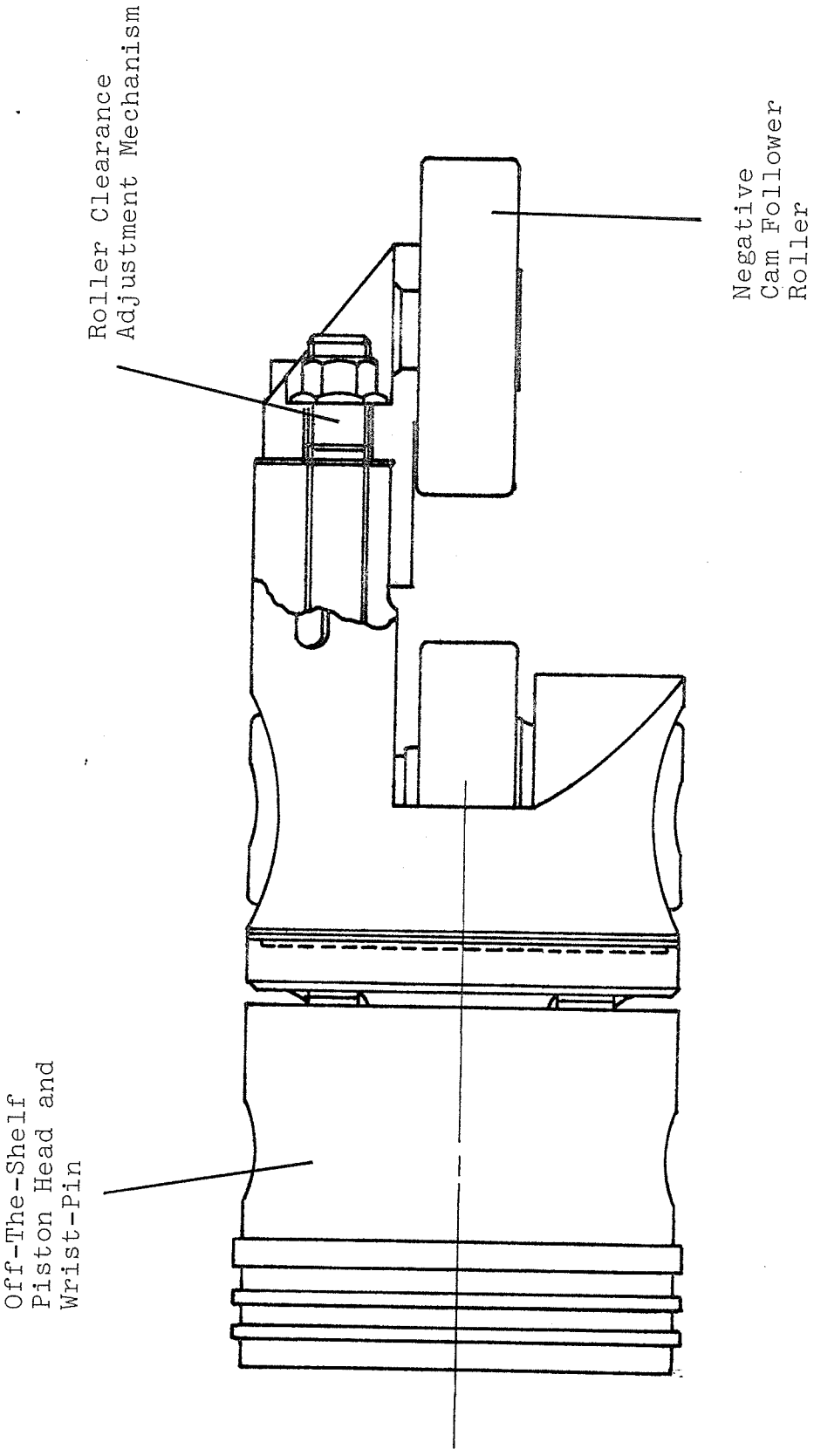

FIGURE 5-2

THE CURRENT MARK I PISTON ASSEMBLY

5.2-2 The Mark I and Mark II Prototype Engine Pistons (Con't)

negative slider was troublesome from its first few hours of use when galling was found on the cam's negative running surface.[21] Despite improved cam lubrication and various slider materials, the slider/cam wear problem continued to worsen until running roller/cam/slider clearances of over 0.125 inches were experienced.[22]

The piston connector was modified to incorporate an off-the-shelf cam follower on an adjustable bracket. This bracket could be shimmed to vary the roller/cam/roller running clearance.

The second major design change consisted of the substitution of an off-the-shelf piston head and wrist-pin sub-assembly. This was mounted to the existing connector via a bolt-on adaptor bracket. This modification was instituted when the original fixed head piston failed: The female thread attaching the piston head to the piston connector failed in bending fatigue with the locking rivit bore acting as a stress-riser.[23]

The addition of the negative roller allowed engine testing to continue unhampered by severe cam wear and the incorporation of theoff-the-shelf piston head assembly was a quick repair that worked.

Although the piston could now function without failure, the repairs drastically increased the weight of the piston assembly: up from 1.75 pounds to 2.4 pounds. This 40%

5.2-2 The Mark I and Mark II Prototype Engine Pistons (Con't)

increase brought the weight even further from the original design goal of 1 pound and raised the inertia loading and frictional losses to only tolerable heights for the low engine speeds and power output encountered.

The piston designed for the Mark II prototype engine was essentially a streamlined version of the repaired Mark I piston (Figure 5-3).

As indicated in Chapter 2, to lower manufacture costs of the Mark II piston, the off-the-shelf piston head and wrist pin was retained while off-the-shelf cam follower bearings were used for both the positive and negative rollers.

Other design changes incorporated in the Mark II Piston included the elimination of the negative roller adjustment bracket and the removal of the grooved surface finish used on the initial pistons.

The Mark II piston technologically was identical to its predessor, and its manufacturing simplification resulted in a slight weight reduction to 2.3 pounds.

5.2-3 Performance of the Mark I and Mark II Pistons

Although the Mark I and Mark II pistons allowed the first two prototype engines to be tested successfully at low power settings without cam follower failures, the apparent high piston friction along with high seal friction and

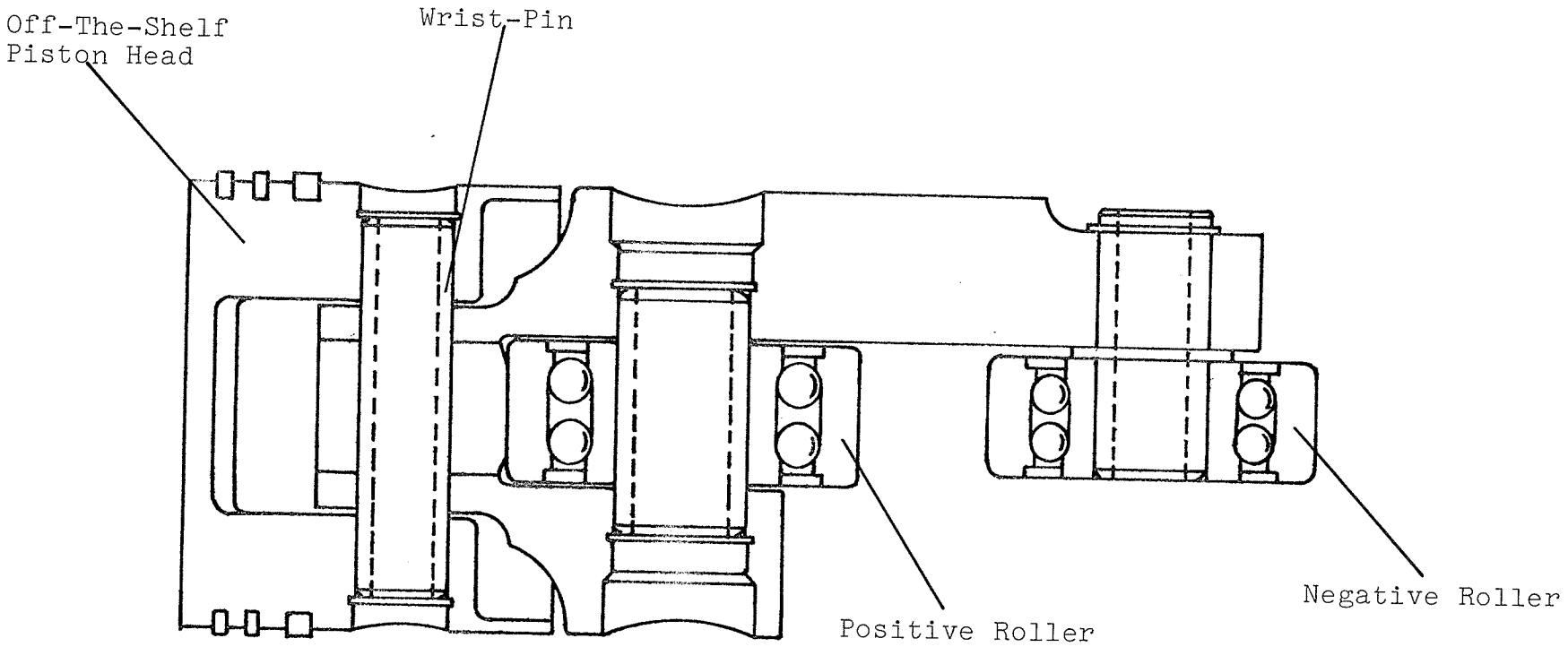

FIGURE 5-3 THE MARK II ENGINE PISTON ASSEMBLY

5.2-3 Performance of the Mark I and Mark II Pistons (Con't)

ineffective combustion limited both engines to low net output. The Mark I Engine developed a maximum of 10 BHP at 800 RPM and had a maximum speed of 1250 RPM. The Mark II Engine developed the same BHP and could reach 1500 RPM.[45] For the Dash-3 engine to have an acceptable level of performance, it must exceed this output by many magnitudes.

To evaluate piston performance a cam and cam follower test rig was devised (Figure 5-4). The cam test rig consisted of two opposed cams, driving a pair of pistons sharing the same cylinder sleeve. The test rig's components were identical to those found in the Mark I Engine except that the rig's cams rotated and the cylinder remained stationary.

Early cam rig test results indicated that the cam follower mechanism suffered from unexpectedly high piston friction and these results were corroborated by non-fired motoring tests of the Mark I Engine.

The tests highlighted several sources that combined to make up the piston friction: the clearance between rollers and the cam running surface, the sliding of the rollers on the cam running surfaces, the piston rings, the sliding friction from the centrifugal loading and the cam pressure angle induced side loading of the piston.

The experimentally derived relationship between engine friction power loss and RPM is illustrated in Graph 5-5.

FIGURE 5-4:

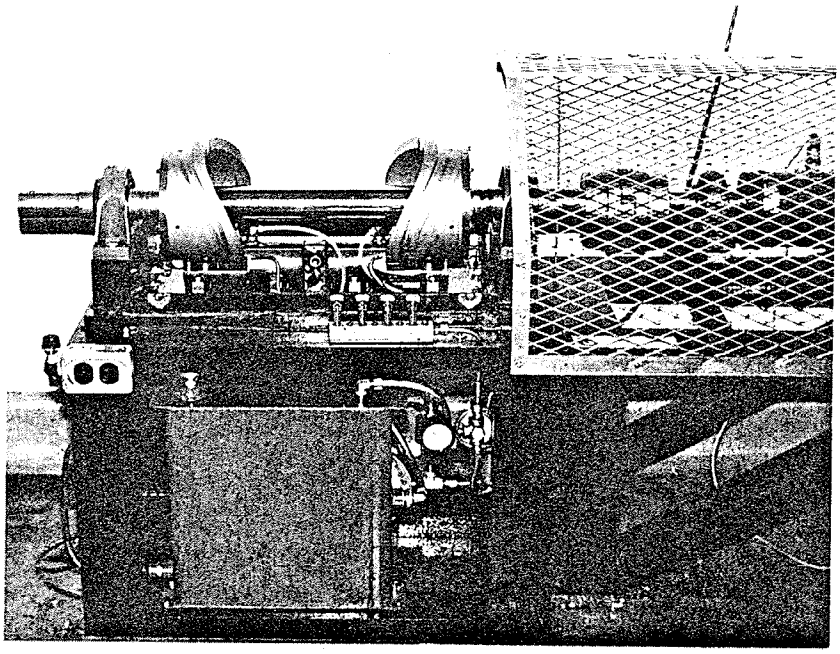

CAM TEST RIG

GRAPH 5-5

THE MARK I ENGINE: BREAKDOWN OF FRICTION LOSSES AS A FUNCTION OF ENGINE SPEED

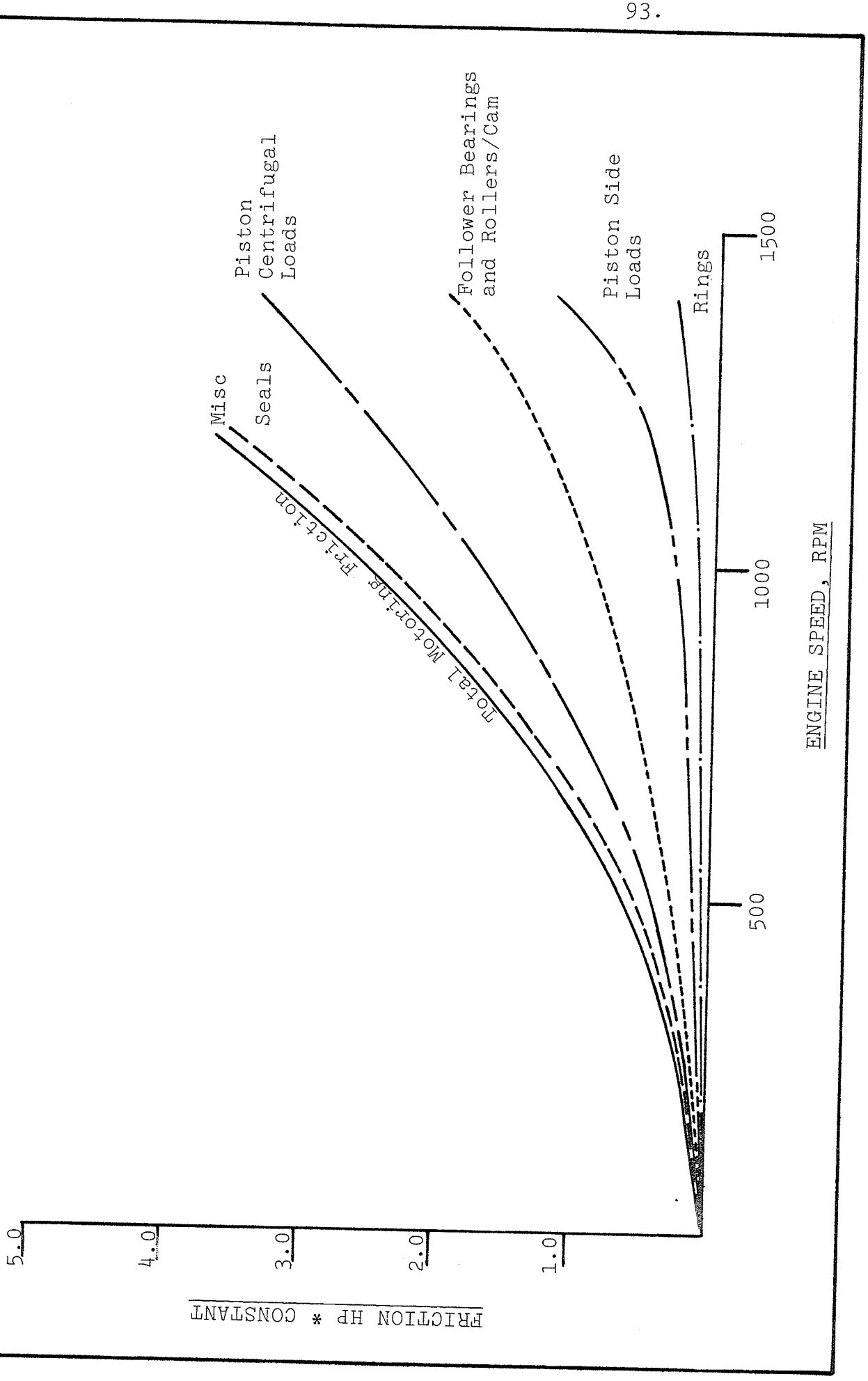

5.2-3 Performance of the Mark I and Mark II Pistons (Cont'd)

The friction components due to the rings, bearings and rollers to cam were isolated in the cam test rig. Piston friction due to the cam pressure angle induced side loads made up the remaining friction generated in the cam test rig. By Subtracting the cam rig friction and the known seal friction from the total engine motoring friction and estimating pumping losses, the remaining centrifugal load piston friction was identified.

It is interesting to note that the majority of the engine friction is produced by the pistons and consequently any effort to significantly reduce engine friction should be focused here.

Graph 5-6 shows the large penalty imposed by the piston friction even with optimum indicated horsepower for the Mark I Engine . The indicated horsepower curves were derived for a 8.0:1 compression ratio, 2.0 expansion ratio spark-ignition engine which results in an ideal inherent thermodynamic efficiency of 60%. A stoichiometric air/fuel ratio and an 80% volumetric efficiency were assumed.

Even with a combustion efficiency of 90% (the amount of fuel burned of that which is available), Graph 5-6 shows that the Mark I Engine will not exceed 50 BHP if the total engine friction is of the magnitude shown in Graph 5-5.

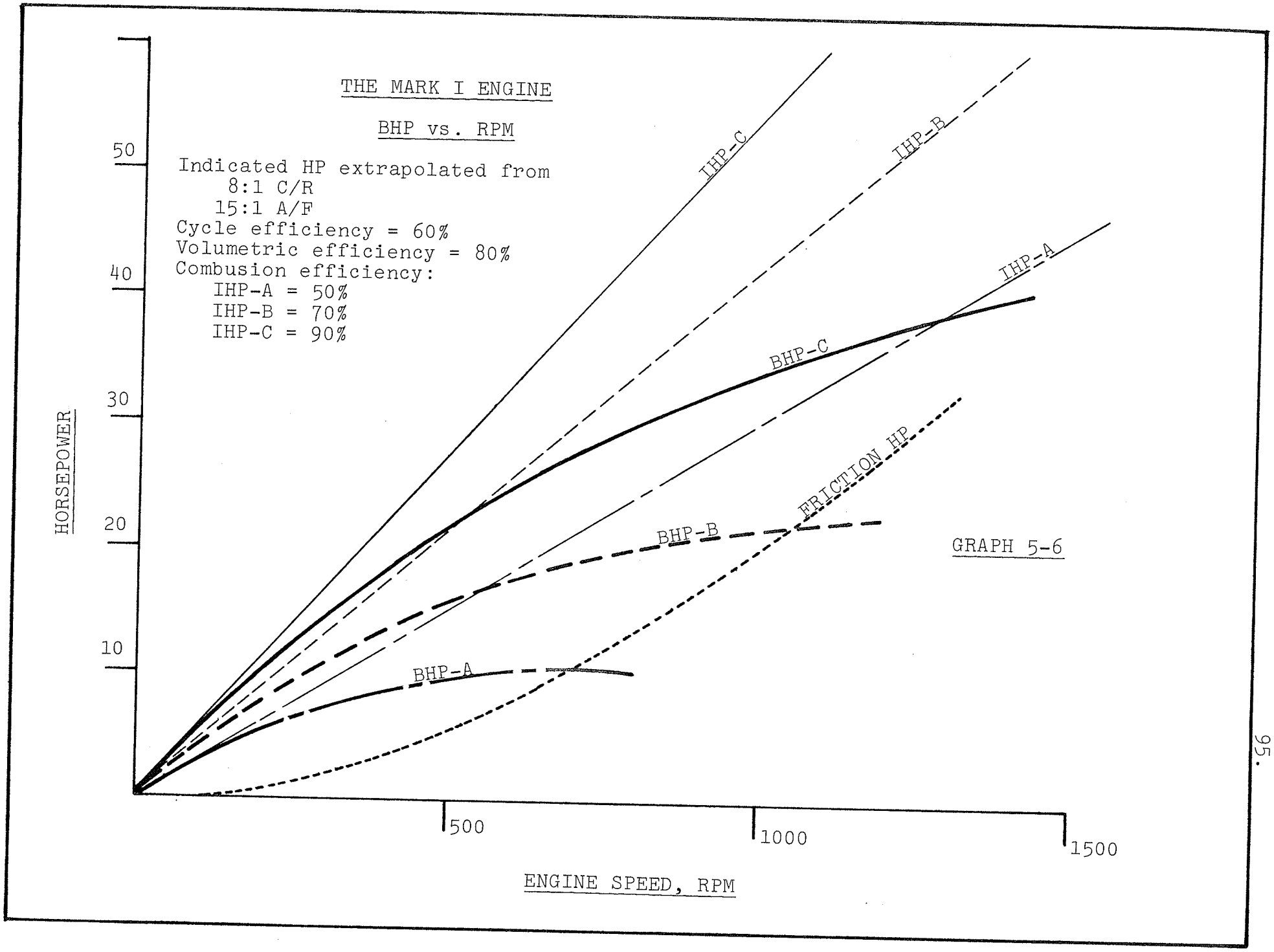
THE MARK I ENGINE
BHP vs. RPM
Indicated HP extrapolated from
8:1 C/R
15:1 A/F
Cycle efficiency = 60%
Volumetric efficiency = 80%
Combusion efficiency:
IHP-A = 50%
IHP-B = 70%
IHP-C = 90%
IHP-C
IHP-B
IHP-A
BHP-C
BHP-B
BHP-A
FRICTION HP
GRAPH 5-6
HORSEPOWER
50
40
30
20
10
500
1000
1500
ENGINE SPEED, RPM

5.2-3 Performance of the Mark I and Mark II Pistons (Con't)

Graph 5-8 shows the mechanical efficiency of the Mark I mechanism for the performance curves of Graph 5-6. This is compared to Graph 5-7 which illustrates the mechanical efficiency and friction losses found in a conventional crankshaft Otto-cycle engine.[25] Clearly the friction will have to be drastically reduced from that of the Mark I Engine, especially at higher speeds, if the Dash-3 level of performance is to approach that of the conventional engine.

5.2-4 Reduction of the Engine Piston Friction

The three types of piston friction defined in the Mark II Engine research will be present and therefore must be dramatically reduced in the Dash-3 Engine in order to obtain respectible output. The rotating cylinders, stationary cam and autonomous piston configuration specified for the Dash-3 prevents the total elimination of any of these three friction components.

Section 4.3-3 demonstrates that at any given engine speed the piston roller to cam loading and the cam pressure angle induced side loading are a function of the gas pressure loading and inertia loading, while the piston centrifugal loading is a function of piston weight.

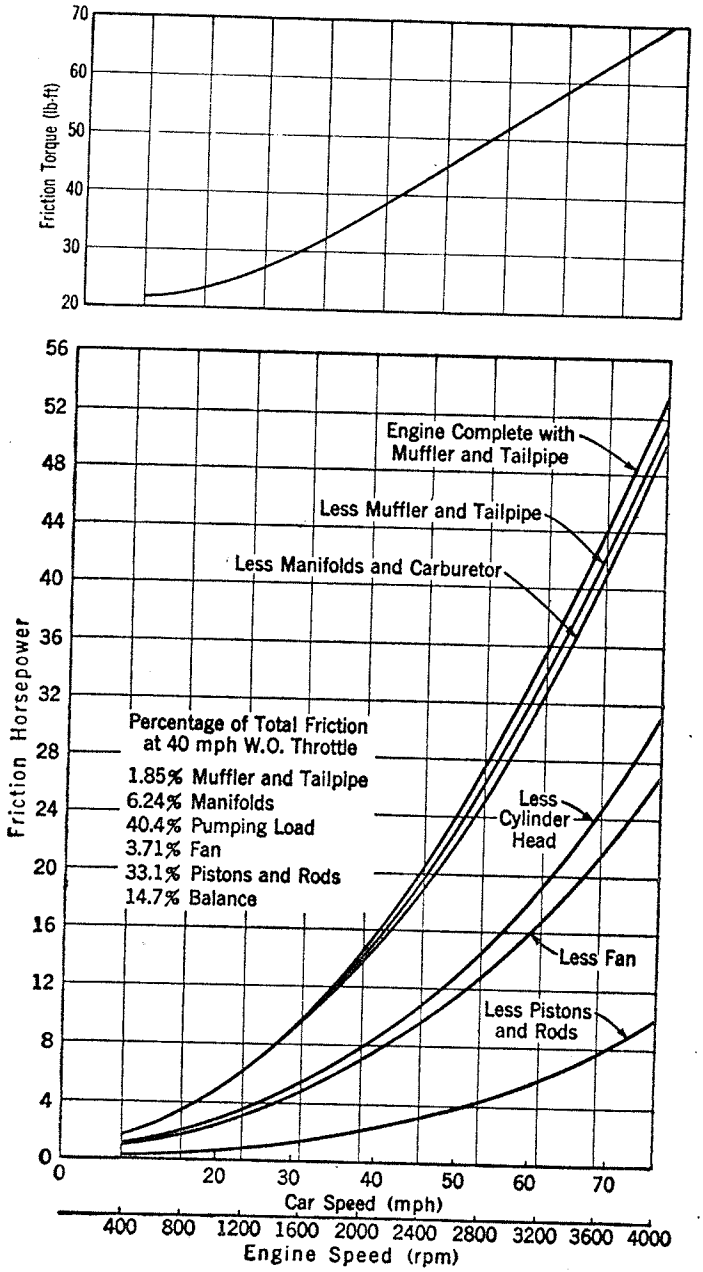

Variation of friction horsepower and torque of an SI engine with speed at wide-open throttle. (After Youngren, Reference 1.)

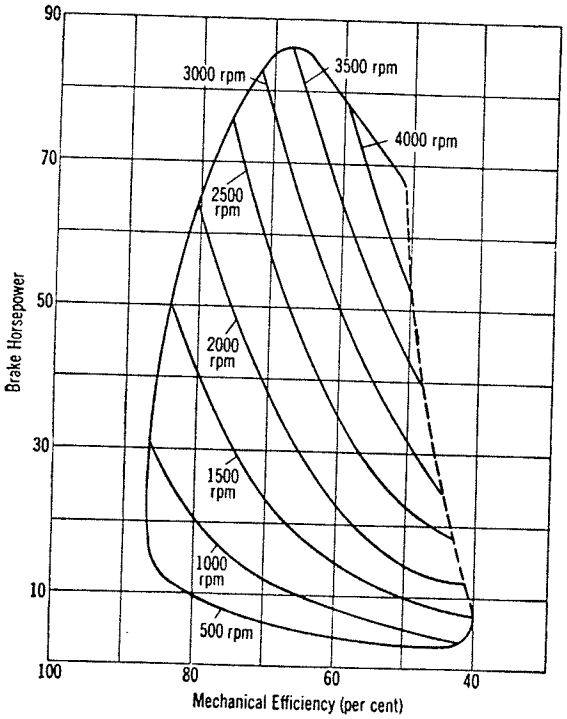

Mechanical efficiency of SI automotive engine. Dash line represents road load. (From Youngren, Reference 1.)

GRAPH 5-7: FROM REFERENCE 25

THE MARK I ENGINE

MECHANICAL EFFICIENCY vs. ENGINE SPEED

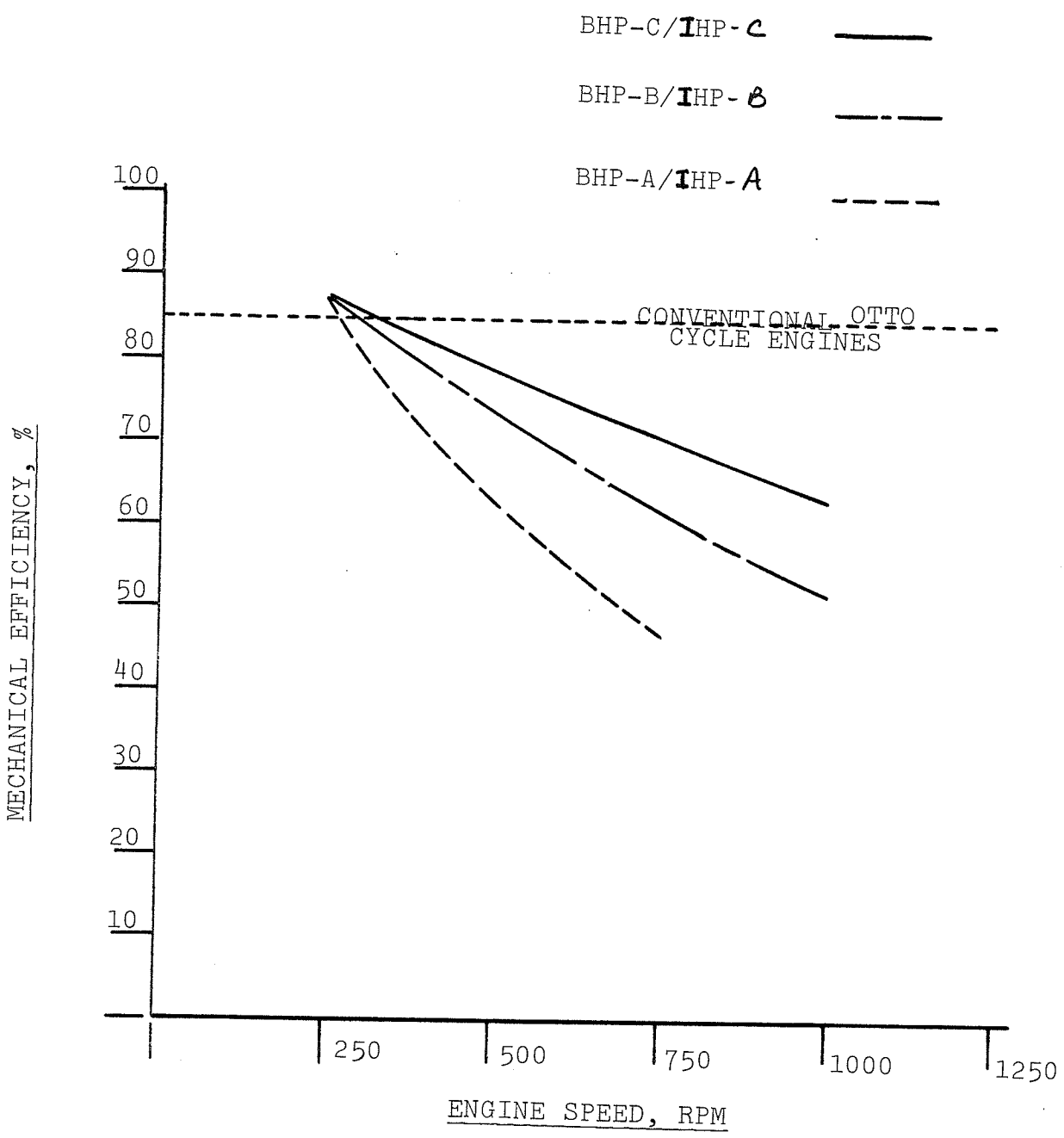

GRAPH 5-8

5.2-4 Reduction of the Engine Piston Friction(Con't)

The magnitudes of the piston friction are a function of the normal force perpendicular to the sliding surface and the coefficient of friction. While it would be detrimental to the indicated horsepower to reduce the cylinder pressure induced gas loading, Equations 4-6, 4-17 adn 4-21 show that any reduction in piston weight will proportionately reduce the inertia loading and hence piston friction for any given engine configuration at any engine speed.

Any reduction in the coefficient of friction generated in the sliding motion of the piston in its bore and the rollers on the cam will also result in a friction horsepower reduction.

The magnitudes of friction coefficients involved in the large power losses illustrated in Graph 5-5 can be examined with the use of Equation 4-7:

$$HP_{CF} = (1.44 \times 10^{-10}) \frac{\mu M Q d^2 N^3}{R k^2 \text{SIN}(\frac{360}{2Q})} (\frac{1}{E_R} + 1)$$

(Equation 4-7)

$$12.0 = (1.44 \times 10^{-10}) \frac{\mu(2.4)(8)(2.5)^2(1200)^3}{(3.27)(.82)^2 \text{SIN}^2 \frac{360}{16}} (\frac{1}{1.96} + 1)$$

Or $\mu = 0.089$

This value is on the upper bounds of that for mixed film lubrication[27] with $\mu = .02$ being possible for a refined

5.2-4 Reduction of the Engine Piston Friction (Con't)

mixed film slider. Any further improvement can only be made with a transition to full thick film lubrication which may not be possible with a reciprocating slider. Such an improvement in the mixed film friction coefficient is possible through careful refinement of the slider mechanism but not within the scope of a basic optimization such as this.

The sliding friction between the rollers and the cam running surfaces can also be reduced. This friction arises from the sliding of the roller line contact. Because of the different inside and outside diameters of the cam running surface, the outside edge of the roller will attempt to run at a higher surface velocity than that of the inside edge resulting in the sliding motion.

There are two possible means of reducing the amount of sliding: introduce a taper into the cam running surface to eliminate the differential surface velocity or to crown the roller contact surface. The tapered roller and cam is not a very satisfactory solution as it imposes an additional piston side load parallel to that of the centrifugal load which is already too high. A tapered surface may also be difficult to machine. The crowned roller can be introduced at any time in the Dash-3 Piston Development Program and can be considered a refinement process.

5.2-4 Reduction of the Engine Piston Friction (Con't)

Because of the line-contact between the roller and cam, marginal thin film or even metal to metal friction coefficients will probably be all that can be expected--at least for the type of configuration being considered for the Dash-3 Engine.

It is quite obvious that the most expedient and efficient method of reducing all three piston friction components is to reduce the total piston weight and subsequent inertia loading. A successful Dash-3 piston must, therefore, undergo a significant weight reduction compared to its predecessors in order to surpass the marginal performance of the first two prototype engines.

5.3 OPTIMIZING THE DASH-3 PISTON

5.3-1 Obtaining a Lightweight Piston

In determining the means of obtaining a lightweight Dash-3 Piston, whose function is essentially identical to its predecessors, the design of the latter should be examined for areas of possible weight reduction. At the same time, the design parameters of the early pistons should be re-examined to determine if they are still valid. Figure 5-9 shows a piston from the Mark II prototype engine with the weight distribution for its components. It should be noted that the total weight is 2.3 pounds: a far cry from the original design goal of one pound for the similar Mark I

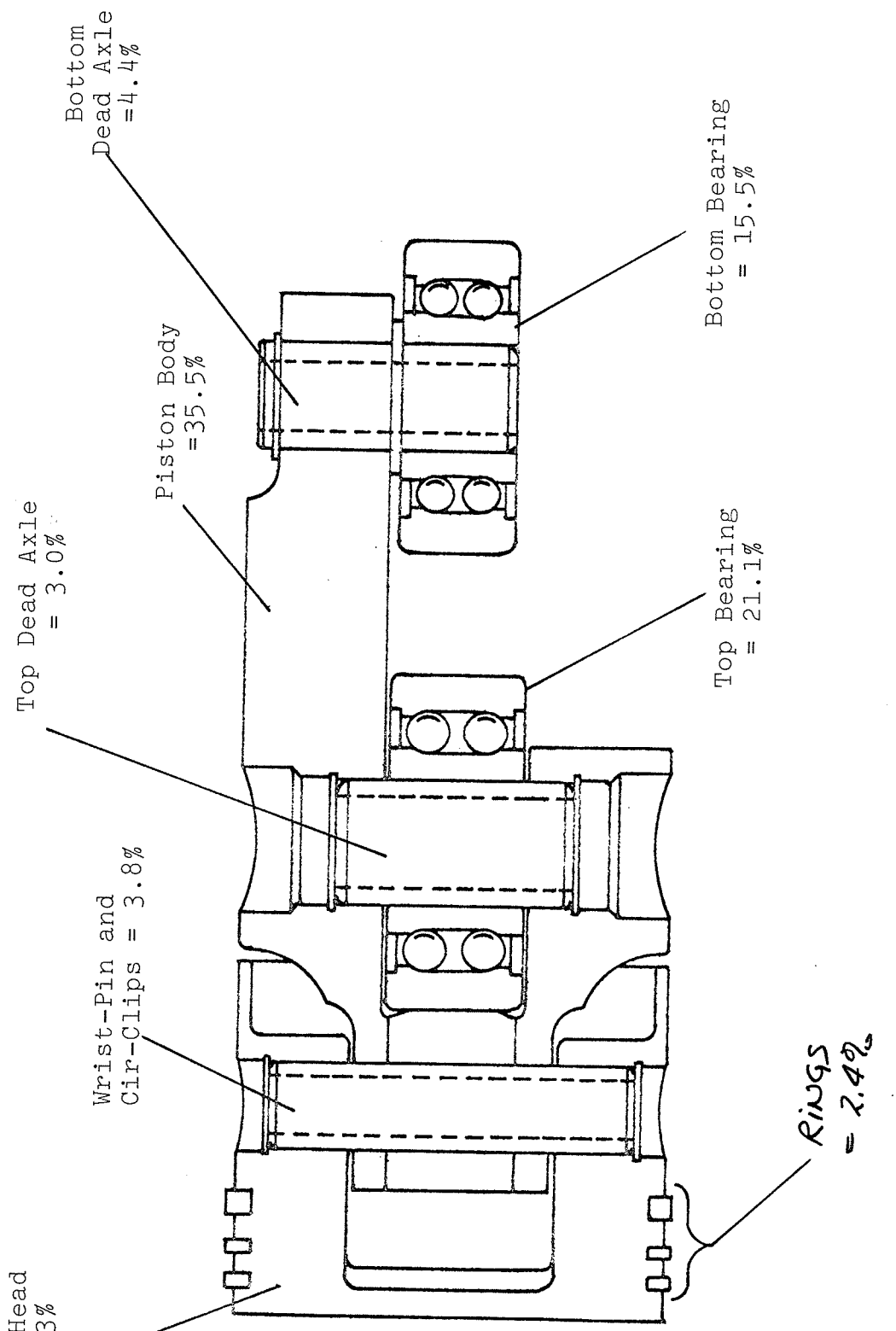

FIGURE 5.9 WEIGHT DISTRIBUTION OF THE MARK II PISTON COMPONENTS
(% of total piston weight of 2.31 pounds)

5.3-1 Obtaining a Lightweight Piston (Con't)

piston (which weighs 2.4 pounds in its current form).

One of the design goals discussed in Chapter 3 is that the total weight of the Dash-3 piston not exceed one pound. As was the case with the original Mark II piston, unless this goal is met, the probability of attaining reasonable component load is quite remote.

Examination of the piston in Figure 5-9 reveals that there are several obvious areas of possible weight reduction. One is the sustitution of a fixed piston head (similar to the original Mark I piston, Figure 5-1) for the heavier off-the-shelf piston head and unnecessary wrist-pin. Another area would be to lighten the piston body by optimizing its strength to weight ratio.

As the piston body is to be constructed of aluminum and will retain the same basic function in the Dash-3 Engine, only marginal reductions in piston body volume and hence overall piston weight are possible without seriously compromising the function of the design.

Scrutiny of Figure 5-9 shows that the bearings and axles account for almost half of the total piston weight and their weight alone exceeds our design goal of one pound. It is obvious that any significant weight reduction will have to take place here.

5.3-2 Optimizing the Roller/Bearing Combination

Three of the possible top cam roller/bearing configurations which use commercially available bearings are illustrated in Figure 5-10: the separate roller and live axle with straddled bearings (5-10A) such as that used in the Mark I Engine, the combination radial and thrust bearing "track-runner" (5-10B) used in the Mark II Engine and the needle roller track runner bearing which requires a separate thrust bearing (5-10C).

It can be seen that in configuration (5-10A) and (5-10C) and to a somewhat lesser extent in (5-10B), that significant weight losses can be obtained by reducing the roller diameter. Since weight is proportional to diameter squared, there are several factors that are a function of roller diameter: the cam/roller Hertz contact stress and the effect of increased roller speed on bearing life.

A measure of the extent that the line contact pressure of the roller loads the running surface of the cam is given by the Hertz contact stress. The Hertz stress assumes that the line contact deforms into an elliptical contact area and for a roller and cam of the same material can be expressed as:

$$Sc = \sqrt{\frac{F\left(\frac{1}{R_1} + \frac{1}{R_2}\right)}{2\,\pi\,b\,\left(\frac{1-\mu^2}{E}\right)}} \qquad \text{psi} \qquad \text{(Equation 5-1)}$$

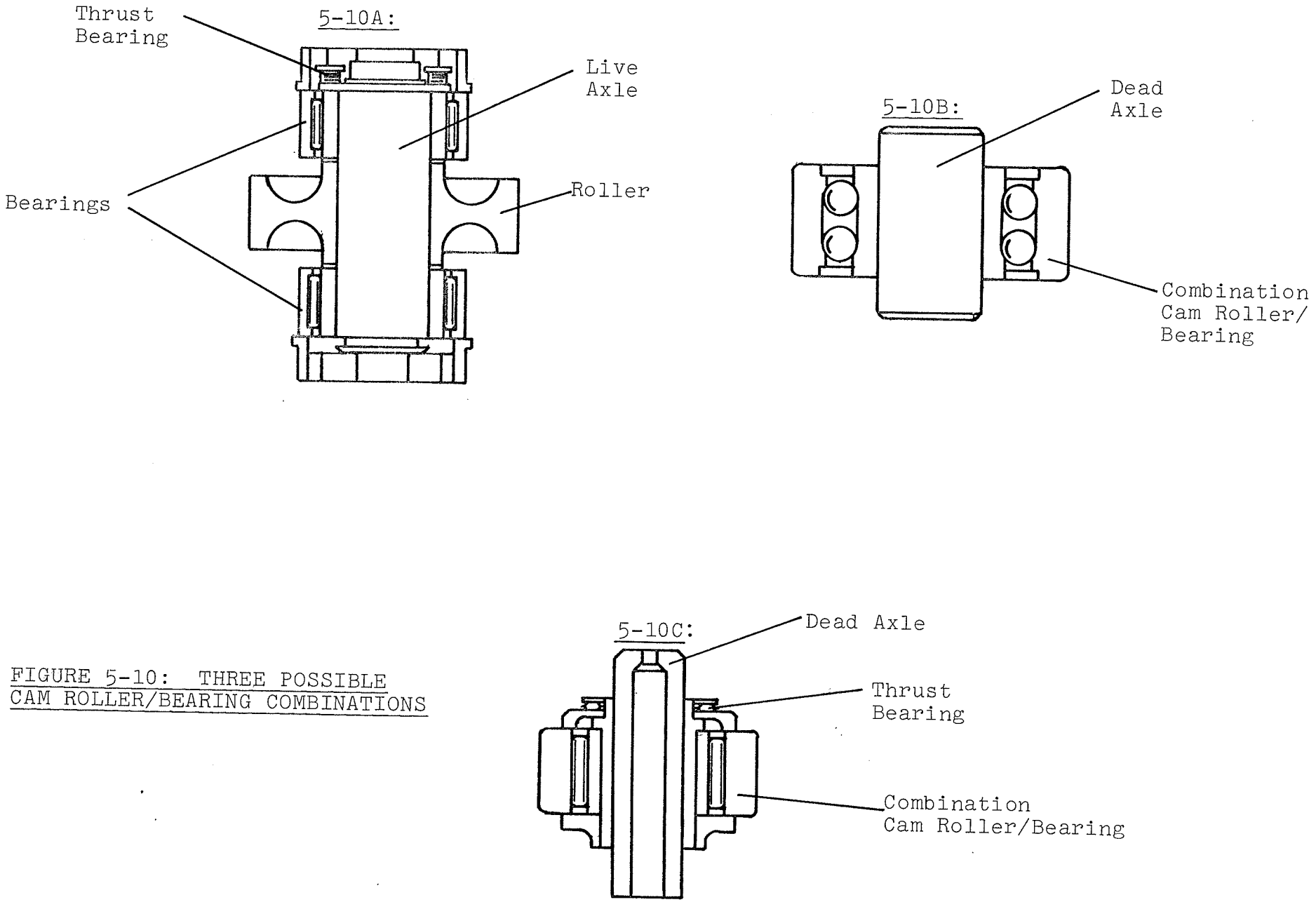

FIGURE 5-10: THREE POSSIBLE CAM ROLLER/BEARING COMBINATIONS

5.3-2 Optimizing the Roller/Bearing Combination (Con't)

WHERE:

S_c = Hertz contact stress

F = Total force acting on the roller

R_1 = Roller radius

R_2 = Cam radius

b = Roller contact width

and μ and E are Poisson's ratio and the modulus of elasticity for the common cam and roller material.

The Hertz contact stress is also a good indicator of the wear life of the meterial if sliding and rolling occurs under lubricated conditions. With the other variables held constant we have the following relationships which are shown in Graph 5-11. It can be seen that reducing the roller diameter or the roller contact width has an equal and non-excessive effect on the contact stress.

Any reduction in roller diameter for a given bearing will result in an increase in bearing speed and a corresponding reduction in bearing life. The rated life equation[29] for bearings operating at constant speed is:

$$L_{10h} = \frac{10^6}{60\ N} \left\{\frac{(C)}{(P)}\right\}^3 \qquad \text{(Equation 5-2)}$$

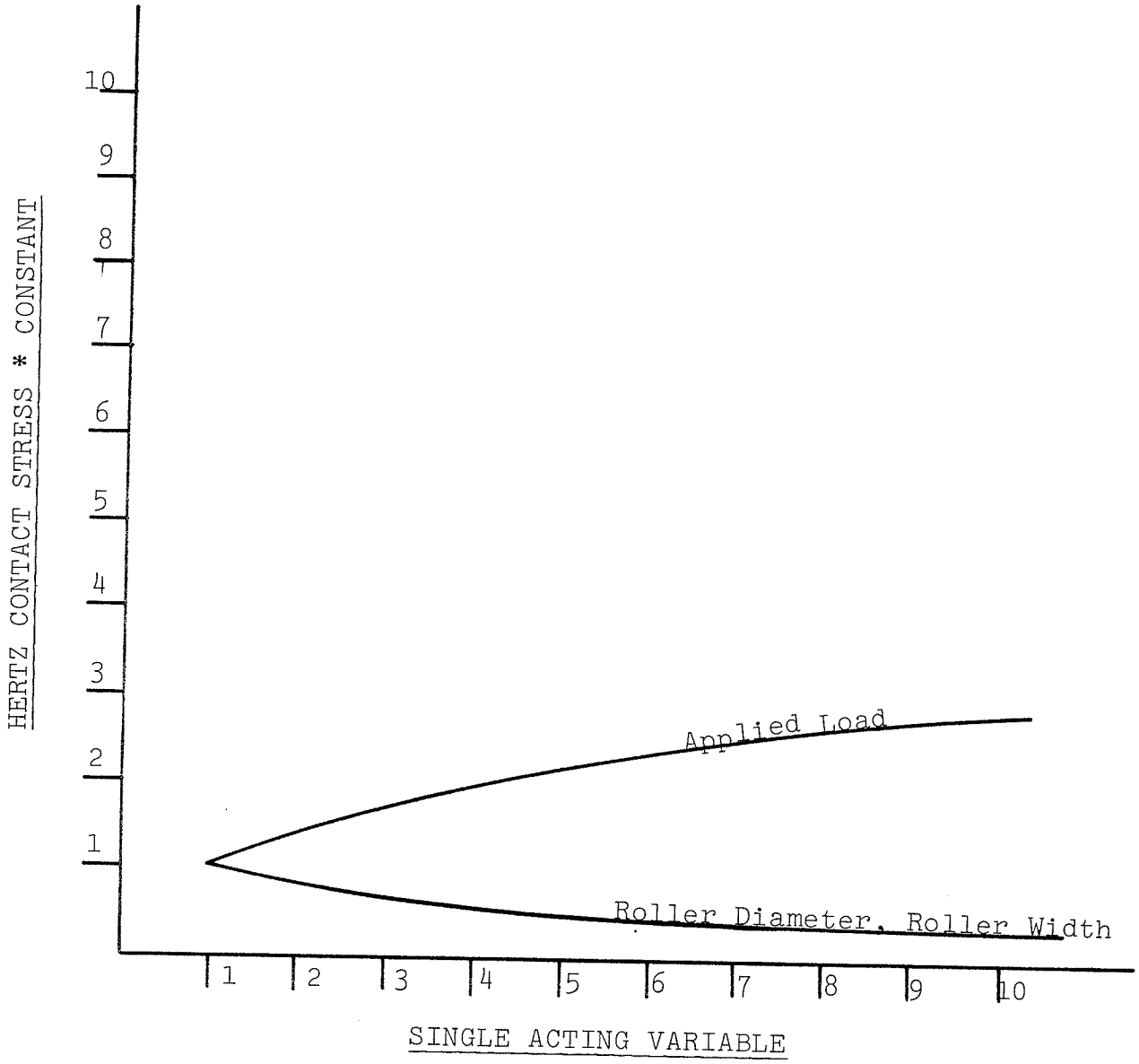

GRAPH 5-11 THE EFFECT OF APPLIED LOAD, ROLLER DIAMETER AND ROLLER WIDTH ON ROLLER/CAM HERTZ CONTACT STRESS

5.3-2 Optimizing the Roller/Bearing Combination (Con't)

WHERE,

L_{10h} = The basic rating life in operating hours

N = Rotational speed, RPM

C = Basic dynamic load rating

P = Equivalent dynamic bearing load

The influence that each variable has on the basic life rating is shown in Graph 5-12. It is quite obvious that bearing speed can undergo a large increase before having a significant effect on bearing life. Graph 5-12 does illustrate the dramatic influence that the ratio of dynamic load rating to equivalent dynamic load has on bearing life. After minimizing the cam roller size with respect to weight, further weight reduction of the roller/bearing assembly can be obtained by specifying a lighter bearing with a proportionally lower dynamic load rating. The (C/P) curve in Graph 5-12 shows that such a reduction in dynamic load results in an overwhelming drop in bearing life.

In summary, it seems more plausible to obtain a reduction in cam roller weight by minimizing its diameter and perhaps increasing the contact width to meet loading requirements rather than reducing the width and increasing the diameter. A reduction in roller diameter alone will not overwhelmingly increase the Hertz contact stresses and the corresponding increase in bearing operating speed willnot appreciably

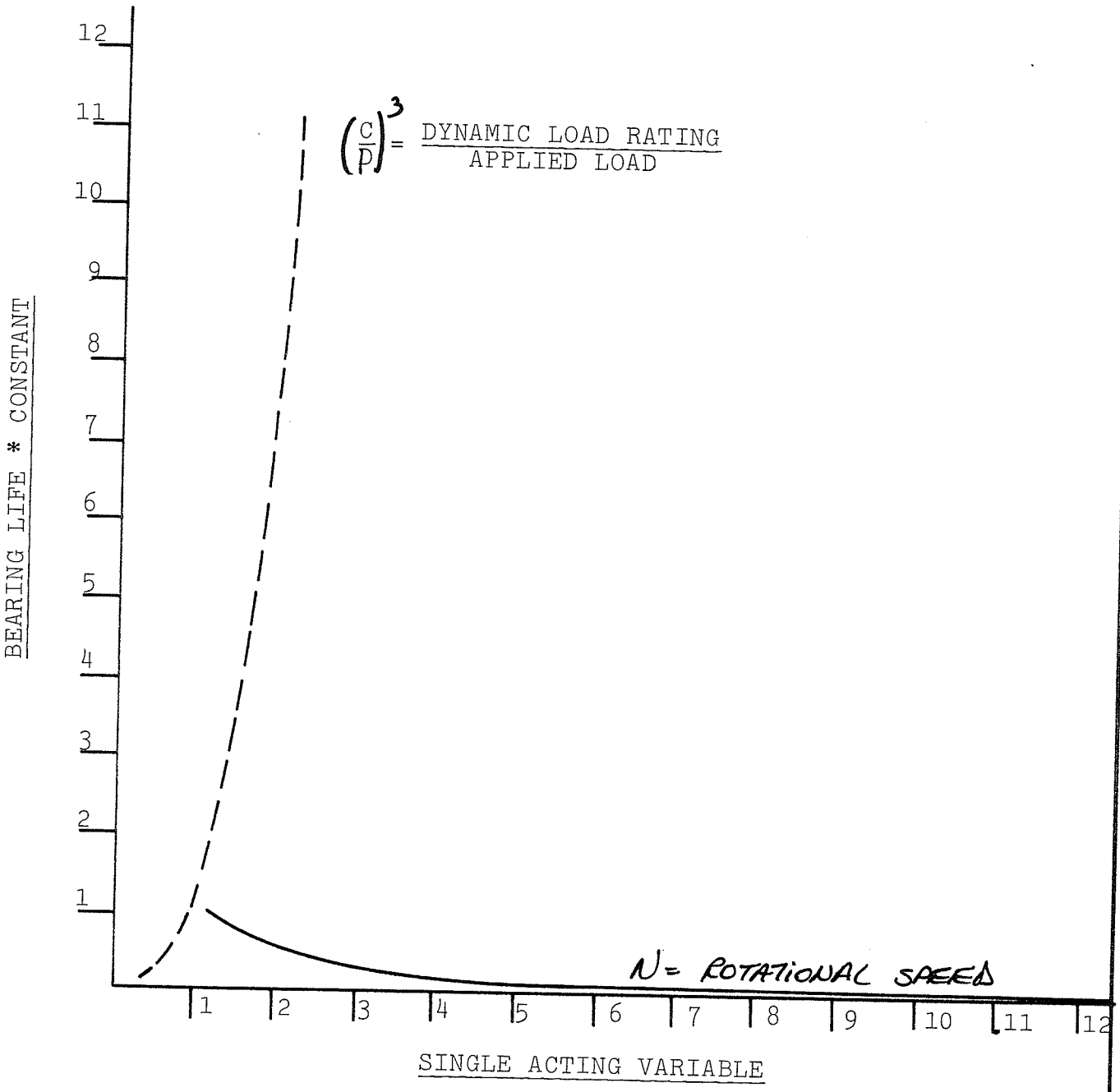

FIGURE 5-12 THE EFFECT OF BEARING SPEED AND THE RATIO OF DYNAMIC LOAD RATING TO APPLIED LOAD ON BEARING LIFE

5.3-2 Optimizing the Roller/Bearing Combination (Con't)

reduce the bearing life. To obtain a truly significant weight reduction of the cam roller/bearing system, a reduction in bearing size should also be considered. This will influence bearing capacity and life and the effect will be considered in the next section.

5.3-3 Dash-3 Piston Revalued Design Parameters

It is quite obvious from Graph 5-6 that even with optimum combustion efficiency that a significant reduction in mechanical losses must occur before respectible engine output can be obtained.

The previous section has concluded that the most expedient method of reducting these losses is by piston weight reduction. Some weight loss can be attained through careful re-design by optimizing the strength to weight ratio of the aluminum piston structure but more than fractional gains with this method are quite unlikely.

The truly significant weight reductions (those in the order of 50%) are only possible with compromised design parameters with the most obvious being those associated with the heavy cam follower rollers and bearings.

It is appropriate at this time to re-examine the design goals of the Mark I piston. The Mark I piston was initially designed

5.3-3 Dash-3 Piston Revalued Design Parameters(Con't)

to transmit the gas and inertia forces of a compression ignition engine with maximum cylinder pressures of 1000 psi via a cam that generated cycloidal motion with a 2.5:1 expansion ratio and a 15° dwell at TDC and was intended to reach a maximum engine speed of 4000 RPM. With the original design weight of one pound the top roller bearings of this piston had a design life of approximately 50 hours at an average engine speed of 2500 RPM when using cubic mean average bearing loads.

The cubic mean is the recommended method for assigning a dynamic load value for a bearing undergoing shock loading such as that encountered with the combustion process.

The final version of the Mark I and Mark II engines were spark ignition engines with a simple harmonic cam using a 2.0:1 expansion ratio. These engines utilized the heavier pistons illustrated in Figure 5-2 and Figure 5-3. Although these pistons increased the inertia loading, the relaxed combustion gas loading resulted in slightly better top and bottom bearing life expectation for both engines in comparison to the original Mark I's 50 hour life. The details of the reduced bearing loads and improved life are shown in Table 5-13.

The Dash-3 Engine will also have the advantage of the more lenient combustion gas loading--being specified as an 8.0:1 compression ratio spark ignition engine (Section 3.3-2)-- and a more gentle cam motion (Section 4.3-2)--such as those of its latter day predecessors.

TABLE 5-13

COMPARISON OF CALCULATED BEARING PERFORMANCE
FOR THE MARK I AND MARK II ENGINES

- simple harmonic motion - no dwell - 2.0:1 expansion ratio	MARK I	MARK II
Engine RPM	2000	2000
Piston Weight, lb.	2.4	2.4
Peak TDC Cylinder Pressure,psi	810	810
Top Bearing(s) cubic mean average load, lbf	5168	5168
Bottom Bearing cubic mean average load lbf	2041	2041
Top Bearing(s) used	TWO SKF NU 4903 (See Fig. 5-10A)	ONE SKF 305704 (See Fig. 5-10B)
Top Bearing Life, hours	226	72
Bottom Bearing Used	ONE SKF 361204	ONE SKF 305703
Bottom Bearing Life, hours	56	559

5.3-3 Dash-3 Piston Revalued Design Parameters (Con't)

Because of the "one off" -- custom fabricated nature of the Dash-3 Engine as were the Mark I and Mark II, its pistons are restricted to commercially available bearings. The most efficient in terms of weight per load capacity being those with integrated cam roller/bearing outer races. A comparison of b/o lives and weights for various "SKF" track runner bearings is shown in Graph 5-14.

In conclusion, the Dash-3 Piston can attain significant improvement in total engine mechanical efficiency via a lightweight design. It has been shown that the greatest reduction in piston weight is obtained by careful seletion of the cam follower rollers and bearings. As bearing capacity and life is proportional to bearing size and weight, bearing life will probably have to be compromized[33] in exchange for reasonable piston friction losses.

GRAPH 5-14

BEARING LIFE vs. BEARING WEIGHT
for commercially available SKF
track runner bearings.

NOTE:
*Comparison is made with the same gas and inertia loading

*$K_s \alpha$ ENGINE RPM $^{-1}$

Indicates bearing used in the Mark II Positive Cam Follower

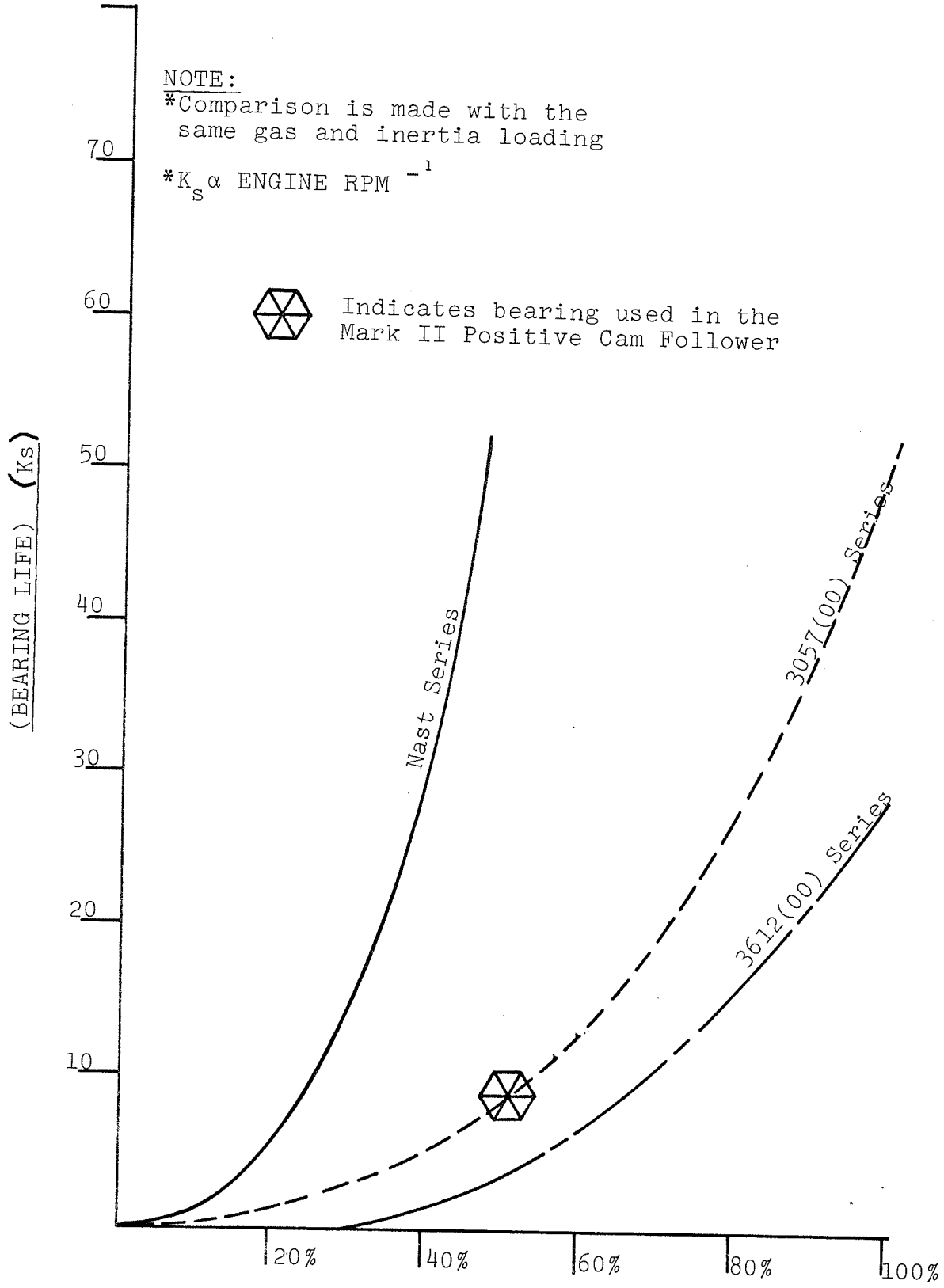

CHAPTER 6

OPTIMIZATION OF THE INDICATED POWER POTENTIAL

6.1 INTRODUCTION

The optimization of the Dash-3 Engine would be a partial one if the only factors considered were those of the mechanical and geometrical configuration presented in Chapter 4, or those contributing to minimal mechanical losses via a light-weight piston in Chapter 5. Not only must the Dash-3 Engine ensure that its power potential is translated to useful work with a minimum of losses, but it must have a configuration that is inherently able to realize this potential in the first place. In this chapter, some of the factors that tend to detract from the optimum combustion process will be examined and it will be determined if the majority can be excluded from the Dash-3 Engine configuration.

6.2 THE COMBUSTION PROCESS

6.2-1 Factors Affecting the Combustion Process

As is the case with the conventional spark ignition engine, the K-Cycle Engine's real life pressure-volume diagram will not realize the magnitude of indicated work associated with its equivalent fuel-air cycle PV diagram. The difference between the ideal and the actual can be attributed to the following factors:

A. Time Loss: Due to the time required for the mixing of the air and fuel and the time taken to complete the combustion process.

6.2-1 Factors Affecting the Combustion Process (Con't)

B. Heat Loss: Due to the flow of heat from the combustion gases to the walls of the combustion chamber.

C. Exhaust-Blowdown loss: Due to the loss of work potential when the exhaust valve or port opens prior to the end of the expansion stroke.

D. Gas Leakage: Due to the piston rings and valves in the crankshaft engine or to the piston rings and seals in the K-Cycle Engine. These losses are negligible in the former but may be significant at low speeds in the latter.

A graphical illustration of how these losses affect the fuel-air cycle of a conventional Otto cycle engine is shown in the PV diagram of Graph 6-1.

In any engine, the magnitude of these losses is governed by a number of primary design and performance variables:

* Spark plug position
* Combustion chamber shape
* Mixture condition at ignition
* Thermal characteristics of the combustion chamber
* Ignition timing

Each of these parameters has an effect on the other in the manner shown in Figure 6-2, and combine and interrelate to determine the efficiency of the combustion process.

The engine configuration chosen in the mechanical and geometrical optimization of Chapter 4 will be examined in

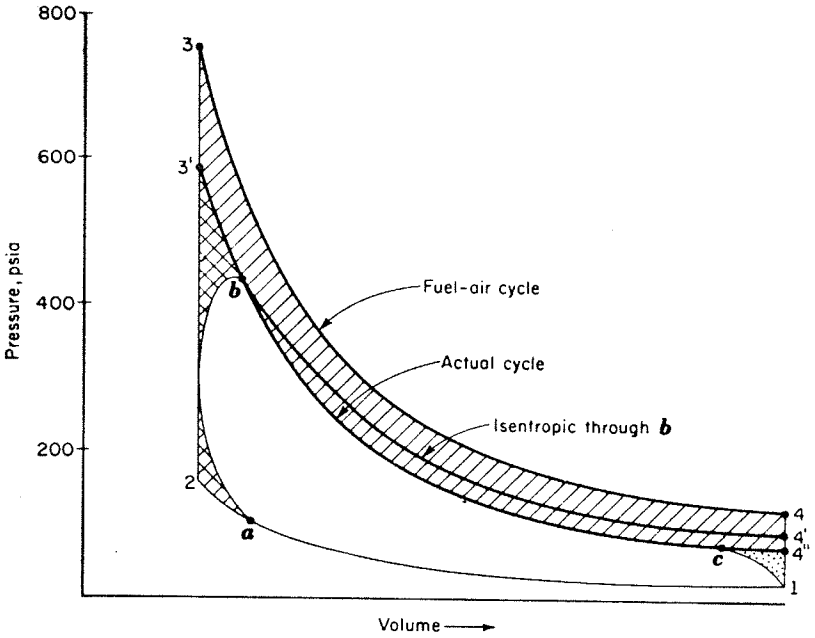

Definition of losses between a real cycle and its equivalent fuel-air cycle; a = beginning of combustion pressure rise, b = end of combustion, c = start of exhaust-valve opening.

Time loss
Heat loss
Exhaust-blowdown loss

GRAPH 6-1: FROM REFERENCE 47

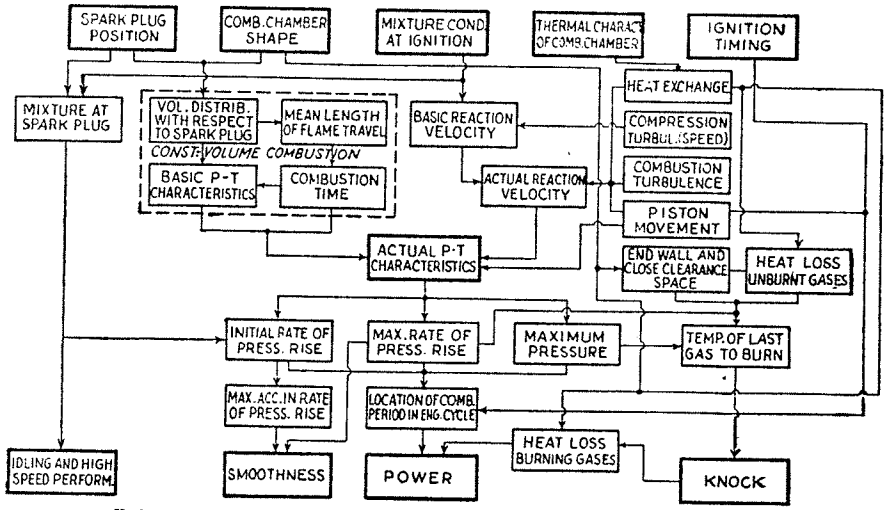

Relation of the various factors affecting the actual combustion process. (*Rabezzana and Kalmar.*)

FIGURE 6-2: FROM REFERENCE 48

6.2-1 Factors Affecting the Combustion Process (Con't)

the following sections for the severity of its inherent heat loss, time loss, and cylinder gas leakage characteristics.

The exhaust blow-down losses encountered in a conventional engine result primarily from the nature of the exhaust poppet-valve port system which requires the early opening of the valve to overcome the mechanism's inertia and the flow restriction presented by the valve itself. The cylinder ports of the K-Cycle face-seal engine are relatively free from these defects; therefore, it is expected that the exhaust blow-down losses will be considerably less than those of the conventional engine. Because of the K-Cycle's longer exhaust stroke the pumping work during this stroke may be slightly greater than that of the same stroke in the conventional four-stroke engine. These losses will be assumed to have a negligible effect on the overall performance of the K-Cycle due to its valveless exhaust port and low exhaust pressure.

6.2-2 Heat Losses from the Dash-3 Engine Configuration

It is generally acknowledged that there are two factors inherent in any piston engine that determine the amount of combustion chamber heat loss: the first is a "size-effect" that is a function of the cylinder bore diameter and the second is the surface-to-volume ratio of the combustion chamber itself.

6.2-2 Heat Losses from the Dash-3 Engine Configuration (Con't)

It has been found in the conventional piston engine that the heat loss varies with cylinder bore diameter: from a "hardly measurable quantity for very large cylinders working at high specific output" to "15 percent of the fuel-air cycle work for cylinders of automotive size operating at moderate piston speed". This difference is illustrated in the pressure-volume diagrams in Graph 6-3 and in Graph 6-4: the former a small bore special CFR engine with a 12 percent heat loss and the latter, a Wright aircraft cylinder with a 6.125 inch bore, and unmeasurable heat loss.

Taylor and Taylor[35] have defined an expression for a heat loss ratio (heat loss to the coolant with respect to the indicated power output of the equivalent fuel-air cycle) that is, among other variables, a function of cylinder bore diameter:

$$\text{Heat Loss Ratio} = C_3 \, f(Gd)^{-0.25} \, (T_g - T_c)$$

(Equation 6-1)

WHERE:

C_3 = Constant

f = Ratio of the indicated heat loss to the actual jacket heat loss

G = Mass flow of gas per unit time divided by piston area

d = The cylinder bore diameter

T_g = Mean cylinder gas temperature

T_c = Mean coolant temperature

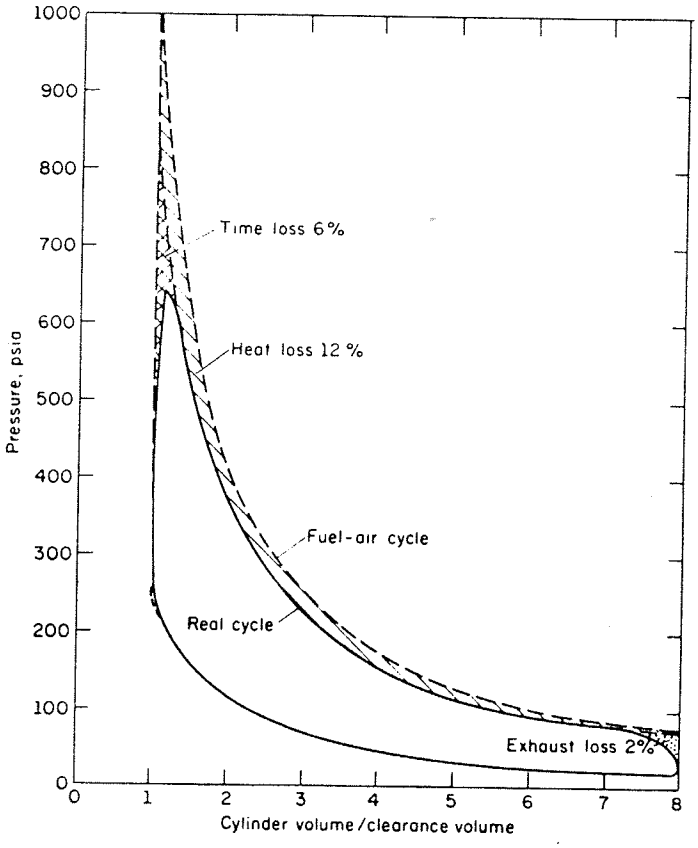

	Actual Cycle	Fuel-Air Cycle	Ratio, Actual Cycle to Fuel-Air Cycle
Imep	143	178	0.802
η_i	0.288	0.360	0.802
Time-loss ratio	0.06	.....	.....
Heat-loss ratio	0.12	.....	.....
Exhaust-loss ratio	0.02	.....	.....

Indicator diagrams for an actual cycle and its equivalent fuel-air cycle; special CFR engine, $F_R = 1.2$, $r = 8$, $s = 1120$ fpm, $M_a = 0.001025$ lbm/cycle, $f = 0.15$, gas temperature at 90° btc = 817°R, $p_i = 16.6$ psia, $p_e = 9.8$ psia, $T_i = T_e = 620$°R, $Gb = 0.072$ lbm/sec ft. (Livingood et al., 9.16.)

GRAPH 6-3: FROM REFERENCE 49

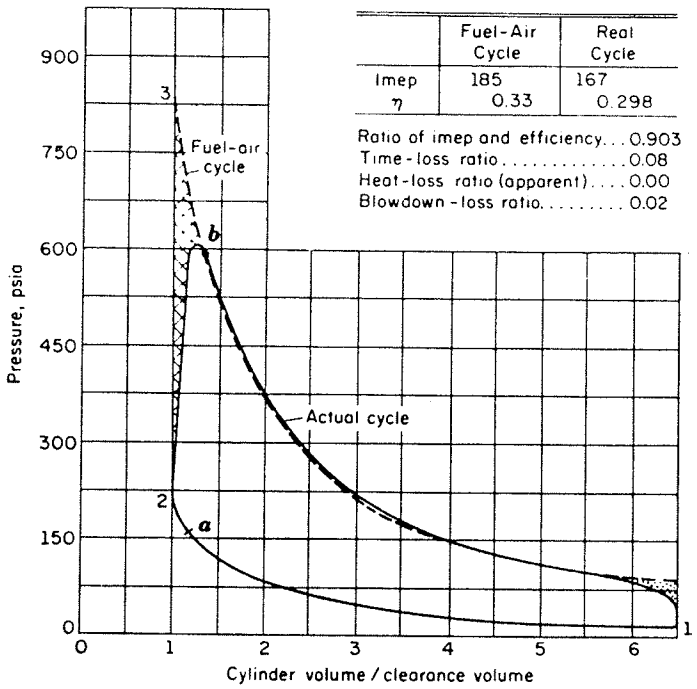

Comparison of pressures, real cycle vs. equivalent constant-volume fuel-air cycle. Wright Aircraft cylinder, 6⅛" x 6⅞", $r = 6.50$, $s = 1850$ fpm, $F_R = 1.175$, $p_i = 16.1$ psia, $p_e = 14.7$ psia, $sa = 15°$, $T_i = 702°$R, $f = 0.038$, air consumption = 0.008 lbm/cycle, $G_b = 0.334$ lbm/sec ft. (Courtesy Wright Aeronautical Corporation.)

GRAPH 6-4: FROM REFERENCE 50

6.2-2 Heat Losses from the Dash-3 Engine Configuration (Con't)

If all the variables other than cylinder bore diameter are held constant:

$$\text{Heat Loss Ratio} = (\text{constant})\ d^{-0.25}$$

(Equation 6-2)

With this relationship, the possible Dash-3 Engine configurations can be examined for inherent heat loss.

The engine configurations presented in Graph 4-19 have their geometric parameters governed by (Equation 4-4):

$$\text{Displ.} = \frac{\pi\ d^3\ Q}{2\ K\ \text{SIN}\ \frac{(360)}{(2Q)}\ (R)\ (ER)}$$

(Equation 4-4)

Combining (Equation 6-2) and (Equation 4-4), setting $k = 0.85$, $R = 2.89$ and $ER = 2.0$, as per the chosen configuration, and solving for the heat loss ratio in terms of intake displacement and the number of cylinders:

$$(\text{Heat Loss Ratio})\ (\text{Constant}) = \left\{\frac{(\text{Displ})\ \text{SIN}\ \frac{360}{2Q}}{(0.320)\ Q}\right\}^{-1/2}$$

(Equation 6-3)

~~This relationship is illustrated in Graph 6-5:~~ it is quite obvious that, as is the case with the conventional engine, the heat loss ratio of the K-Cycle Engine is reduced by increasing the cylinder bore.

Leaf blank to correct
numbering

6.2-2 Heat Losses from the Dash-3 Engine Configuration (Con't)

It can be concluded that the heat loss ratio of the configurations of Graph 4-19 can be minimized by approaching the maximum displacement with the lowest number of cylinders allowed by the continuous combustion port duration parameters.

The heat transfer from the combustion gases to the walls of the combustion chamber is proportional to the surface area of the combustion chamber itself. For any given cylinder bore diameter, the lower the surface-to-volume ratio, the lower the thermal losses. In addition, a combustion chamber with a low surface/volume ratio will tend to have minimal exhaust emissions with respect to unburned hydrocarbons, resulting from fuel plating on the walls of chamber.[36]

The surface-to-volume (S/V) ratio at TDC is governed by the actual shape of the combustion chamber itself. The "double hemisphere" chamber with a hemispheric depression in the piston to match the hemispheric dome in the cylinder head has one of the lowest possible S/V ratios, while a now obsolete 'L' head chamber has one of the highest. The combustion chamber shape and TDC S/V ratio of the Dash-3 Engine will be determined during the detailed design of the engine and is not a function of the primary design parameters in our configuration optimization.

While the TDC surface-to-volume ratio will control some of the engine's exhaust emissions and heat loss, the majority of

6.2-2 Heat Losses from the Dash-3 Engine Configuration (Con't)

the heat loss to the chamber walls occurs not at TDC but during the expansion stroke and the exhaust blowdown process. The distribution of the heat loss during the four strokes of a conventional Otto cycle engine are shown in Table 6-6 which was compiled by Taylor and Taylor.[37] For this particular example, 88% of the heat loss occurs during expansion and blowdown while only 8% occurs during combustion. It is quite likely that the majority of the heat loss of the K-Cycle Engine will also occur during its expansion stroke.

The tendency of the Dash-3 Engine configuration to reject heat during expansion is a function of the cylinder wall area presented to the gases, and can be examined via the cylinder's S/V ratio at the BDC of the expansion stroke (BDC-EXP).

In the K-Cycle Engine, for a given combustion chamber shape, intake displacement, and number of cylinders, the S/V ratio at BDC-EXP is controlled by the maximum allowable cam pressure angle. In the configuration optimization of Section 4.3, a pressure angle of 30^{o} was chosen for the dwell-free simple harmonic cam. This choice and its influence on the configuration optimization with respect to inherent heat loss will now be re-examined.

For the sake of simplicity, assume a BDC-EXP volume bounded by a flat-topped piston and a flat-faced cylinder head. The

Relative Heat Lost During Different Phases of the Cycle of a Spark-Ignition Engine

Phase	Duration, Crankshaft Degrees	Average Relative Area Exposed	Average Relative Density = 1 at Inlet	Estimated Average Relative Velocity = 1 at Inlet	Estimated Average Temperature, R	Average Temperature Diff, °F	Heat Lost	
							Relative %	% Heat in Fuel
Compression....	150	0.7	3	0.8	810	60	1	0.2
Combustion....	40	0.4	5	0.7	2860	2100	8	1.2
Expansion.....	125	0.7	3	0.6	3860	3100	40	6.0
Blowdown.....	90	1.3	0.7	3	3260	2500	48	7.2
Exhaust.....	135	1.1	0.3	0.9	2050	1300	5	0.7
Inlet.....	180	0.7	1	1	560	−200	−2	−0.3
Total.....	...	...	...	...	...	...	100	15

TABLE 6-6: FROM REFERENCE 37

6.2-2 Heat Losses from the Dash-3 Engine Configuration (Con't)

S/V ratio of such a chamber can be expressed as:

$$\frac{S}{V} = \frac{2\left\{\frac{\pi d^2}{4}\right\} + \pi d E}{\frac{\pi d^2}{4} E} = \frac{2 (d/E) + 4}{d}$$

(Equation 6-4)

WHERE:

d = Cylinder bore dia.

E = Expansion stroke length

AND (d/E) = bore to expansion stroke ratio

$$d/E = R\ k\ SIN\ \frac{(360)}{(2Q)}$$

(Equation 6-5)

By solving (Equation 4-4) for 'd' and substituting this into (Equation 6-4):

$$\frac{S}{V} = \frac{2 (d/E) + 4}{\left\{\frac{(Displ.)\ 2\ k\ SIN\ \frac{(360)}{(2Q)}\ (R)\ (ER)}{\pi Q}\right\}^{1/3}}$$

(Equation 6-5)

Rearranging to obtain S/V ratio for any intake displacement:

$$\left(\frac{S}{V}\right)\ (Displ)^{1/3} = \frac{2 (d/E) + 4}{\left\{\frac{2 (d/E)(ER)}{\pi Q}\right\}^{1/3}}$$

(Equation 6-6)

This relationship, as a function of the number of cylinders and maximum cam pressure angle, is shown in Graph 6-7. The maximum pressure angles were obtained from Graph 4-10 and incorporated into (Equation 6-5) via the term 'R'.

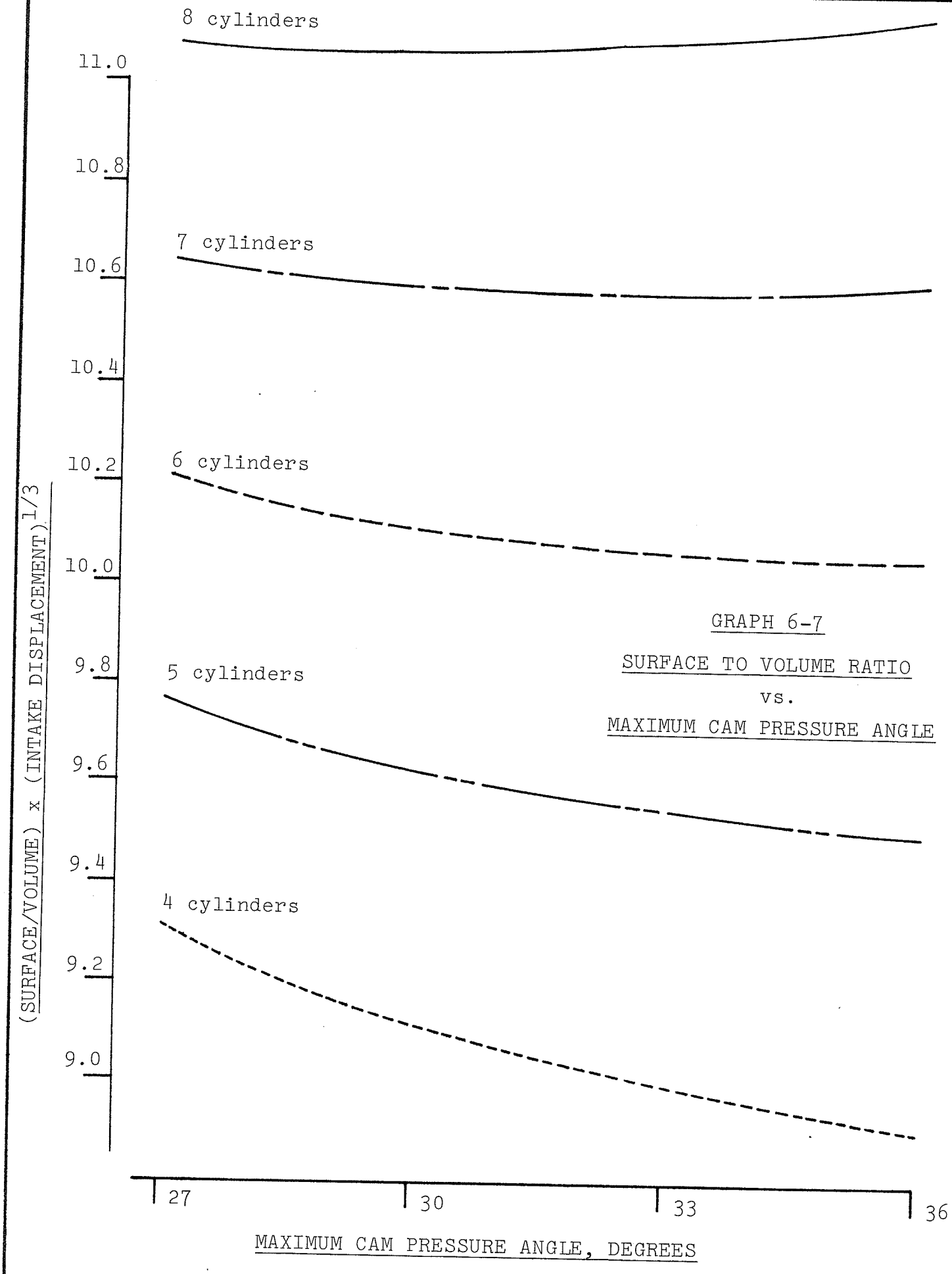

GRAPH 6-7

SURFACE TO VOLUME RATIO

vs.

MAXIMUM CAM PRESSURE ANGLE

6.2-2 Heat Losses from the Dash-3 Engine Configuration (Con't)

Graph 6-7 indicated that for engines with less than 7 cylinders, the S/V ratio at BDC-EXP can be reduced by increasing the maximum pressure angle with the amount of S/V ratio reduction increasing with a decreasing number of cylinders.

For a six cylinder engine, such as that specified for the Dash-3 Engine, in Section 4.3-5, increasing the maximum pressure angle beyond the specified 30 degrees will result in only a marginal drop in the S/V ratio. In light of this, there is no great advantage to increasing the Dash-3 maximum cam pressure angle.

For engines with more than 7 cylinders, Graph 6-7 shows that the S/V ratio increases with cam pressure angles greater than 30^{o}.

In summary, the 6 cylinder configuration specified for the Dash-3 Engine does not appear to suffer from overly large heat losses in comparison to the remaining available configurations for the chosen 30^{o} maximum pressure angle. Some marginal reductions in heat loss are available--but at the expense of compromising some of the primary configuration design parameters: the optimum continuous combustion cylinder port duration being one example.

6.3 TIME LOSS AND COMBUSTION CHAMBER SHAPE

6.3-1 Introduction

As indicated in Section 6.2-1, next to heat loss, time loss is the next largest deviation accounting for the differences between an actual indicator diagram and its equivalent fuel/air cycle.

The time loss arises from the fact that in a spark ignition engine, the flame starts from a single ignition point and spreads at a finite speed. The distance that the flame must travel to complete the combustion process, and the rate at which it travels, will determine the effectiveness of the combustion process and the efficiency of the shape of the chamber within which it is confined.

Two of the primary factors in Figure 6-2, which are inherent to the engine configuration and which affect the actual combustion process, are the spark plug position and the combustion chamber shape. Both of these factors determine the total distance the flame front must travel and control the sensitivity of the chamber to detonation. The shape of the combustion chamber governs the rate of pressure rise as flame travel progresses and the point at which maximum pressure occurs.

6.3-2 Performance of the Mark I Combustion Chamber

The combustion chamber of the Mark I engine was originally designed for continuous combustion with continuous fuel

6.3-2 Performance of the Mark I Combustion Chamber (Con't)

injection. The chamber was ideally suited for this with the narrow peripheral port enabling the cylinder to receive a highly homogeneous spray pattern as it rotated by the stationary fuel injector.

The conversion of the Mark I Engine from fuel injection to carburetion and spark ignition (S.I.), (Section 2.4-3), transformed the combustion chamber into a poor S.I. chamber with an unacceptably long flame travel distance similar to that of the conventional "L-head" engine now considered obsolete.

Combustion experiments conducted by K-Cycle confirmed that the peripheral port was ill-suited to spark ignition: Graph 5-6 shows that even with the existing excessive engine friction, to attain the measured BHP the indicated power output of the combustion process could only be half of what might be expected from a well designed chamber.

Two factors were suspected as being responsible for the low indicated power: excessive leakage of the peripheral seals and poor placement of the spark plug resulting in an unacceptably long flame travel distance.

To measure the influence of the spark plug position, the cylinder head of a single cylinder "L-head" crankshaft engine was modified to incorporate a combustion chamber shape similar to that of the Mark I Engine.[38] This test showed

6.3-2 Performance of the Mark I Combustion Chamber (Con't)

that with the modified chamber similar to that of the Mark I Engine, the power output was 50% of that obtained with the original cylinder head which had a more central ignition point. The ignition points and chamber shapes of these cylinder heads are shown in Figures 6-8A & B.

Because of the nature of the experiment, exact comparisons between the Mark I chamber in the K-Cycle Engine and the simulated chamber in the single cylinder engine should be avoided because of the overwhelming differences between a valved stationary chamber and a ported rotating one.

The test did highlight that a less than optimum combustion chamber shape and ignition point, as in the Mark I Engine, can dramatically cut the indicated power of that engine.

The single cylinder crankshaft engine was also used to measure the effect of leakage on the power output. This test[38] found that with the leakage increased by a factor of six to that of the original engine's piston rings and valves (a leakage more severe than that in the Mark I), the engine's power output dropped by only 21%. With the results of these tests, it became obvious that the poor combustion resulted from the Mark I's chamber shape and spark plug location and not from seal leakage. Similar results were found in the development of the Wankel Engine[39] where increased apex seal leakage increased engine oil consumption without dramatically reducing power output.

FIGURE 6-8A: MODIFIED SINGLE CYLINDER ENGINE COMBUSTION CHAMBER SHAPE

- To simulate the Mark I Engine

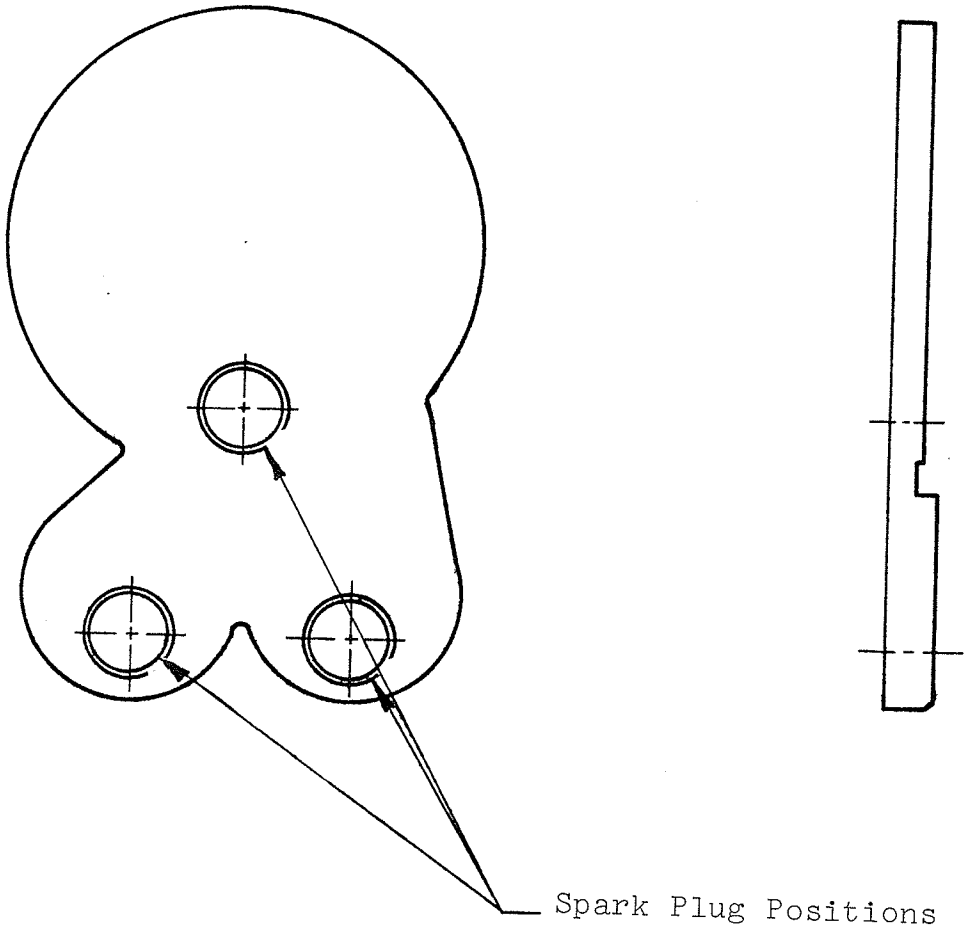

Simulated Mark I Chamber

Volume = 1.59 in^3

Surface Area = 16.92 in^2

FIGURE 6-8B: SINGLE CYLINDER ENGINE ORIGINAL COMBUSTION CHAMBER SHAPE

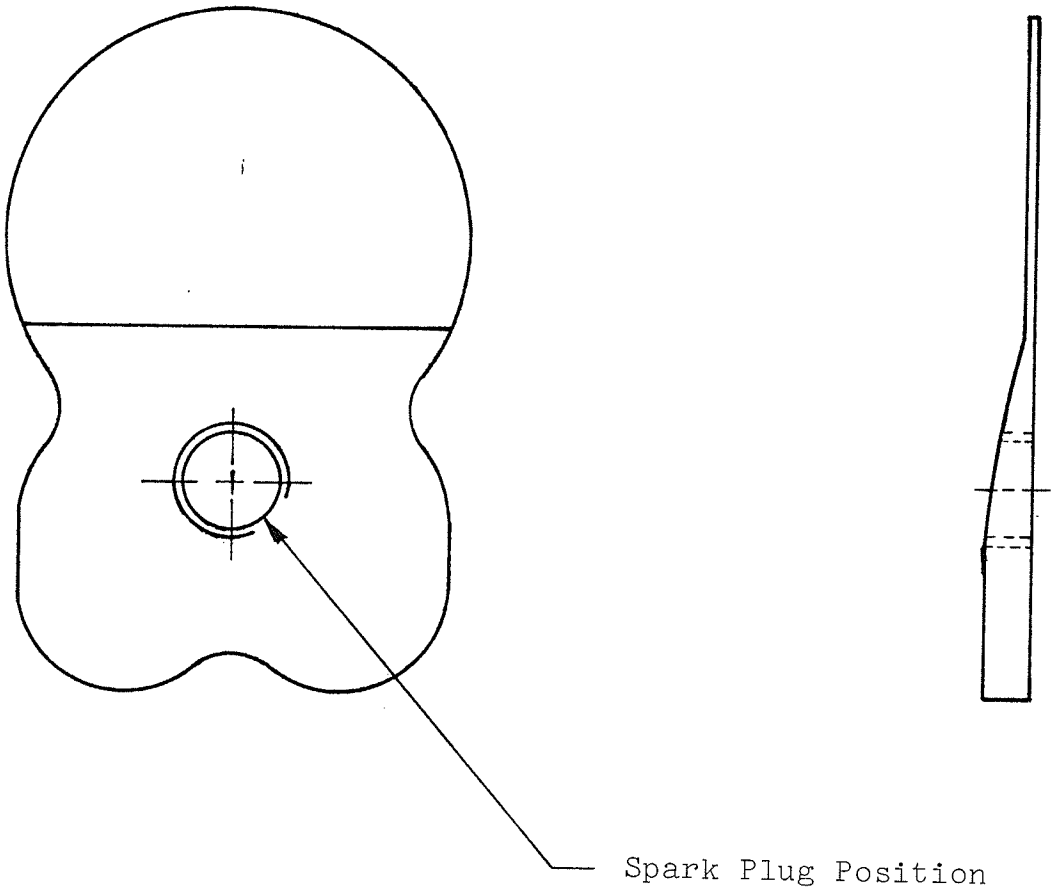

Standard Combustion Chamber

Volume = 1.59 in^3

Surface Area = 15.61 in^2

6.3-3 Determining the Shape of an Effective Combustion Chamber

Despite the ease of ascertaining that the peripheral port chamber in the Mark I Engine is ill-suited to spark ignition, the determination of what constitutes an efficient combustion chamber is quite difficult. Obert[40] points out that even for the combustion chamber of the conventional S.I. engine, analytical relationships of the primary design variables are unknown and the modern combustion chamber has evolved through years of experimental development.

Obert does point out some general rules than an efficient combustion chamber must follow. Such a chamber must have the following attributes:

A. Short combustion time obtained by faster burning (this is the primary consideration).

B. Minimum flame travel obtained by central location of the spark plug.

C. Turbulence during inlet and compression.

D. High piston coverage of the cylinder head to concentrate the charge near the spark plug.

E. Minimum quench thickness or clearance between the piston and the cylinder head.

A short combustion time is desired so as to obtain the maximum combustion pressure as close to TDC as possible without intruding on the compression stroke. Some control over the timing of the peak combustion pressure is exercised by the ignition timing, but the shape of the combustion chamber itself has

6.3-3 Determining the Shape of an Effective Combustion Chamber (Con't)

also to promote an early attainment of this peak pressure without excessive combustion roughness.

Combustion theory explains that the flame front expands from the point of ignition as the surface area of a sphere of increasing diameter. The pressure rise is not directly proportional to the volume consumed by the spherical flame front, but follows the relationship illustrated in Graph 6-9. Obert[41] explains that the ideal combustion chamber shape would be that of a cone with a point of ignition located in the middle of its base. Such a chamber would obtain the required early peak pressure while minimizing the volume of the chamber's end gas so as to avoid detonation.

The piston in cylinder mechanism does not lend itself to a conically shaped combustion chamber, and past experience with chamber in conventional engines has shown that minor changes in chamber shape can transform a workable chamber to one of unacceptable performance.

Taub[42] proposed that the rate of pressure rise in a combustion chamber be controlled by designing the chamber shape to have the rate of change of the burned volume (with respect to the flame travel) increase at a specified rate. This method is called volume control. Taub established empirical limits that a successful combustion chamber must fall within and substantiated the validity of these limits with experimental verification. Two examples of this are illustrated in Figure 6-10.

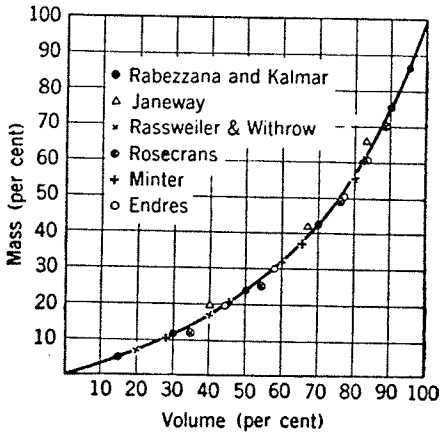

Relation between mass and volume of burned charge. (From Rabezzana, Kalmar, and Candelise, "Gasoline Engine Combustion," *Automotive and Aviation Industries*, Nov. 15, 1939.)

GRAPH 6-9: FROM REFERENCE 51

Note: rate of pressure rise has been found to be directly proportional to mass burned.

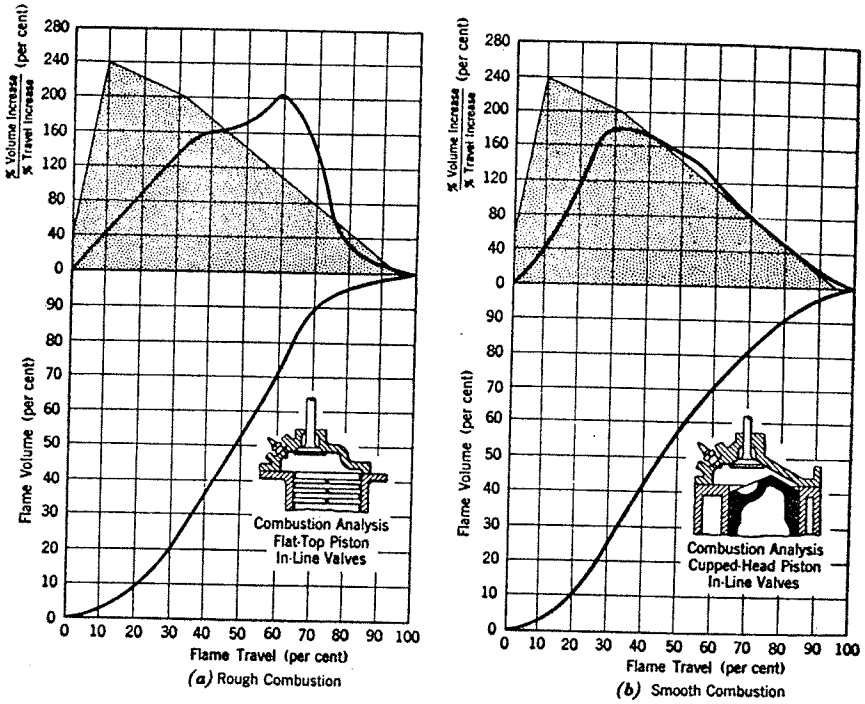

Volume-distribution and rate curves. (From Taub, Reference 3.)

GRAPH 6-10: FROM REFERENCE 52

6.3-3 Determining the Shape of an Effective Combustion Chamber (Con't)

Volume distribution does not give the total picture of a combustion chamber's characteristics in that piston movement, flame velocity (which is often variable), mixture distribution and turbulence are not taken into account. Despite this, Obert[43] claims that a general idea of the relative performance of chambers of the same size range and environment can be established with volume control analysis.

6.3-4 Volume Control Analysis of the K-Cycle Combustion Chamber

In an effort to characterize the poor performance of the first prototype engine in a spark ignition situation, volume control analysis was conducted. The combustion chamber shapes evaluated are shown in Figure 6-11. The curves for the Mark I and Mark II Engines are shown in Graphs 6-12A & B and are compared to Taub's empirical limits.

Taub set his empirical parameter so as to obtain maximum rate of change of flame area, or rate of pressure rise within the first 10% to 30% of flame travel, so as to position the peak combustion pressure rise as close to TDC as possible without encountering combustion roughness. He then had the rate of increase decrease linearly until completion of flame travel so as to avoid detonation. It is quite obvious that both the Mark I and Mark II chambers do not stay within Taub's prescribed volume control limits.

FIGURE 6-11: THE MARK I AND MARK II COMBUSTION CHAMBER SHAPES

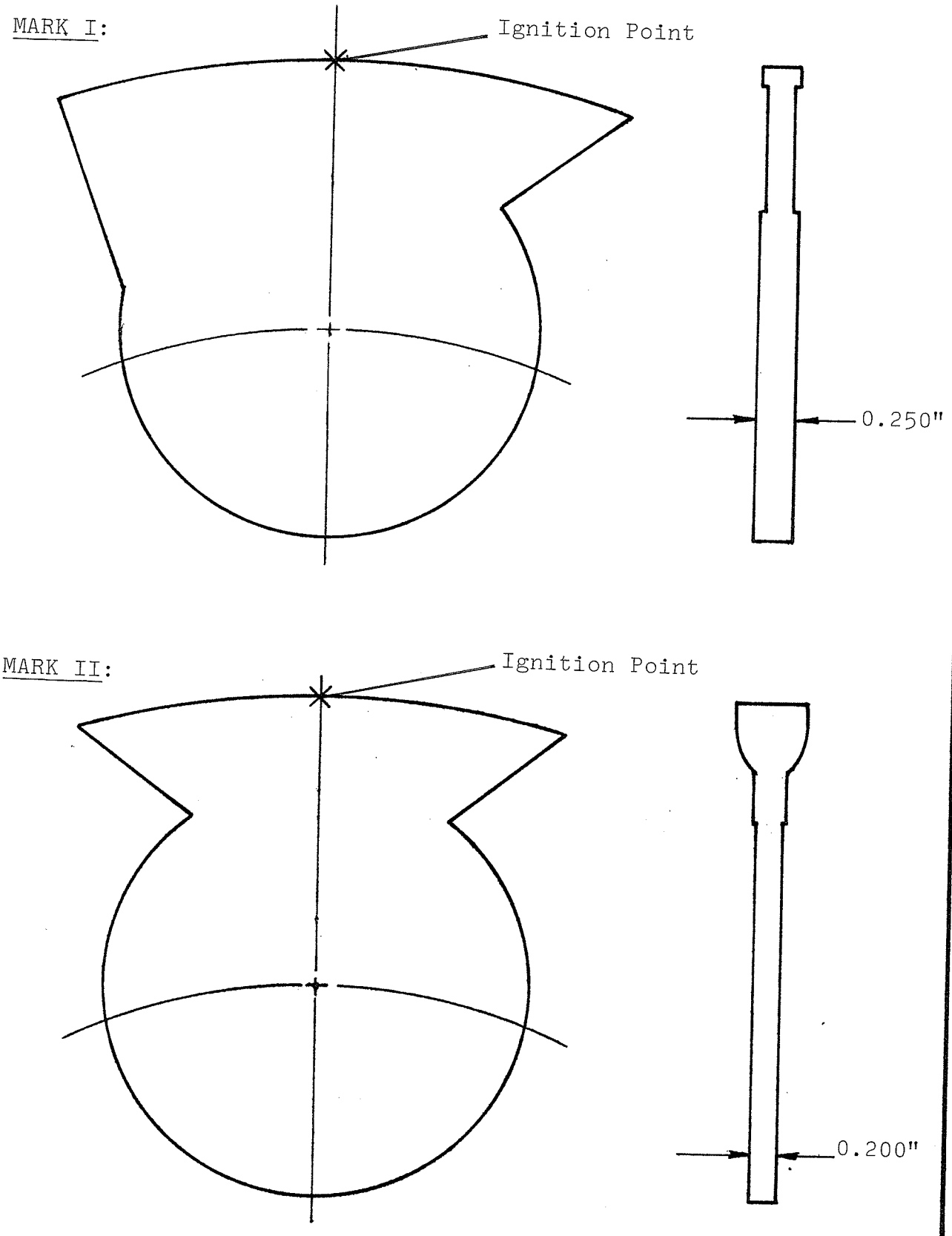

GRAPH 6-12A: VOLUME RATE DISTRIBUTIONS FOR THE MARK I AND MARK II COMBUSTION CHAMBER SHAPES (FIGURE 6-11)

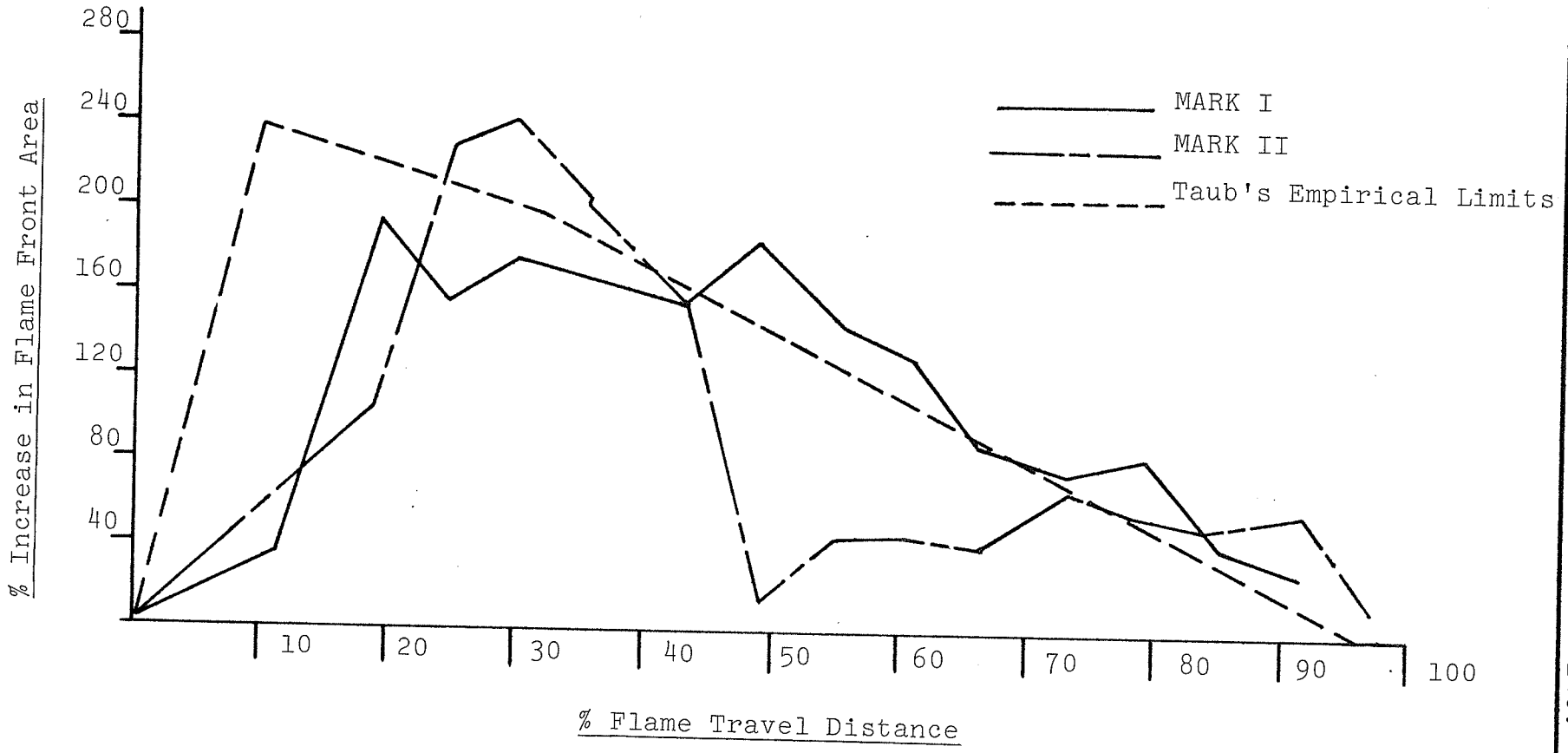

GRAPH 6-12B: RATE % VOLUME AND PRESSURE INCREASE VS % FLAME TRAVEL DISTANCE FOR THE MARK I AND MARK II COMBUSTION CHAMBER SHAPES (FIGURE 6-11).

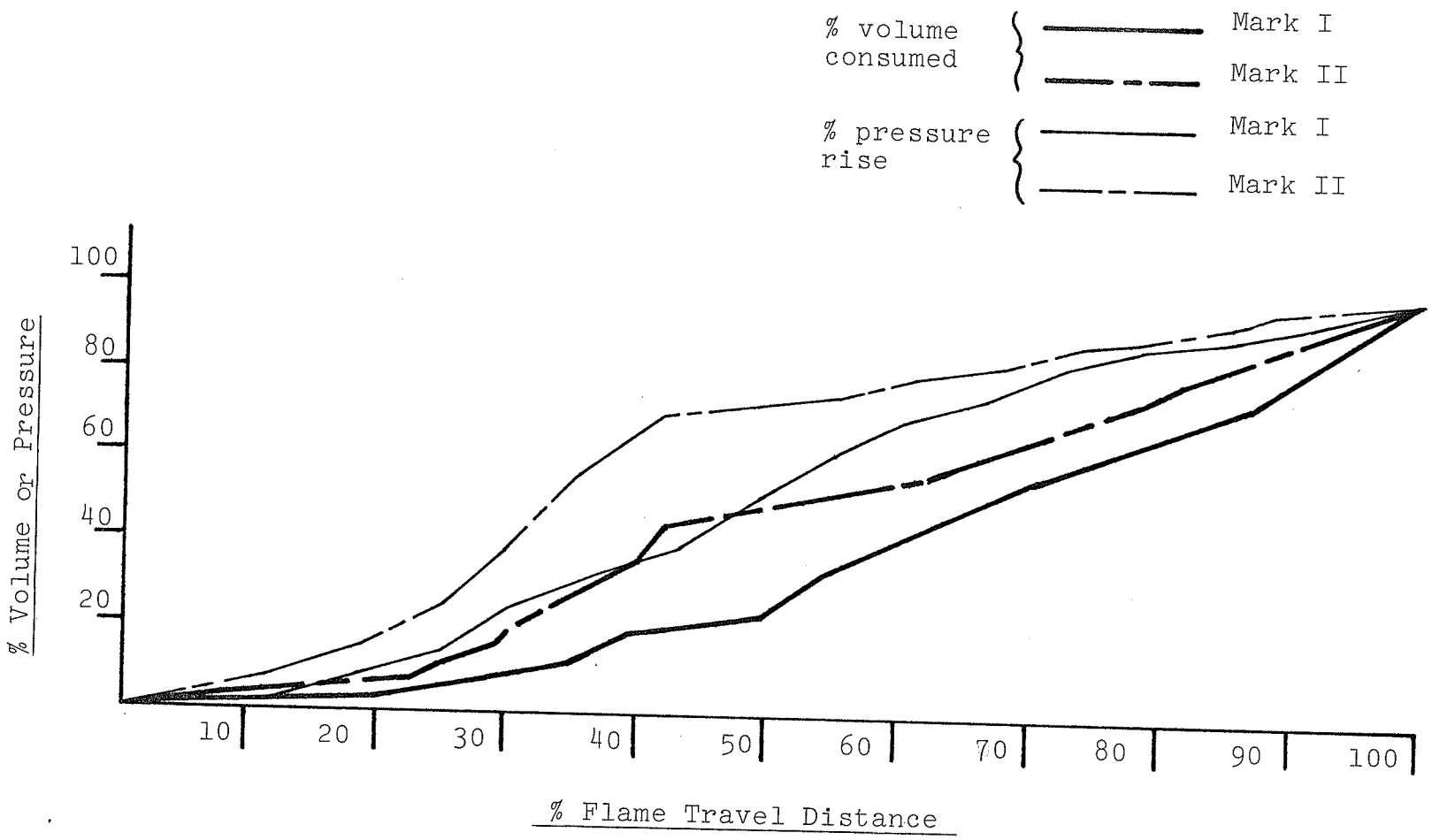

6.3-4 Volume Control Analysis of the K-Cycle Combustion Chamber (Con't)

An estimate of the rate of pressure rise can be obtained by applying the relationship between the volume consumed/mass burned and pressure rise relationship in Graph 6-13 to the percent volume consumed vs. percent flame travel curve. It should be noted that this is only a very rough estimate as Graph 6-13 was established by examining constant volume combustion.

The resulting pressure rise versus flame travel curves are also shown in Graph 6-12B. The particularly slow rate of pressure rise shown may indicate that Mark II's poor combustion efficiency is due to late and possibly incomplete burning of the air/fuel mixture.

While it is beyond the scope of Taub's volume control theory to pinpoint the exact cause of the poor indicated power of the Mark I and II Engines, his theory can certainly be used to compare the performance of the proposed Dash-3 Engine face seal spark ignition combustion chamber to its predecessors.

The Dash-3 Engine configuration chosen in Section 4.3-5 has the seal pitch circle diameter smaller than the cylinder PCD. The resulting envelope for the Dash-3 combustion chamber shape is shown in Figure 6-14.

The proposed Dash-3 combustion chamber shape has, for simplicity, a flat piston top and a flat faced cylinder head. The port opening is curved to match the seal PCD, and its

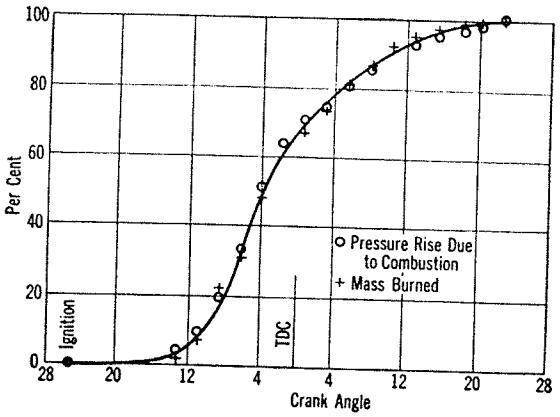

Relationship between pressure rise of combustion and mass burned. (From L. Withrow and G. M. Rassweiler, General Motors Corp.)

GRAPH 6-13: FROM REFERENCE 53

FIGURE 6-14: THE DASH-3 ENGINE COMBUSTION CHAMBER SHAPE

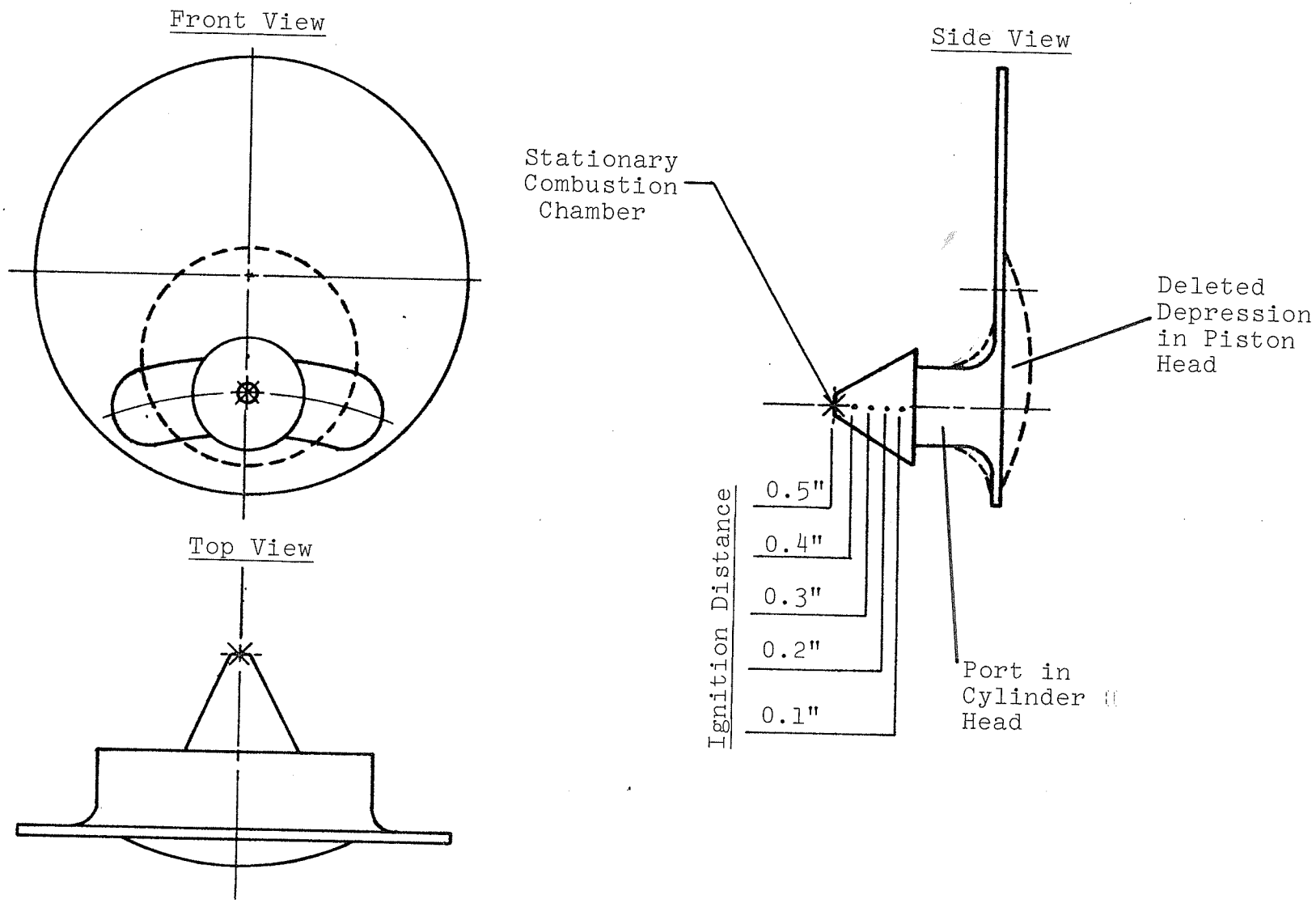

6.3-4 Volume Control Analysis of the K-Cycle Combustion Chamber (Con't)

width is set to obtain a maximum flow velocity recommended by Obert[44] of 240 ft/sec at maximum engine speed. The depth of the port is set at 1/2 inch. The stationary combustion chamber which contains the spark plug is conically shaped and positioned at the mid-point of the cylinder port opening. The piston to cylinder head clearance was set to obtain an 8.0:1 compression ratio. Graphs 6-15 A & B show the volume rate distribution for the combustion chamber of Figure 6-14.

The chamber shape of Figure 6-14 was altered by increasing corner radii and adding a spherical depression to the piston head surface in an attempt to approach Taub's recommended volume rate distribution. It was found that although these modifications had some effect on the volume rate distribution, the primary variable that had the greatest influence was the distance of the ignition point from the cylinder head. By shifting the ignition point from a distance of 0.40" from the cylinder head to 0.10" away, the volume rate distribution changes from an unacceptable one to one that falls within Taub's arbitrary limits.

For the 0.1 "ignition distance", the volume rate peaks at 32% of the flame travel distance rather than at the 10% recommended by Taub. This is due to the thickness of the cylinder head and cannot be avoided.

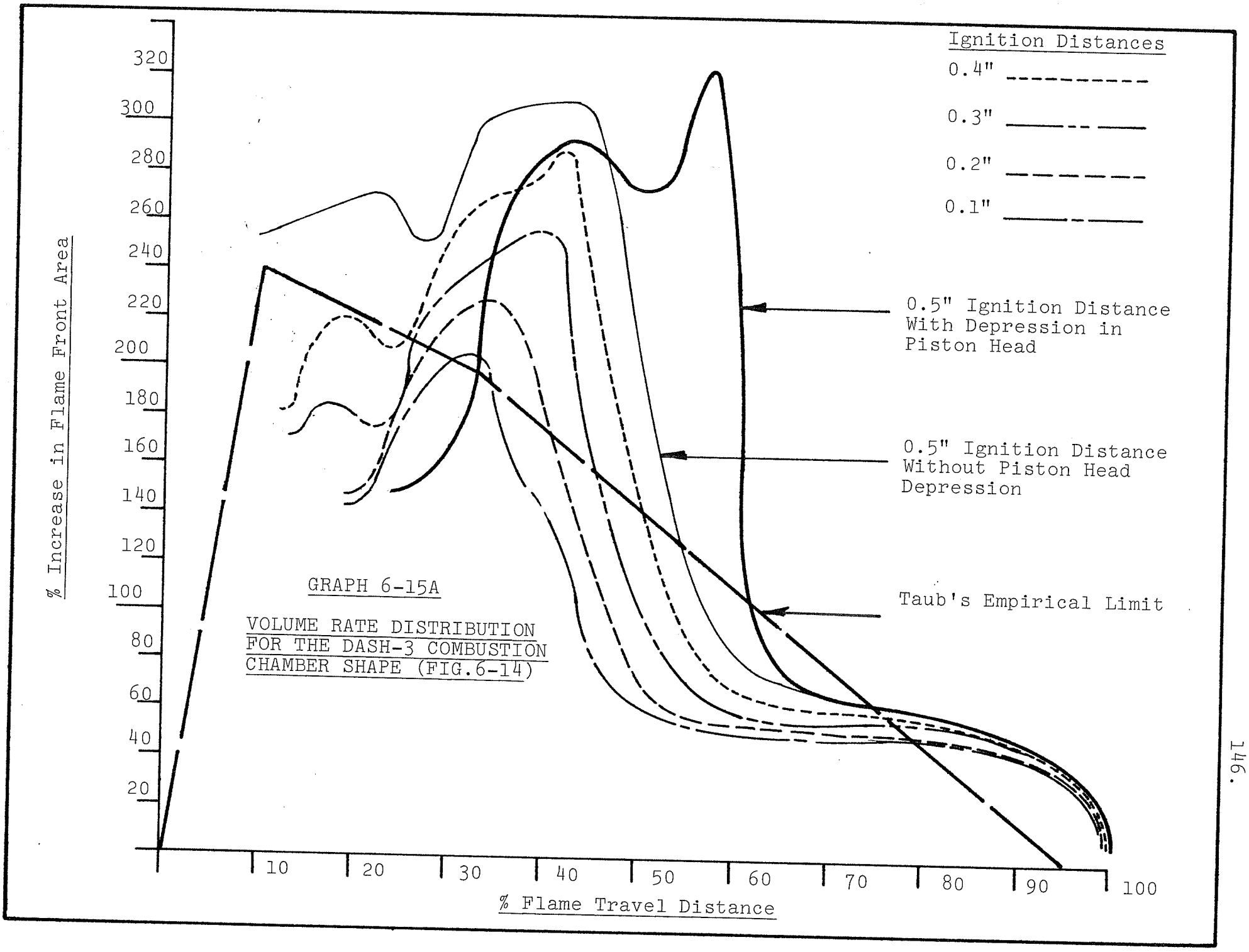

GRAPH 6-15A

VOLUME RATE DISTRIBUTION FOR THE DASH-3 COMBUSTION CHAMBER SHAPE (FIG.6-14)

GRAPH 6-15B

% OF TOTAL PRESSURE RISE
vs.
% FLAME TRAVEL DISTANCE
FOR THE DASH-3 COMBUSTION
CHAMBER SHAPE (FIG. 6-14)

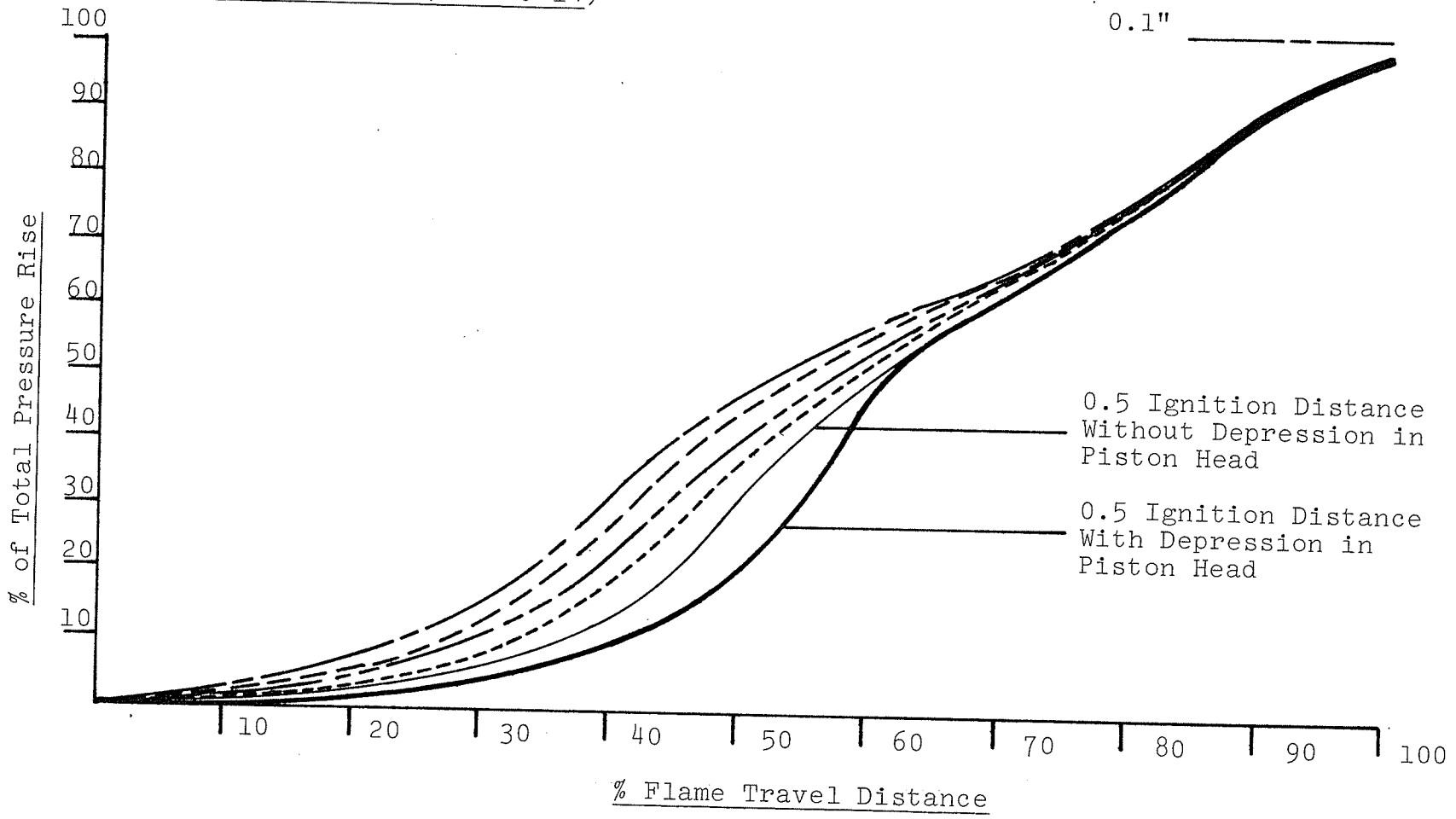

6.3-4 Volume Control Analysis of the K-Cycle Combustion Chamber (Con't)

In comparing the Dash-3 chamber to that of the Mark I and Mark II Engines, several improvements are noted:

* The volume rate distribution of the Dash-3 chamber is quite close to that recommended by Taub's theory.
* The flame travel distance is significantly shorter and should result in faster burning and more effective combustion.
* The closeness of the piston face to the cylinder head should provide significant squish and quench promoting the creation of turbulence during compression and cooling the end to reduce the tendency to detonate.

The recommended chamber shape for the Dash-3 Engine shown in Figure 6-14 will not be a success until all the combustion variables are considered and optimized. Such an optimization process will continue past the detailed design stage into test bench evaluation.

It is hoped that the analysis of this chapter has provided the Dash-3 Engine configuration with a combustion chamber without inherent handicaps.

CHAPTER 7

CONCLUSION

Although the material presented in the previous chapters has established the general direction that an optimization of the K-Cycle mechamisn should take, such an optimization and the subsequent refinement process can only be brought to a successful conclusion if the process is calibrated with actual test results. It is hoped that the conclusions reached within will result in a fundamentally correct Dash-3 Engine configuration that can be fine-tuned by the use of its designed-in component interchangeability to allow a respectable engine output.

It should be once again noted that the Dash-3 Engine configuration was evolved within the confines of the K-Cycle Engines Ltd. company "Design Manual". Some of the design goals, while appearing quite valid at the time of the writing of this document, may impose restrictions on the future development of the Dash-3 Engine. For example, the requirement of a low surface-velocity face seal may impose detrimental parameters on the combustion chamber shape. The final performance of the Dash-3 Engine should therefore be evaluated in not only how the engine met the goals specified in Chapter Three, but how it performed in light of the restrictions imposed by these goals.

The gas sealing between the cylinder ports and the stationary inlet and outlet ports will ultimately be brought to an

acceptable level because the required technology has already been evolved in similar situations such as the seals of the current Wankel Engine. The face seal is highly desirable for the K-Cycle Engine at this stage as it operates at conventional "pressure-velocity" values (similar to the Wankel seals and piston rings) and it removes the now significant centrifugal friction seal power loss. The high velocity technology required by the original peripheral seal design will eventually have to be developed if the ultimate potential of detonation free combustion with low grade fuels, via continuous combustion and fuel injection, is to be realized. Although fuel injection can be incorporated into a face seal engine with some compromises, it will never be capable of the performance of the much simpler pheripheral port combustion chamber.

One of the areas that offers a great deal of freedom to the designer of a K-Cycle Engine is that of the cam generated piston motion. A conservative approach was taken in specifying a dwell-free simple harmonic motion with equally split stroke angular durations for the Dash-3 Engine. It was felt that until respectable seal performance is obtained, a TDC dwell should not be considered as it megnifies the effect of seal leakage. Once the sealing and other problems are overcome, the multitude of available cam motions can be investigated. Some of the interesting possibilities are tailoring the combustion process with a TDC dwell to limit exhaust emissions and optimizing the expansion stroke angular duration to reduce combustion chamber thermal losses.

The optimization of any of the available cam motions will be incomplete unless the influence of maximum cam pressure angle on characteristics such as piston side loads, piston friction, combustion chamber surface to volume ratio and expansion ratio is determined. If the maximum cam pressure angle is constant with respect to cam motion and engine size, then the method of engine configuration optimization presented in Chapter Four is fundamentally correct. If the maximum cam pressure angle varies with one or more engine characteristics, the configuration optimization will have to be re-evaluated.

Another aspect of the Dash-3 Engine which was limited to a conservative value, because of the lack of test data, was the expansion ratio. The practical limit of this variable will be determined by part-throttle operation of the engine and the maximum potential of the K-Cycle principle cannot be realized until the upper limit of the expansion ratio is defined.

It was indicated that piston friction accounts for the majority of the K-Cycle Engine's mechanical losses and that a significant reduction in this friction can be obtained by reducing piston weight. Unfortunately, bearing life is greatly compromised in a light weight piston, and part of the future development of the K-Cycle Engine will have to focus on increasing bearing life. The cam followers of the current pistons are restricted to commercially available

"off-the-shelf" bearings and the acquisition of superior performance non-standard--non-catalogue bearings may be the most expedient method of improving bearing life.

Until additional test results are obtained, it is unclear as to which of the three piston friction components (centrifugal, side reaction, or roller to cam) has the greatest magnitude. If the centrifugal load friction is the most significant, the number of cylinders in the Dash-3 Engine should be reduced while the opposite holds true if the roller/cam sliding friction is the greatest. Excessive piston side load friction can be countered with a reduction in the maximum cam pressure angle. Centrifugal friction losses can be totally eliminated by the conversion of the K-Cycle Engine concept to a stationary cylinder - rotating cam engine, but this configuration is not being seriously considered at this time because of the many associated disadvantages.

As indicated in Chapter Six, it is not enough to minimize the mechanical losses, but the ability of the combustion chamber to develop maximum indicated power must also be optimized. Although Taub's "Volume Rate Distribution Theory" is capable of defining the general characteristics that an efficient combustion chamber must have, final chamber definition must have experimental guidance.

Once the combustion chamber is capable of producing sufficient indicated power the heat losses to the surrounding walls must

be minimized so as to obtain optimum brake thermal efficiency. Another area which must be contended with is that of exhaust emissions: these must be easily minimized either inside the engine or with the help of external apparatus if the K-Cycle Engine is to present itself as a viable alternative to the conventional crankshaft engine.

It is hoped that the optimization of the Dash-3 Engine presented within will result in an engine configuration that is fundamentally correct and with the assistance of its component interchangeability, will be able to bring the K-Cycle Engine concept closer to being a truly more efficient internal combustion engine.

REFERENCES

1. W. D. Alexander, "A New Dimension in Heat Engine Technology", P. 1, K-Cycle Engines Ltd. Publication.

2. L. C. Lichty, "Combustion Engine Processes", P.10, 7th Edition, McGraw-Hill Book Co.

3. W. D. Alexander, "Design Considerations for Continuous Combustion", Feb. 79, K-Cycle Engines Ltd. Publication.

4. J. E. Shigley, "Kinematic Analysis of Mechanisms", P.213, 2nd Edition, McGraw-Hill Book Co.

5. V. M. Faires, "Design of Machine Elements", P.529, 4th Edition, The MacMillan Book Company.

6. J. P. Norbye, "The Wankel Engine", P.36, 1st Edition, The Chilton Book Co.

7. "Engine Design Series, Automotive Design Engineering", January 1975, Part I

8. W. Froede, "The NSU-Wankel Rotating Combustion Engine", SAE Transactions, Vol. 69, 1961.

9. E. F. Obert, "Internal Combustion Engines", P.453, 2nd Edition, The International Textbook Company.

10. Reference 5, P.529.

11. B. Lanoway, "Mark I P-V Diagram-Motoring", K-Cycle Engines Ltd. Report

12. K-Cycle Engines Ltd., Mark I and Mark II Engines Monthly Test Logs.

13. D. Fisher, "Ford Fairmont Test Data", K-Cycle Engines Ltd. Report.

14. Reference 7, Part 4.

15. Reference 4, P.216.

16. The SKF "General Catalogue", Catalogue 3000 E/GB 666, November 1975, P.372.

17. Reference 3.

18. W. H. Crouse, "Automotive Engine Design", P.143, 1st Edition, The McGraw-Hill Book Co.

19. J. W. Winship, "Engine Piston Design - Art or Science?", SAE Paper 660474.

20. Reference 18, P.144.

21. Reference 12, February 1978.

22. Reference 12, January 1978 Inspection Report.

23. Reference 12, February 1978.

24. K-Cycle Engines Ltd. Engineering Report No. 62, P.3

25. Reference 9, P.433, Figure 13-4.

26. Reference 18, P.24.

27. J. E. Shigley, "Mechanical Engineering Design", P.456, 2nd Edition, The McGraw-Hill Book Co.

28. Reference 5, P.37.

29. Reference 16, P.28.

30. Reference 16, P.50.

31. B. Lanoway, K-Cycle Engines Ltd., Engineering Report No. 35, Appendix B.

32. A. Palmgren, "Ball and Roller Bearing Engineering", P.104, S. H. Burbank Co. Inc.

33. Reference 16, P.31.

34. C. F. Taylor and E. S. Taylor, "The Internal Combustion Engine", P.197, 2nd Edition, The International Textbook Company.

35. Reference 34, P.220.

36. Reference 18, P.140.

37. Reference 34, P.198.

38. G. Reese, K-Cycle Engines Ltd., Engineering Report No.63.

39. Reference 6, P.134.

40. E. F. Obert, "Internal Combustion Engines", P.502, 3rd Edition, International Textbook Company.

41. Reference 9, P.453.

42. Taub, "SAE Transactions", Volume 30, P.159.

43. Reference 40, P.502.

44. Reference 40, P.473.

45. R. Herbert, K-Cycle Engines Ltd., Engineering Report No.72, Figure 1.

46. Reference 9, P.432-433.

47. Reference 34, P.215.

48. L. C. Lichty, "Internal Combustion Engines", P.374, 6th Edition, The McGraw-Hill Cook Co.

49. Reference 34, P.217.

50. Reference 34, P.219

51. Reference 9, P.451

52. Reference 9, P.454

53. Reference 9, P.452.